Title: ABI5 Binding Proteins are substrates of key components in the ABA core signaling pathway

Short title: SnRK2s and PP2Cs regulate AFP2 phosphorylation

Author for contact: Ruth Finkelstein

Email: finkelst@ucsb.edu

Authors: Tim J Lynch[1], B. Joy Erickson McNally[2,3,4], Teodora Losic[1,5], Jonas Lindquist[1,6], Ruth Finkelstein[1]

[1]Department of Molecular, Cellular and Developmental Biology, University of California at Santa Barbara, Santa Barbara, CA 93106

[2] Biomolecular Science and Engineering Program, University of California at Santa Barbara, CA 93106

[3]Current address: Biological Sciences Department, Santa Rosa Junior College, Santa Rosa, CA 95401

[4]Current address: Dominican University of California, San Rafael, CA 94901

[5]Current address: Dren Bio, Inc., Foster City, CA 94404

[6]Current address: Diffuse Bio, San Carlos, CA 94070

One-Sentence Summary: An inhibitor of ABA-INSENSITIVE5 is proposed to act as a hub in ABA signaling, and its stability, localization and function are regulated by changes in phosphorylation state.

Author contributions: RRF conceived the project and supervised construction of genetic lines and physiological assays; all authors performed experiments; RRF wrote the article, with contributions from BJEM and TL, and serves as the author responsible for contact.

ABSTRACT

The central components of the ABA core signaling pathway are families of receptors, clade A type 2C protein phosphatases (PP2Cs), SNF1-Related Protein Kinases (SnRK2s), and diverse sets of proteins regulated by phosphorylation via these kinases, including bZIP transcription factors such as ABA-INSENSITIVE(ABI)5. The larger network of ABA signaling factors includes additional kinases and E3 ligases that modify these components to affect their activity and stability. The ABI5-Binding Proteins (AFPs) are negative regulators of ABA response. This study shows that the AFPs interact with specific family members of all components of this pathway and are substrates for SnRK2s and PP2Cs. AFPs also interact with subsets of MAP kinases (MPKs) and 14-3-3 proteins previously found to regulate activity of the ABI5-related clade of transcription factors. Residues predicted to be phosphorylated are conserved between AFPs, but are located within regions predicted to be unstructured. ABA promotes phosphorylation of AFP2, but conditions that prevent phosphorylation of AFP2 result in decreased stability, a shift in localization toward dispersed foci, and reduced effectiveness for inhibiting ABA response at germination. Thus, AFP2 appears to be an important hub in the ABA core signaling pathway.

43 **INTRODUCTION**

44

45 The phytohormone ABA regulates diverse responses in plants, in part mediated by large changes in gene
46 expression. Although transcriptome experiments in diverse tissues at various stages of growth have
47 identified many thousands of ABA-regulated genes, very few of these are consistently ABA responsive
48 across all of these conditions (reviewed in Finkelstein, 2013) and most transcriptome comparisons focus
49 on co-expressed genes to construct gene regulatory networks acting in specific responses or tissues
50 (reviewed in Ko and Brandizzi, 2020). However, some loci encode core components regulating these
51 diverse responses. The central components of the ABA core signaling pathway are families of receptors,
52 protein phosphatases, protein kinases, and diverse sets of proteins regulated by phosphorylation via
53 these kinases (Cutler et al., 2010; Chen et al., 2020; Ali et al., 2020). In the absence of ABA, PP2C clade A
54 protein phosphatases bind to SNF1-Related Protein Kinase2s (SnRK2s), sterically preventing them from
55 becoming phosphorylated and active. When ABA is present, PYRABACTIN RESISTANT
56 (PYR/PYL)/REGULATORY COMPONENT OF ABA RECEPTOR (RCAR) receptors bind and inactivate these
57 PP2C phosphatases, thereby permitting phosphorylation and activation of the SnRK2 class kinases .
58 These kinases can then phosphorylate regulatory proteins such as the ABA- INSENSITIVE(ABI)5/ABA
59 RESPONSE ELEMENT BINDING FACTOR (AREB/ABF) clade of bZIP transcription factors, leading to ABA-
60 induced changes in gene expression, including feedback regulation by inducing expression of the PP2C co-
61 receptors (Wang et al., 2019). Several of these bZIP proteins are bound in a phosphorylation-dependent
62 manner by 14-3-3 proteins, and this interaction can be required for gene activation by the bZIP factor
63 (Schoonheim et al., 2007; Camoni et al., 2018).

64

65 The clade A PP2Cs are monomeric Ser/Thr phosphatases that were initially identified genetically by
66 dominant mutations in ABA-INSENSITIVE(ABI)1 and ABI2 (Koornneef et al., 1984), resulting in ABA
67 resistance due to their inability to be inactivated (Park et al., 2009; reviewed in Finkelstein, 2013).
68 Additional members of the clade, e.g. ABA-HYPERSENSITIVE GERMINATION(AHG)1 and AHG3, were
69 identified based on loss of function mutations conferring hypersensitivity to ABA, reflecting their role as
70 negative regulators of ABA response (Yoshida et al., 2006; Nishimura et al., 2007). These PP2Cs have
71 overlapping expression patterns and functions, such that double mutants are more hypersensitive than
72 the single mutants. Interactome and other studies have identified numerous substrates or other
73 interaction partners for these PP2Cs, including members of multiple families of kinases and transcription
74 factors involved in response to ABA and abiotic stresses (Lumba et al., 2014; Yilmaz et al., 2022).

75

76 The SnRK2 Ser/Thr kinases are a plant-specific subfamily of the SnRKs, comprising 10 family members in
77 *Arabidopsis thaliana* (reviewed in Kulik et al., 2011; Maszkowska et al., 2021). Although all SnRK2s
78 function in stress responses, this subfamily is further divided into 3 groups distinguished by their
79 response to ABA. Group 1 does not respond to ABA, group 2 shows minimal response to ABA, and group
80 3 is strongly activated by ABA (Kobayashi et al., 2004). In Arabidopsis, group 3 consists of SnRK2.2,
81 SnRK2.3 and SnRK2.6. These kinases have partially redundant functions, with SnRK2.2 and SnRK2.3
82 playing major roles in seed dormancy, control of germination and seedling growth, while SnRK2.6 has
83 greater effects on stomatal regulation (Fujii and Zhu, 2009; Nakashima et al., 2009). Triple mutants
84 defective in all three are highly resistant to ABA and exhibit extreme drought sensitivity and severely
85 stunted growth (Fujita et al., 2009). In contrast, SnRK2.10 is a member of group 1 and responds to
86 osmotic stress, but is not part of the ABA core signaling pathway (Kobayashi et al., 2004).

87 Mitogen activated protein kinases (MAPKs, also known as MPKs) are another conserved family of
88 Ser/Thr kinases, some of which regulate abiotic stress and ABA response. MAPKs are the final step in the
89 MAPK cascade, composed of MAP kinase kinase kinases (MAPKKKs/MAP3Ks/MEKKs) that phosphorylate
90 and activate MAP kinase kinases (MAPKKs/MAP2Ks/MEKs), which in turn phosphorylate/activate the
91 MAPKs (Jagodzik et al., 2018). Over 100 genes encode members of these families in *Arabidopsis*
92 *thaliana,* regulating diverse processes with substantial overlaps in function. Although not part of the
93 ABA core signaling pathway, cross-talk between these pathways occurs at various levels: SnRK2s
94 phosphorylate some MAPKs (Umezawa et al., 2013), while MAP3Ks phosphorylate SnRK2s and are
95 required for their activation by ABA (Takahashi et al., 2020). MAPK cascades regulate ABA response
96 through effects on gene expression, including induction of transcription factors such as ABI3 and ABI5
97 (Lee et al., 2014), and activation or stabilization of other factors, e.g. ABI4, by phosphorylation (Guo et
98 al., 2016; Eisner et al., 2021; Maymon et al., 2022). The 20 MAPKs of Arabidopsis are divided into 4
99 clades (A-D), distinguished by their domain structures and the sequence at the site phosphorylated by
100 MAPKKs, which is different in clade D (Group et al., 2002). Clade D also lacks a “common docking”
101 domain that is recognized by MAPKKs, phosphatases and other proteins. The most extensively studied
102 MAPKs are MPK3, MPK4 and MPK6, which are members of clades A and B; these have been shown to
103 function in diverse pathways including stomatal development, root growth, pollen tube growth, immune
104 response, and response to abiotic stress and/or ABA (Wang et al., 2007; Shao et al., 2020; Galletti et al.,
105 2011; Zou et al., 2021; Guan et al., 2014; de Zelicourt et al., 2016). All members of the C clade are also
106 activated by ABA by inducing synthesis of the upstream MAP3Ks via the PYR/PYL/RCAR-PP2C-SnRK2 core
107 signaling pathway (Danquah et al., 2015). Within this clade, MPK7 has been specifically implicated in

108 dormancy release (Chen et al., 2023).
109
110 Although not initially characterized as part of the core signaling pathway, a group of ABI5-binding
111 proteins (AFPs) identified by a yeast two-hybrid screen using ABI5 as bait were shown to be important
112 ABA-inducible negative regulators of ABA response (Garcia et al., 2008). One of these, AFP3, is among the
113 few genes that are ABA-induced in many different contexts, but especially during vegetative growth
114 (Finkelstein, 2013). In contrast, AFP1 and AFP2 are most active during germination and seedling
115 establishment. The AFPs have three highly conserved domains, including an ethylene-responsive element
116 binding factor-associated amphiphilic repression (EAR) domain in the "A domain" and a nuclear
117 localization signal in the "B domain," in addition to the C-terminal domain initially shown to interact with
118 the ABI5/ABF/AREB transcription factors (Garcia et al., 2008). Overexpression of the AFPs results in
119 extreme ABA resistance, including decreased expression of many seed maturation genes, failure to
120 acquire desiccation tolerance, and ability to germinate on 100-fold higher ABA concentrations than wild-
121 type seeds (Lynch et al., 2017).
122
123 Studies addressing the mechanism by which AFPs inhibit ABA response have demonstrated interactions
124 with co-repressors including TOPLESS/TOPLESS-RELATED (TPL/TPR) and Histone Deacetylase (HDAC)
125 subunits, suggesting effects on chromatin remodeling (Lynch et al., 2017). Although mechanistically
126 more obscure, the AFPs also interact directly with DELLA proteins, antagonizing their inhibitory effects
127 on germination (Finkelstein and Lynch, 2022). The AFPs have also been proposed to confer ABA
128 resistance by promoting ABI5 degradation, functioning as adaptors for E3 ligases that ubiquitinate ABI5
129 and possibly related bZIP proteins, based in part on colocalization of AFP1 with ABI5 and COP1 in nuclear
130 bodies (Lopez-Molina et al., 2003). However, the interactions with several such E3 ligases (DWA1, DWA2
131 and KEG1) are rather weak and loss of function mutations for these ligases do not block the ABA
132 resistance conferred by AFP2 overexpression (Lynch et al., 2022). Furthermore, tests of the timecourse
133 of germination show that germination mostly precedes degradation of ABI5 (Lynch et al., 2022) and
134 COP1 promotes ABI5 accumulation in the dark (Peng et al., 2022).
135
136 Outside of the conserved domains, much of the AFP sequences are predicted to be intrinsically
137 disordered (Lynch et al., 2017; Varadi et al., 2023) (Supp. Fig.1), raising the possibility that the AFPs
138 can assume a variety of structures due to post-translational modifications, consistent with the
139 diversity of their observed protein interactions. Furthermore, much recent work highlights the
140 tendency of intrinsically disordered regions to drive phase transitions forming bimolecular

141 condensates (Liu et al., 2023). The current work reports interactions between AFPs and the PP2Cs,
142 SnRK2s and MPKs previously shown to regulate ABA response, and addresses the functional
143 significance of these interactions. Additional interactions with ABA receptors and 14-3-3 proteins
144 may affect the activity of signaling complexes containing some of these factors.
145
146 **RESULTS**
147
148 **Interactions between AFPs and components of the ABA core signaling pathway**
149
150 Our early studies of the AFPs revealed no obvious biochemical function, so we used AFP2 as bait in a
151 yeast two-hybrid screen to identify additional interacting partners that might provide clues regarding
152 function. This screen produced a diverse set of potential interactors including multiple ABI5/ABF/AREB
153 clade bZIP proteins, ABI clade protein phosphatases (PP2Cs), and a variety of kinases. Further specific
154 pairwise yeast two-hybrid assays, expanding this study to include all four members of the AFP family and
155 seven members of the ABI PP2C clade, showed strong interactions between all AFPs and AHG1 and
156 AHG3. When the AFPs were present as Binding Domain (BD)-fusions, additional interactions were limited
157 to either AFP1 or AFP2 for only one other PP2C tested, ABI1 (Fig.1). Interactions mapped to the C domain
158 of AFP1, but to several regions of AFP2.
159
160 Tests of interactions with kinases showed all AFPs except AFP4 interacted with SnRK2.3, SnRK2.6,
161 MPK3, MPK4, and MPK7, but not with SnRK2.10 (Fig.2). The BD-MPK6 fusion conferred growth without
162 requiring an AD- interaction partner, but reporter activation was again enhanced by interaction with AD-
163 fusions to AFP1,2 and 3 (Supp. Fig. 2). Surprisingly, activity was impaired when BD-MPK6 was co-
164 expressed with AFP4 or AFP2-C. Only AFP2 interacted with SnRK2.2 in this assay. Interactions with
165 subdomains were very weak, suggesting that regions across the entire protein were required for these
166 interactions. Although several D clade MPKs are highly co-expressed with the AFPs in maturing, dry and
167 germinating seeds (Supp.Fig 3), only MPK17 and MPK20 interacted with the AFPs in yeast, and the
168 interactions were relatively weak.
169
170 In contrast to the strong interactions between AFPs and bZIPs, PP2Cs and kinases, relatively weak
171 interactions were observed between AFPs and a few members of the PYR/PYL/RCAR family of ABA
172 receptors: PYLs 2, 7, 9, 11 and 12 (Fig. 3A, Supp Fig. 4). All of these are expressed in maturing, dry
173 and/or imbibing seeds, coinciding with peak expression of AFP1, AFP2, and ABI5 (Supp. Fig. 5).
174 Furthermore, PYLs 11 and 12 promote ABI5-mediated ABA response during germination and their

175 expression is regulated by ABI5 (Zhao et al., 2020), and PYLs 7 and 9 are members of the small subset
176 of receptors that can interact with AHG1 (Tischer et al., 2017). This result suggests that several AFPs
177 can interact with all components of the ABA core signaling pathway.
178
179 Many phosphorylation-dependent protein activities, including hormone signaling, are regulated by 14-3-
180 3 proteins that bind to phosphorylated Ser or Thr residues within specific contexts (Camoni et al., 2018).
181 The Arabidopsis genome encodes thirteen expressed 14-3-3 proteins, designated GENERAL REGULATORY
182 FACTORS(GRFs), many of which are also expressed in maturing, dry and germinating seeds (Supp Fig 5).
183 Previous studies in multiple cereal grains and Arabidopsis have shown a role for 14-3-3 proteins in ABA-
184 regulated transcriptional complexes, including direct interactions with members of the ABI5/ABF clade of
185 bZIPs (Jaspert et al., 2011). We initially tested the Arabidopsis 14-3-3 proteins with the highest homology
186 to the barley and rice proteins shown to interact with HvABI5 and HvABF1 (Schoonheim et al., 2007), and
187 that are expressed in dry, imbibed or germinating seeds: GRF1 (14-3-3 chi), GRF2 (14-3-3 omega), GRF3
188 (14-3-3 psi), GRF4 (14-3-3 phi), and GRF7 (14-3-3 nu). AD fusions with GRF1,2,3, and 4 all interacted
189 weakly with a BD-AFP1 fusion, but only the AD-GRF3 and -GRF4 fusions interacted above background
190 with BD-AFP2 (Fig. 3BC). Interaction with ABI5 was substantially stronger (Supp Fig 6). Consistent with the
191 importance of phosphorylation for 14-3-3 binding, a BD-fusion to AFP2 with alanine substitution
192 mutations in 2 binding sites predicted by 14-3-3-Pred
193 (https://www.compbio.dundee.ac.uk/1433pred/)(Madeira et al., 2015) had greatly reduced interactions
194 with the GRFs (Supp Fig 6). In addition to their relatively strong interactions with AFP1 and AFP2,
195 transcripts for both GRF3 and GRF4 are present at similar levels to those of these AFPs in dry and imbibed
196 seeds (Supp. Fig. 3), so our further studies focused on interactions with these family members.
197
198 We previously found that AFP1 and AFP2 could form homo- and heterodimers in yeast two-hybrid and
199 BiFC assays (Lynch et al., 2017). Attempts to map the interacting domains by further yeast two-hybrid
200 assays showed that the AB domain was sufficient for interactions with full-length AFP2, but not with itself,
201 implying that multiple domains are required for interaction (Supp. Fig. 7A). Consistent with this, Alphafold
202 modeling suggests that the most likely interface between AFP2 subunits includes residues present in the B
203 and C domains (Supp. Fig. 7B).
204
205 The interactions between AFP1, AFP2, PP2Cs, kinases, receptors and GRFs were further tested by BiFC
206 assays, using split YFP fusions in transiently transformed *N. benthamiana*. These studies showed
207 interactions between both AFPs and SnRK2.3, SnRK2.6, MPK3, MPK4, MPK6, AHG1, AHG3, GRF3, GRF4,

208 PYL2 and PYL9, confirming the yeast two-hybrid results, but interactions with GRF7 and AHG3 were much
209 weaker in these assays (Fig.4). AFP2 also interacted with MPK7 in this assay. Although none of the 14-3-3
210 proteins showed any specific interaction with PP2Cs or a SnRK that interacts with AFP2 in the yeast two-
211 hybrid assay, GRF4 interacted strongly with MPK3 and SnRK2.6, and very weakly with AHG1, in BiFC
212 assays (Supp Fig.6). Further mapping of the BiFC interactions between domains of the AFPs with AHG1
213 and SnRK2.3 showed that all AFP domains interacted with AHG1 (Supp Fig 8) (Erickson McNally, 2016). In
214 contrast, SnRK2.3 interacted with only the B and C domains of AFP2, and the A and B domains of AFP1.
215
216 The BiFC assays also showed some differences in localization. Fluorescence was generally diffuse
217 throughout the nuclei when AFPs and kinases were co-expressed, but localized to nuclear punctae when
218 AFPs and AHG1 were combined (FIg 4 and Supp Fig. 8). Although GRF4 was distributed throughout the
219 cell when forming homodimers, or heterodimers with GRF3 and GRF7, the GRF interactions with AFPs
220 were mostly limited to nuclei (Fig.4).
221
222 **AFPs are substrates for SnRK2s and PP2Cs**
223
224 We had previously observed that YFP-AFP2 fusions migrate as doublets and occasionally even triplets on
225 SDS-PAGE, suggesting the possibility of post-translational modifications (Erickson McNally, 2016). These
226 doublets are especially pronounced in any fusions containing the B domain of AFP2 (Fig. 5A). To
227 determine whether the observed interactions between AFP2 and these kinases and phosphatases
228 reflected a substrate role of AFP2, these proteins were transiently co-expressed in *N. benthamiana*. Co-
229 expression with SnRK2.3 shifted the YFP-AFP2-AB fusion to predominantly the slower mobility form,
230 whereas co-expression with AHG1 or AHG3 resulted in a shift toward the higher mobility form (Fig.5B).
231 YFP-AFP2-AB affinity purified with GFP-trap beads cross-reacted with an anti-phosphoserine antibody,
232 and this reaction was enhanced in the slower migrating form, confirming that the altered mobility was
233 due at least in part to phosphorylation (Fig.5C).
234
235 AFP2 contains 40 serines and 22 threonines, constituting nearly 18% of the total amino acids in AFP2,
236 many of which are conserved between AFP1 and AFP2 (Supp. Fig. 9). Of these, 17 serines and 11
237 threonines were predicted to be phosphorylated by the PhosPhAt database (Zulawski et al., 2012), but
238 only 9 serines and 1 threonine are predicted at high stringency by http://musite.sourceforge.net/ (Table
239 1). PhosPhAt lists only three documented phosphorylated residues, following ionizing radiation stress
240 and dependent on the ataxia telangiectasia-mutated (ATM) and Ataxia telangiectasia-mutated and Rad3-

241 related (ATR) kinases: T76, S232 and S234 (Roitinger et al., 2015). Of these, only T76 was predicted by
242 both programs. Based on the consensus target sites of R-X-X-S and S-D for ABA-induced phosphorylation
243 by SnRK2s (Wang et al., 2013), potential targets in AFP2 are S85, S112, S150, S187, and S259. Of these,
244 only S85 and S112 are conserved between AFP1 and AFP2. Similarly, two consensus sequences, P-X-S/T-P
245 and S/T-P, are highly abundant in protein substrates of MAPKs (Seger and Krebs, 1995) such that
246 potential targets of MAPKs are T76, S221 and T319 of AFP2, all of which are conserved between AFP1
247 and AFP2. Three consensus motifs have been proposed for 14-3-3 target binding sites, two of which are
248 present in AFP2: S112 fits the mode I consensus and both S346 and T347 fit the C-terminal mode III
249 consensus (reviewed in Camoni et al., 2018). The 14-3-3 Pred program scores S112 and S85 as highly
250 likely binding sites, with relatively moderate scores for T16, S38, and S259.
251
252 We took two approaches to identifying actual phosphorylation sites: *in vitro* phosphorylation with
253 purified recombinant proteins, and site-directed mutagenesis of predicted phosphorylation sites. We
254 focused on specific target sites of SnRK2s by incubating recombinant His6-AFP2-AB (aa1-149) fusions
255 with GST-SnRK2.6 *in vitro*, resulting in a shift of the His-AFP2-AB fusion to a higher apparent molecular
256 weight (Fig. 5D). Mass spectrometric analysis of this slower mobility form identified S112 as a
257 phosphorylated residue (Supp Fig 10). *In vitro* kinase assays including gamma-labeled ATP, comparing
258 wild-type to either S112A or phosphomimetic S112E or S112D mutants of His6-AFP2-AB, showed that
259 phosphorylation by SnRK2.6 was still possible until the S85 was also converted to alanine (Fig. 5E). The
260 phosphomimetic mutants appeared to have an intermediate degree of phosphorylation between the wild
261 type and S112A forms, suggesting that true phosphorylation at S112 affected the likelihood of additional
262 phosphorylation. In contrast, a His6-AFP2-C fusion (aa-149-348) was not phosphorylated by SnRK2.6
263 (Supp Fig 11A).
264
265 Immunoblot analyses of possible *in vivo* phosphorylation by Myc-MPK3 showed either no shift in mobility
266 for the YFP-AFP2-AB domain fusion or an apparent compression to the higher mobility form for the YFP-
267 AFP2-BC domain fusion (Fig.5F). Surprisingly, although neither the S85A, S112A double mutant nor the
268 T76A, S85A, S112A triple mutant of the His6-AFP2-AB domain fusion could be phosphorylated by SnRK2.6
269 *in vitro* (Fig 5G), only the double mutant ran as a single high mobility form when transiently expressed as
270 a YFP-fusion *in planta* (Fig.5H). The triple mutant ran at the same mobility as wild-type when expressed as
271 a YFP fusion *in planta*. and the T76A mutant of the His6-AFP2-AB domain fusion showed a greater shift
272 toward lower mobility forms than the wild-type fusion (Fig. 5H). However, similar to the wild-type fusion,
273 its mobility was not altered by co-expression with Myc-MPK3 (Supp. Fig. 11B).

274 *In vitro* kinase assays with His6-AFP2-BC domain fusions showed that an S112A substitution greatly
275 reduced phosphorylation of this domain by SnRK2.6 (Fig.5I). Similarly, S112A mutations blocked *in planta*
276 phosphorylation of YFP-AFP2-BC fusions by SnRK2.3 when transiently co-expressed in *N. benthamiana*
277 (Supp Fig. 12A). Although phosphorylation of S112A in the *in vitro* reactions was not affected by
278 phosphomimetic mutations in S221 and T319, these mutations reduced mobility of the fusion (Fig. 5I).
279 Transiently expressed YFP-AFP2-BC mutant fusions converting S112, S259, S221 or T319 to alanine all still
280 appeared as doublets in immunoblot analysis, as did double mutants combining predicted SnRK2 targets
281 (S112, S259)A or potential MPK targets (S221, T319)A (Fig. 5J). However, both single and double mutants
282 affecting S221 and T319 reduced the shift toward lower mobility, and both double mutants were under-
283 accumulated relative to the wild type. The triple mutant (S112,S221,T319)A fusion was rarely detectable.
284 Unlike the alanine substitution mutants, YFP-AFP2-BC fusions with phosphomimetic mutations converting
285 S221 alone or in combination with S112 and T319 to aspartic acid all resulted in compression to a single
286 intermediate mobility form (Fig.5K). Co-expression with MPK3 also converts most of the wild type AFP2-
287 BC fusion toward higher mobility forms, but has little effect on the (S221,T319)A mutant which already
288 displays a higher mobility than the wild type (Fig.5F,K). In contrast to the higher mobility on Laemmli SDS-
289 PAGE of AFP2-BC co-infiltrated with MPK3, analysis on Phos-tag gels showed a shift toward decreased
290 mobility, reflecting increased phosphorylation (Supp Fig 12B). The S221A mutation alone blocked the
291 phosphorylation seen in the wild-type BC domain, but a phosphorylated form reappeared in the
292 (S221,T319)A mutant. Although the (S221,T319)A mutant migrated similarly to the wild-type BC domain,
293 co-expression with MPK3 resulted in the appearance of a novel phosphorylated form, visible in both gel
294 systems, suggesting that loss of both "consensus" MPK targets led to phosphorylation of an as-yet
295 unknown alternative residue, possibly by an unidentified endogenous kinase.
296
297 In contrast to the AB and BC domain fusions, full-length YFP-AFP2 transiently co-expressed with Myc-
298 AHG1 in *N. benthamiana* shows as much or more phosphorylation than YFP-AFP2 alone, even when the
299 SnRK2 and potential MPK target residues have been converted to alanines, again suggesting that
300 alternative residues are being modified (Supp Fig.12D). Surprisingly, YFP-AFP2 co-expressed with Myc-
301 SnRK2.3 appeared less phosphorylated than YFP-AFP2 alone. However, alanine substitutions in the SnRK
302 target residues (S85 and S112) resulted in the appearance of novel bands, reflecting both less and more
303 phosphorylation, but including the additional S259A mutation fully blocked SnRK2-induced
304 phosphorylation (Supp Fig.12D). Alanine substitutions in potential MPK target residues (S221 and T319)
305 also blocked phosphorylation by SnRK2.3. Collectively, these results suggest that modification of the

306 primary SnRK2 or MPK targets affects accessibility of the SnRK2 target sites and may lead to
307 phosphorylation of novel sites.
308
309 **ABA effects on AFP2 phosphorylation state**
310
311 Given that ABA activates the group 3 SnRK2s, we tested whether these mutations affected any post-
312 translational modifications induced by ABA treatment. Transiently expressed wild type YFP-AFP2-AB
313 domain fusions shifted from roughly 40% slower mobility forms in control conditions to 60% slower
314 mobility forms after 4 hrs exposure to 30 µM ABA (Fig. 6A). In contrast, the S112A mutation alone, or in
315 combination with T76A and S85A ("3xA"), blocked this shift (Fig. 6A). Similarly, the highest mobility form
316 of the YFP-AFP2-BC domain fusion shifted to an intermediate slower mobility following ABA treatment
317 and this was blocked in the (S112,S259)A mutant. In contrast, the (S221,T319)A mutant of the BC domain
318 continued to show a shift of the highest mobility form in response to ABA, but had greatly reduced
319 expression of the slowest mobility form under any condition.

320 In stable transgenic Arabidopsis lines carrying the wild-type YFP-AFP2-BC domain fusion, this shift in
321 mobility was induced by exposure to as little as 1 µM ABA for 6 hrs or by 1 hr of treatment with 20 µM
322 ABA (Supp Fig 13AB). Similar to the transient expression assays, only those lines with the S112A mutation
323 blocked the shift to slower mobility (Fig. 6B), suggesting that this residue is modified in response to ABA
324 treatment. Phos-tag gel analysis showed that the ABA-induced shift in mobility correlated with S112-
325 dependent changes in phosphorylation (Supp Fig 12C), but surprisingly, "phosphomimetic" Asp
326 substitutions at S112, S221, and T319 ("3xD") did not prevent phosphorylation of this fusion. A slight
327 mobility shift of the YFP-AFP2-BC domain fusion was also seen in response to salinity stress imposed by at
328 least 100 mM NaCl (Fig.6C).

329 Although transiently expressed full-length YFP-AFP2 fusions showed no difference in phosphorylation
330 between control and ABA treatments, there was generally a higher degree of phosphorylation in proteins
331 with more ala substitutions, again consistent with modifications at novel sites (Fig.7A). In contrast,
332 transgenic lines carrying the full-length YFP-AFP2 fusion showed an ABA-induced shift toward slower
333 mobility/greater phosphorylation of the fusion (Fig.7B). The stable transgenic lines with (S85,S112)A
334 substitutions showed no change in fusion mobility in response to ABA, whereas the phosphomimic
335 mutations (S85,S112)E displayed a shift toward slower mobility on control media.
336

337 Comparison of transcript levels for wild-type vs. mutant fusions in tissue harvested in parallel to that used
338 for protein extracts showed that levels were somewhat variable for all constructs, as expected for a
339 transient system, but the reductions in protein levels of the mutant forms were far greater than any
340 changes in transcript levels (Supp Fig 14). Although some transiently expressed transgene transcripts
341 were two- to three-fold lower for the mutant constructs, this was not sufficient to explain the at least
342 ten-fold decreases in YFP-AFP2-AB protein or the five- to ten-fold decreases in YFP-AFP2-BC protein
343 fusions (Supp. Fig. 14C). Stable transformants carrying the (S221,T319)A mutant YFP-AFP2-BC fusion also
344 showed at least five-fold less protein despite a similar transcript level as the wild-type fusion. Similarly,
345 the YFP-AFP2-BC(S112A) mutant form showed a roughly four-fold reduction in protein:transcript in stable
346 transformants (Supp. Fig. 14E). All of these results are consistent with possible defects in stability or
347 translation of the fusions. Protein levels were greatly reduced for full-length YFP-AFP2 fusions with ala
348 substitutions in stable transgenic lines, but transcript levels were similar for wild type and the
349 (S85,S112)A variant (Fig. 7).
350
351 **Effects of phosphorylation on AFP2 stability**
352
353 To further address the functional relevance of these differences in phosphorylation, we tested stability
354 and potential proteasomal degradation by assaying accumulation following treatment with either the
355 translation inhibitor cycloheximide (CHX) or the proteasome inhibitor MG132. In transient expression
356 assays, the higher mobility form of the AB domain decreased from roughly 58% in control conditions to
357 50% of the total in CHX, but the high mobility form was stabilized by MG132 (Fig.6D), consistent with
358 proteasomal degradation of the high mobility/unphosphorylated form. Accumulation of the low mobility
359 form was still seen in the T76A mutant, but was reduced in all the mutant fusions affecting SnRK2
360 targets: S85A, S112A, (S85,S112)A and the (T76,S85,S112)A triple mutant, consistent with a role for
361 SnRK2-mediated phosphorylation in regulating protein stability. The S85A mutant appeared to have an
362 even higher mobility than the wild-type fusion forms (Fig.5H,6D).
363
364 The YFP-AFP2-BC domain fusions were tested in both transient and stably transformed tissue. All stable
365 transformants showed reduced fusion accumulation following CHX treatment and most increased
366 accumulation in MG132-treated seedlings (Fig. 6E,F). The fusion combining S221A and T319A mutations
367 had severely decreased accumulation in both stable and transiently transformed tissue (Fig. 6E,F and
368 Supp.Fig. 14DE). ABA treatment primarily stabilized accumulation of the phosphorylated form (Fig 6G).
369 Although the double mutant proteins were stabilized by MG132 treatment, this treatment was not

370 sufficient to increase accumulation of the (S112, S221, T319)A (3xA) mutant in transiently transformed
371 tissue (Supp.Fig. 15). Furthermore, the limited YFP-AFP2- BC(3xA) fusion visible was present in only a
372 small fraction of cells, mostly in small punctae throughout the cytoplasm, not concentrated in the nuclei
373 as for all other YFP-AFP2 fusion constructs (Supp. Fig. 15C).
374
375 In stable transformants with full-length wild-type YFP-AFP2, the phosphorylated form was more stable
376 than the faster-migrating form (Fig.7C). Consistent with this, lines with either alanine or phosphomimetic
377 substitutions affecting S112 have substantially lower fusion protein levels, despite transcript levels that
378 are similar or higher than those for the wild-type fusion (Fig. 7CF). All of these full-length YFP-AFP2
379 fusions are proteasomally degraded, but the effects of CHX and MG132 are more limited for those with
380 ala substitutions (Fig. 7CE, Supp. Fig. 17F). In contrast, the only stable lines expressing the (S221,T319)A
381 variant had extremely low fusion protein accumulation, which was not increased by MG132 treatment
382 (Fig.7D) and reflected very low transcript levels (less than 0.1% of that for the wild-type fusion
383 transcript).
384
385 **Effects of phosphorylation on AFP2 localization**
386
387 Having observed that co-expression of either nYFP-AFP fusions with cYFP-AHG1 or YFP-AFP2 with Myc-
388 AHG1 led to formation of nuclear punctae we tested whether mutations preventing phosphorylation
389 would lead to similar changes in localization in transient expression assays. Whereas full-length YFP-AFP2
390 fusions appear mostly diffuse through nuclei, but generally excluded from nucleoli, YFP-AFP2-AB domain
391 fusions display as dense bundles of foci (Fig. 8). YFP-AFP2-AB(S112A) and (3xA) mutants appear to form
392 fewer foci. Although not uniform across the leaf, the two double mutants of the YFP-AFP2-BC domain
393 fusions tend toward more discrete areas of accumulation, appearing either more excluded from some
394 regions (S112A,S259A) or more focused in a few foci (S221A,T319A), consistent with effects of
395 phosphorylation state on changes in aggregation state.
396
397 Full-length YFP-AFP2 fusions with ala substitutions in S85,S112, and S259 are generally diffuse in the
398 nuclei, but occasionally form condensates. Similar to their effects on the BC domain, the full-length
399 (S221,T319)A mutants are also diffuse with occasional foci within nuclei, but become more diffuse when
400 coexpressed with SnRK2.3. Combining the (S85,S112,S221,T319)A mutations in a full-length protein
401 results in many dispersed nuclear foci and some punctae at the cell periphery. Fusions with ala
402 substitutions in T76 alone are sufficient to produce multiple nuclear foci, but become diffuse when co-

403 expressed with SnRK2.3. Combinations including T76A and ala substitutions in SnRK2 targets produce
404 many nuclear foci, whether or not SnRK2.3 is co-expressed.
405
406 Complexes of signaling proteins may be scaffolded by 14-3-3 proteins such as the GRFs, which recognize
407 phosphorylation in several consensus motifs. The S85 and S112 residues of AFP2 are both SnRK2 target
408 sites and predicted binding sites for 14-3-3 proteins. Similar to the yeast two-hybrid result, comparison of
409 BiFC assays with GRF4 and either wild type AFP2 or a (S85,S112)A mutant show greatly reduced
410 interactions with the mutant (Fig. 8). However, GRF4 still interacts with the S112A mutant of the AFP2-BC
411 domain, consistent with the potential for additional 14-3-3 binding sites in this domain. Unlike the
412 nuclear interactions with AFP2, GRF4 dimers are primarily cytoplasmic.
413
414 **Effects of AFP2 phosphorylation on ABA sensitivity of germination**
415
416 We previously showed that overexpression of YFP fusions to either full-length AFPs or just the BC
417 domains were sufficient to confer resistance to ABA inhibition of germination in transgenic Arabidopsis,
418 but AB-domain fusions had almost no effect (Lynch et al., 2017). The full-length AFP2 fusions conferred up
419 to 100-fold reductions in ABA sensitivity and produced desiccation intolerant seeds, while the AFP2-BC
420 domain fusions conferred up to 30-fold reductions in ABA sensitivity and did not impair seed viability.
421 Arabidopsis carrying transgenes with mutations either blocking phosphorylation or creating
422 phosphomimetics in the SnRK2 target sites were tested for effects on ABA sensitivity of germination.
423
424 Although overexpression of full-length AFP2 with a variety of mutations permitted germination on up to
425 50 µM ABA, lines carrying phosphomimetic (S85,S112)E or non-phosphorylatable (S85,S112)A mutant
426 YFP-AFP2 fusions differed from those with the wild-type fusion in that seedling greening was still greatly
427 impaired by any ABA (Fig. 9AB and Supp Fig 16). Transgenic seeds overexpressing YFP-AFP2 with
428 mutations in the C domain sites (S221,T319)A differed from those affecting the SnRK2 targets in that they
429 were not able to germinate on media with ABA exceeding 3 uM, but greening was not impaired by this
430 lower concentration of ABA (Fig. 9AB). In contrast, transgenic seeds overexpressing YFP-AFP2 combining
431 all of these ala substitutions (S85,S112,S221,T319)A blocked seed maturation, resulting in production of
432 green seeds lacking desiccation tolerance (Supp. Fig.17AB). ABA sensitivity of germination of seeds
433 expressing this quadruple mutant protein was tested by removing maturing seeds from developing
434 siliques. Although also able to germinate on at least 50 uM ABA, subsequent seedling development was
435 severely impaired even in the absence of ABA (Supp. Fig.17CDE). The relatively weak ABA resistance of

436 transgenic lines with the (S221,T319)A variant reflected the low level of fusion protein (Fig.7 and Supp.
437 Fig. 17G). In contrast, the (S85,S112,S221,T319)A mutant constructs produced similar levels of fusion
438 protein as the wild-type construct in seeds, and were highly effective in blocking ABA response, but the
439 mutant protein was not maintained during seedling growth (Supp. Fig. 17EFG).
440
441 The poor viability of seeds and seedlings expressing the full- length YFP-AFP2 resulted in partial silencing
442 of these transgenes over generations, and led us to focus on AFP2-BC domain fusions for additional
443 mutant analyses. When overexpressed in a wild-type background, all YFP-AFP2-BC domain fusions
444 conferred similar resistance (Fig. 9C). The well-expressed transgenes from the wild-type background were
445 backcrossed into the *afp2* mutant to create isogenic lines with similar transgene expression levels (Supp
446 Fig. 13C), resulting in similar resistance to ABA as seen in the wild-type background up to 10 µM ABA (Fig.
447 9D). However, the mutants with alterations in the residues predicted to be phosphorylated by MPKs were
448 less effective than the wild-type fusion in permitting germination on ABA higher than 30 µM in this
449 background (Fig. 9D). Comparison of protein levels showed that only the (S221,T319)A mutant had
450 reduced fusion protein accumulation, but accumulation could be increased by MG132 treatment (Fig.6E).
451 Germination *sensu stricto* is defined as complete when the radicle emerges from the seed coat, and is
452 usually followed by cotyledon greening during seedling establishment in the light. However, some ABA
453 resistant lines including *abi5* mutants and AFP over-expressors often reverse this order when
454 germinating in the presence of ABA, such that their cotyledons turn green prior to radicle emergence.
455 Consequently, at the higher ABA concentrations, the fraction of seeds that have turned green may be
456 higher than the fraction that has completed germination (Fig. 9EF). This was especially true for seeds
457 expressing the wild-type and S112A mutants of the YFP-AFP2-BC fusion in the *afp2* mutant background.
458 In contrast, the (S221,T319)A mutant was less effective than the other constructs in reducing ABA
459 sensitivity in the *afp2* background and severely delayed greening when germinating on ABA.
460
461 **Effects of AFP2 phosphorylation on seed maturation**
462
463 In addition to decreasing ABA sensitivity at germination, AFP2 overexpression inhibits various aspects of
464 seed maturation including accumulation of storage proteins (e.g. cruciferins) and some late
465 embryogenesis abundant (LEA) proteins (Lynch et al., 2022). To determine whether the phosphorylation
466 state of AFP2 was important for this regulation, we compared storage protein accumulation in wild-type
467 vs transgenic seeds with either wild-type or mutant AFP2 fusions. Surprisingly, even though most
468 mutants were less effective than wild-type AFP2 for conferring ABA resistance, only the mutant forms

469 with substitutions in multiple target residues resulted in a decrease in storage protein accumulation (Fig.
470 10, Supp. Fig.17H). The most dramatic reductions in cruciferin accumulation were seen in seeds
471 producing the AFP2 quadruple mutant (S85,S112,S221,T319)A (Supp. Fig. 17H).
472
473 The two BC domain mutant fusions producing the greatest reduction of storage protein accumulation
474 ((S112,S259)A and "3xD") had similar effects on ABA sensitivity of germination and seedling
475 establishment (Figs. 9,10 and Supp Fig 16). However, they differ in that the (S112,S259)A mutations also
476 adversely affect seed longevity, resulting in decreased viability within 4 months and complete lethality
477 by 6 months (Fig. 10, Supp. Fig 18). It is noteworthy that the (S112,S259)A mutant form of AFP2-BC
478 accumulates to higher levels in seeds than the wild-type construct (Fig.10), suggesting that this form
479 might have greater effects on disrupting seed maturation, but this difference fades away during seedling
480 growth (Supp Fig 19).
481
482 Examination of multiple ages of seed lots producing different AFP2-BC fusion variants showed that the
483 major differences in storage protein levels reflected loss during aging (Supp Fig 18). Furthermore, this
484 was not directly related to the level of ABI5 accumulation in that lines with very little storage protein still
485 had ample ABI5. ABI5 is activated by phosphorylation and already appears as a triplet in dry seeds of all
486 genotypes, but shifts to a more highly phosphorylated state when incubated on ABA (Supp Fig 19).
487
488 **DISCUSSION**
489
490 **Post-translational modification of ABA core signaling components**
491
492 The core signalosomes of ABA signaling comprise the PYR/PYL/RCAR receptors, clade A PP2C protein
493 phosphatases, and SnRK2 kinases (reviewed in Lim et al., 2022; Née and Krüger, 2023). Each of these
494 components is encoded by a multigene family that is differentially expressed, with different interaction
495 characteristics and ABA sensitivities, creating the potential for a range of responses at different ABA
496 concentrations in different tissues (Tischer et al., 2017). In the canonical view, ABA bridges the receptors
497 with PP2Cs, effectively inactivating the PP2Cs and releasing the SnRK2s to become phosphorylated and
498 active. When active, the SnRK2 kinases regulate the activity of many effector proteins, including the
499 ABI5/ABF/AREB clade of bZIP transcription factors and ion channels. However, AHG1 differs from the
500 other clade A PP2Cs in that it does not bind to the active sites of group 3 SnRK2s, interacts with only a
501 subset of receptors and requires high ABA concentrations to do so (Tischer et al., 2017; Krüger et al.,

502 2024). In addition to this central de-repression mechanism for activating ABA response by
503 phosphorylation of effectors, all signalosome components are also subject to post-translational
504 modifications including phosphorylation and ubiquitination. Both of these modifications may be either
505 activating or inhibitory, depending on the target protein residues and the specific kinases or E3 ligases
506 involved (reviewed in Lim et al., 2022).
507
508 Activity and stability of the ABI5/ABF/ABRE clade of bZIP transcription factors is also regulated by a
509 variety of post-translational modifications including phosphorylation, ubiquitination, sumoylation, and S-
510 nitrosylation (reviewed in Yu et al., 2015). Multiple kinases, including SnRK2s, CBL-interacting protein
511 kinase (CIPK)26, SOS2-like protein kinase 5 (PKS5), BRASSINOSTEROID INSENSITIVE(BIN)2, and MPK3,
512 phosphorylate overlapping and discrete subsets of amino acid residues within ABI5 (Wei et al., 2022;
513 Lyzenga et al., 2013; Zhou et al., 2015; Bhagat et al., 2021). Our immunoblots detected multiple forms of
514 ABI5 in dry seeds and seeds germinating in the presence of ABA, but it is currently not clear which
515 modifications are present on these ABI5 proteins.

516 The AFPs interact with multiple members of this clade of bZIPs (Garcia et al., 2008) and AFP1 was initially
517 proposed to assist degradation of these bZIPs by promoting interactions with E3 ligases that ubiquitinate
518 ABI5 (Lopez-Molina et al., 2003). Although these proposed E3 ligase interactions appear weak at most
519 (Lynch et al., 2022), subsequent studies including the present one have expanded the list of AFP
520 interactors to include proteins representing all elements of the ABA signalosome, some MPKs, several
521 14-3-3 proteins, the DELLA repressors of GA signaling (Finkelstein and Lynch, 2022), the flowering
522 regulator CONSTANS (Chang et al., 2019), WRKY36 and AHG1 in dormancy regulation (Deng et al., 2023;
523 Krüger et al., 2024), several chromatin modifying factors (Pauwels et al., 2010; Lynch et al., 2017), and
524 the protein kinase SALT OVERLY SENSITIVE(SOS)2 in regulating germination under salt stress (Wang et al.,
525 2024). This extensive list of interactions is consistent with a role for AFPs as signaling hubs in a variety of
526 processes, but raises the question of how specificity is achieved. Some of the likely options are regulated
527 expression affecting availability of these proteins in different organs or stages of growth, and changes in
528 phosphorylation state or other post-translational modifications leading to changes in structure of the
529 disordered regions.
530
531 **Kinases regulating ABA response target AFPs**
532
533 The kinase families most highly associated with ABA or osmotic stress signaling are the SnRK2 kinases
534 acting in the ABA core signalosome, SnRK3/CBL interacting kinases (CIPKs), MAP kinases and calcium-

535 dependent protein kinases (CDPKs). Many proteins can be phosphorylated at multiple sites, by multiple
536 kinases, and the different sites may be phosphorylated sequentially with initial modifications altering the
537 efficiency of subsequent events (reviewed in Miller and Turk, 2018). For example, mammalian GSK3
538 kinases often require "priming" by phosphorylation at a residue 4 or 5 amino acids C-terminal to the
539 target (Sutherland, 2011). Furthermore, modifications at different sites may have opposing effects on
540 activity of the substrate.
541
542 We focused on specific SnRK2s and MAP kinases that interacted with AFP1 and/or AFP2 in yeast two-
543 hybrid and/or BiFC assays, using *in vitro* kinase assays and co-expression to test for altered mobility on
544 SDS-PAGE and Phos-tag gels. Mass spectrometric analysis identified Ser-112 of AFP2 as the sole residue
545 phosphorylated by SnRK2.6, consistent with results reported for a phosphorylated site conserved in all
546 four AFPs (Krüger et al., 2024). Mutagenesis converting this residue to either alanine or a
547 phosphomimetic amino acid reduced, but did not eliminate, phosphorylation of the AFP2-AB domain.
548 This indicated that SnRK2.6 could phosphorylate additional residues, albeit not efficiently enough to be
549 detected by mass spectrometry. Mutagenesis converting an additional predicted SnRK2 target, Ser-85, to
550 alanine eliminated phosphorylation of the AFP2-AB domain. In contrast, combining the S112A mutation
551 with alanine substitution of Ser-259, the residue with the next highest match to the SnRK2 consensus
552 target in the AFP2-BC domain, was not sufficient to eliminate phosphorylation of this domain *in vitro*, but
553 did block ABA-induced changes in mobility of the YFP-AFP2-BC fusion in stable transgenic plants.
554 Mutations affecting predicted MAP kinase target residues did not block ABA-induced changes in mobility
555 of protein fusions, but severely reduced stability and consequently accumulation of these proteins.
556 Surprisingly, transient expression of full-length AFP2 fusions containing alanine substitutions at multiple
557 documented or predicted kinase targets produced even more distinct phosphorylated products than the
558 wild-type fusion. These mutant fusion proteins in stable transgenics were barely detectable, but some
559 were slightly stabilized by inhibiting proteasomal degradation.
560
561 **AFPs can form biomolecular condensates**
562
563 Predictions of AFP structures show a series of likely protein binding regions separated by intrinsically
564 disordered regions (Lynch et al., 2017) and the AFPs have been reported to interact with diverse
565 proteins. The structure predicted by AlphaFold for the AFP2 monomer shows most of the predicted
566 SnRK2 and MAPK phosphorylation sites in regions predicted to be disordered (Supp. Fig.1). Only T319 is
567 predicted with high confidence to be at the junction between beta-sheet and helical regions, while T76

568 and S112 are predicted to be near regions that might form helices. Our interaction data show that AFP2
569 forms dimers requiring regions in both the AB domain and the full-length protein (Supp. Fig.7). When
570 modeled as a dimer, the relatively structured regions of the B domain (aa 115-143) and the C domain (aa
571 281-326) of distinct chains are in proximity, and T76 is predicted to be in a fully unstructured region. The
572 AB domain does not dimerize and is predicted to have all potential phosphorylation sites in disordered
573 regions. Substrates are often bound to the kinase active site in an extended conformation (reviewed in
574 (Miller and Turk, 2018) and these structural predictions are consistent with the observation that the AB
575 domain is more accessible to SnRK2s than full-length AFP2.
576
577 Intrinsically disordered regions are recognized as drivers of biomolecular condensate formation, often
578 through multivalent interactions, i.e. with multiple other molecules (Emenecker et al., 2021). Post-
579 translational modifications such as phosphorylation alter the charge distribution, and consequently the
580 potential for interactions leading to condensate formation. Modeling possible effects of modification at
581 the potential target residues tested in our mutant constructs showed limited impact of phosphorylation
582 at either the two primary SnRK2 targets (S85 and S112) or the predicted MPK targets (S221 and T319),
583 but additional phosphorylation of T76 or S259 was predicted to promote helix formation across much of
584 the unstructured regions (Supp. Fig. 20). Further phosphorylation at additional target residues is
585 predicted to give the AFP2 dimer even more structure, albeit with low confidence. In contrast, the ala
586 substitutions tested in this study are predicted to maintain the dimer in a largely disordered state, such
587 that additional residues might be accessible to additional kinases.
588
589 Initial descriptions of the AFPs showed a variety of localization patterns, depending on the experimental
590 conditions. Transient over-expression of AFP(1)::CFP in either onion epidermal cells or Arabidopsis
591 seedlings treated with ABA produced diffuse nuclear localization, but co-bombardment with 35S::ABI5
592 resulted in co-localization in nuclear bodies (Lopez-Molina et al., 2003). Stable expression of
593 *AFP2pro:AFP2:GFP* in an *afp2* mutant background was also primarily nuclear, but excluded from nucleoli,
594 in ABA- or NaCl-treated seedlings (Garcia et al., 2008). These conditions enhanced accumulation of both
595 AFP2 and ABI5, but did not result in restriction to nuclear bodies, consistent with diffuse nuclear
596 localization of AFPs likely to be in a phosphorylated state due to ABA or stress exposure. However, within
597 7 hrs of removal from these stress treatments AFP2:GFP was no longer visible in the nuclei, but still
598 detected by immunoblot. In addition, some punctate fluorescence was visible in the cytoplasms of a few
599 cells near the root meristem. Subsequent studies of interactions between AFPs and ABI5/ABF proteins by
600 split YFP BiFC assays using transient over-expression in *N. benthamiana* also showed nuclear localization,

601 but no foci (Lynch et al., 2017).
602
603 In the current BiFC assays, we found that co-expression of AFPs with kinases revealed interactions in
604 nuclei, but excluded from nucleoli, whereas co-expression with PP2Cs resulted in formation of nuclear
605 bodies over a broad range of sizes (Fig.4), suggesting that dephosphorylated AFPs were more prone to
606 form condensates. However, YFP-AFP2 co-expressed with cYFP-GRF4 also formed numerous small
607 nuclear condensates, consistent with interactions dependent on phosphorylation. In an effort to
608 determine which residues were most important for regulating condensate formation, we tested
609 localization of YFP-AFP fusions with alanine substitutions at known or predicted phosphorylation sites.
610 Surprisingly, the wild-type YFP-AFP2-AB domain fusion formed clusters of nuclear bodies, similar to the
611 "grapebunch-like" condensates observed for ARF proteins (Powers et al., 2019), but the alanine-
612 substituted mutant AFP2-AB domain fusions formed fewer clusters. This might reflect formation of
613 complexes by phosphorylation-dependent interactions with 14-3-3 proteins that are reduced in the
614 mutants. In contrast, the wild-type YFP-AFP2-BC fusion was mostly diffuse, but YFP-AFP2-BC fusions with
615 mutations preventing phosphorylation of the predicted kinase target residues were more likely to form
616 condensates, sometimes with small internal areas of exclusion (donut-shaped). When co-expressed with
617 the tagged PP2C phosphatase Myc-AHG1, full-length AFP2 formed punctae whether or not the SnRK2 or
618 GRF target residues could be phosphorylated. The AFP2-AB domain also continued to form punctae
619 when co- expressed with AHG1, but fewer punctae formed when AHG1 and the AFP2-BC domain were
620 co- expressed. In combination with the previously described diffuse nuclear localization in ABA-treated
621 roots, this suggests that condensate formation is negatively correlated with ABA-induced
622 phosphorylation.
623
624 **Physiological significance of AFP phosphorylation state**
625
626 The AFPs have recently been reported to function as a downstream element of DOG1 control of
627 dormancy. Proteomic and genetic studies showed that DOG1 maintains dormancy by repressing AHG1
628 and AHG3 activity (Krüger et al., 2024). In non-dormant or *dog1* mutant seeds AHG1 dephosphorylates
629 AFP2 at S112 and AFP1 at the corresponding conserved serine, allowing the AFPs to function as
630 repressors of ABA response, resulting in germination. These results are consistent with our observation
631 that ABA promotes a shift to the phosphorylated state, whereas co-expression with AHG1 has the
632 opposite effect. Our studies used a gain of function approach, such that overexpression of the AFP
633 domains and mutant forms leads to ABA resistance if the AFPs are physiologically active.

634

635 Functional tests of the physiological significance of these phosphorylation options focused on effects on
636 ABA sensitivity of germination, cotyledon greening, storage protein accumulation, and seed longevity. We
637 previously reported that overexpression of YFP-AFP2 could reduce ABA sensitivity nearly 100-fold and
638 was so extreme in a wild-type background that homozygous transgenic lines failed to complete seed
639 maturation and become desiccation tolerant (Lynch et al., 2017). Overexpression of the quadruple
640 mutant (S85A,S112A,S221A,T319A), even though present at barely detectable levels, had a more extreme
641 effect, also blocking maturation of heterozygous seeds. Homozygous YFP-AFP2 transgenes are tolerated
642 in an *afp2* mutant background, where the total AFP2 concentration is lower, and YFP-AFP2-BC domain
643 fusions are sufficient to reduce sensitivity only 30- to 50-fold, also resulting in viable seeds. The reduced
644 impact of the truncated protein might reflect the loss of the EAR domain, and therefore interactions with
645 TPL/TPR co-repressors. However, these fusions could still inhibit ABI5 and related AREB/ABF clade
646 transcription factors via interactions with their C domains (Garcia et al., 2008). Further truncation of
647 AFP2, removing the B domain, results in much weaker reduction of ABA inhibited germination (Lynch et
648 al., 2017). Surprisingly, removal of the unstructured region between the B and C domains to produce the
649 "LITTLE NINJA" microprotein creates a dominant negative effect on jasmonic acid signaling resulting in
650 stunted growth, but this construct was not tested for effects on ABA sensitivity (Hong et al., 2020).

651 Comparison of endogenous AFP and ABI5 levels over a range of ABA concentrations showed that ABI5 is
652 usually in excess post-stratification, ranging from 8-10 fold higher than AFP1/2 when exposed to 1 µM
653 ABA, but increasing to as much as 30 fold higher after 5d post-stratification on media containing 10 µM
654 ABA (Garcia et al., 2008). Extended incubation on the higher ABA concentrations led to accumulation of
655 more AFP protein, effectively reducing the ABI5/AFP ratio, which was accompanied by increased
656 germination. If this ratio is a sensor of physiological state that regulates germination, the severe
657 disruption of the ratio by the AFP over-expression approach might be acting by titrating their interacting
658 factors.
659

660 Mutations of the BC domain fusions converting only the SnRK2 targets, S112 or both S112 and S259, to
661 alanine had minimal effect on ABA sensitivity of germination. However, the double mutant substantially
662 reduced seed longevity. In contrast, mutants preventing phosphorylation of both predicted MPK target
663 residues, S221 and T319, were less effective than the wild-type BC domain in conferring ABA resistance
664 to concentrations higher than 10 µM ABA. This might reflect the reduced accumulation of this mutant
665 form due at least in part to its reduced stability. Overexpression of phosphomimetic mutants did not

666 confer greater ABA resistance than provided by the wild-type YFP-AFP2-BC. Although the mutants with
667 the strongest effects on ABA sensitivity ((S112,S259)A and 3xD) had cruciferin levels similar to wild-type
668 seeds when fresh, they showed accelerated loss of these storage proteins during shelf storage.
669 Cruciferins have been found to serve as protectants from oxidative stress leading to seed deterioration
670 during ageing (Nguyen et al., 2015), but the 3xD mutants remained viable despite a massive loss of
671 cruciferins within a year, suggesting that they rely on alternative protectants. A more detailed
672 comparison of the proteomes or metabolomes of these mutants might identify components critical for
673 seed longevity.
674
675 Although phosphomimetic substitutions are often used to simulate phosphorylated forms of proteins,
676 they frequently do not confer the expected activities, especially if the phosphorylation is a binding site
677 for an adaptor protein, e.g. 14-3-3 proteins (Kozeleková et al., 2022; Dephoure et al., 2013).
678 Consequently, it is not surprising that the alanine and aspartic acid substitutions have some similar
679 effects since both types of mutations prevent true phosphorylation. Given that AFP2 phosphorylation is
680 required to interact with the 14-3-3 proteins, this might represent a sequestered state induced by ABA,
681 maintaining ABI5 and other downstream signaling factors in an active state. As ABA levels decrease post-
682 stratification, increased activity of the AHG PP2Cs could release the AFPs from complexes with the 14-3-
683 3 proteins, permitting more inhibitory interactions with ABI5/ABFs/AREBs.
684
685 Finally, what is the physiological significance of these condensates? In other well-characterized plant
686 systems, condensates include miRNA processing bodies (Xie et al., 2021), light response complexes
687 regulating translation (Jang et al., 2019), high temperature-induced de-repression of gene expression
688 (Bohn et al., 2024), sensors of hydration regulating germination (Dorone et al., 2021), and cytoplasmic
689 sequestering of inactive transcription factors (Powers et al., 2019). Thus, they may represent complexes
690 required for activity or inactivity of the relevant proteins. In the current work, all AFPs or AFP domains
691 tested were present as overexpressed fusions to all or part of YFP. A trivial explanation is that at least
692 some of these simply reflect high protein concentrations produced by over-expression in transient
693 systems. However, some fusions formed foci despite accumulating to barely detectable levels, different
694 mutations or co-expression conditions led to different localizations, and the BiFC studies permit
695 visualization of only the fusion pairs being tested. As discussed above, the AFPs interact with many
696 different proteins and are likely to be modified at additional sites by kinases not yet tested.
697 Consequently, it is possible that these AFPs, and their variants created by distinct post- translational
698 modifications, are present in diverse complexes with different functions, i.e. acting as signaling hubs.

699

700 **Materials and Methods**

701

702 **Plant Materials and Transgenes**

703

704 Split YFP fusions for MPKs, GRFs and PYLs were constructed using the Gateway compatible pSITE-nEYFP-
705 C1 (GenBank Acc# GU734651) and pSITE-cEYFP-C1 (Acc# GU734652) vectors and PCR products with attL
706 ends added as described in (Fu et al., 2008), following manufacturer's instructions for LR Clonase
707 reactions (Invitrogen). The *35S::YFP:AFP2* fusion in pEarleyGate104 (Earley et al., 2006) and split YFP
708 fusions for AFP1 (AT1G69260) and AFP2 (AT1G13740) were also constructed by LR Clonase
709 recombinations, as described in (Lynch et al., 2017). The split YFP fusions for SnRK2s and AHGs were
710 described in (Lynch et al., 2012). The *35S::YFP:AFP2* fusion lines in the wild-type (Col-0) and *afp2-1*
711 (SALK_131676) (Alonso et al., 2003) mutant backgrounds were lines #4A2 and H1, respectively,
712 reported in (Lynch et al., 2017). All genes included in this study are listed in Supp. Table 1. Mutations
713 affecting potential phosphorylation sites were created by PCR using the high-fidelity polymerase ExTaq
714 (TaKaRa Bio) and primers shown in Supp. Table 2, designed using PrimerX
715 (https://www.bioinformatics.org/primerx/documentation.html), with plasmids encoding cDNAs for full-
716 length AFP2 or specific subdomains as templates. The AFP2-AB domain includes aa 1-149 and the AFP2-
717 BC domain includes aa 94-348. For multi-site mutations, fragments overlapping at the mutation sites
718 were amplified, then annealed and amplified by attL primers at the end points to create Gateway-
719 compatible fragments.

720

721 Arabidopsis plants were grown in pots in growth chambers under continuous light at 22°C.
722 *Agrobacterium tumefaciens*-mediated direct transformation of constructs with mutations in potentially
723 phosphorylated residues was performed by the floral dip method (Clough and Bent, 1998), followed by
724 selection of BASTA-resistant seedlings on Germination Medium (GM: 0.5x MS salts and vitamins, 1%
725 sucrose) supplemented with 8 µg/mL BASTA ("Finale", AgrEvo Environmental Health). Homozygous
726 lines were identified by production of 100% BASTA-resistant progeny. Following crosses between
727 *35S:YFP:AFP2-BC* fusion lines and *afp2-1* mutants, YFP-AFP2-BC overexpressing progeny were selected
728 by BASTA resistance and homozygous *afp2-1* segregants were identified by PCR-based genotyping, as
729 described at http://signal.salk.edu/tdnaprimers.2.html.

730

731 **Yeast Two-Hybrid Constructs and Assays**

732

733 Fusions between the GAL4 activation domain (AD) and full-length PP2C cDNAs were described in (Lynch
734 et al., 2012). Fusions between the AD domain and full-length and partial AFP cDNAs were described in
735 (Lynch et al., 2017). Fusions between the AD domain and 14-3-3 cDNAs were constructed by CRE-lox
736 recombination between pUNI clones and the pACT2-lox vector (Liu et al., 1998). Fusions between the
737 GAL4 DNA binding domain (BD) and either AFP or PYL cDNAs were constructed using the pGBKT7-DEST
738 vector (Lu et al., 2010) and PCR products with attL ends. BD fusions with SnRK2.2, 2.3 and MPK6 were
739 constructed by CRE-lox recombination using the pAS2lox vector and by LR Clonase reactions with the
740 pGBKT7-DEST vector and pDONR clones for SnRK2.6, SnRK2.10, and MPK3.
741

742 BD fusions were transformed into yeast line PJ69-4A selecting for growth on yeast synthetic medium
743 (YSM) without trp. AD fusions were transformed into Y187, selecting for growth on YSM without leu.
744 Interactions were tested by matings between pairs of lines carrying BD- and AD-fusions; following
745 overnight incubation on YPD plates, matings were replica plated to YSM lacking leu and trp to select for
746 diploids or YSM also missing histidine (his) and, in some cases, adenine to screen for diploids that had
747 activated the HIS3 and ADE2 reporter genes. Diploids carrying BD-PYLs and AD vector or AD-AFPs were
748 grown in YSM lacking leu and trp, then diluted to an OD600 of 0.9, before making serial 10-fold dilutions
749 that were spotted in replicates on YSM lacking lacking leu and trp, or also lacking his. Diploids combining
750 BD-AFPs with AD vector or AD-GRFs were also analyzed by growth assays with serially diluted cultures.
751

752 **Plant growth conditions**

753

754 Germination assays testing ABA sensitivity of age-matched seeds were performed on minimal nutrient
755 media supplemented with ABA at concentrations over the range from 0- 50 µM, as described in (Lynch
756 et al., 2017). Accumulation of fusion proteins was assayed by immunoblots of seeds or seedlings
757 harvested after 5d incubation on Germination Medium (GM: 0.5x MS salts and vitamins, 1% sucrose) or
758 minimal media solidified with 0.7% agar, then subjected to ABA at the indicated concentrations, or 100
759 µM cycloheximide (CHX) (Acros Organics, #357420010) or MG132 (UBPBio, # F1101) for the indicated
760 times.
761

762 For transient expression *Agrobacterium* lines expressing fusion proteins were combined with GV3101
763 expressing the P19 protein of tomato bushy stunt virus to enhance transient expression, as described in
764 (Voinnet et al., 2003). Cultures of all bacteria to be used in infiltration were grown overnight in YEP media
765 with appropriate selective antibiotics, diluted to an OD_{600} of 1.0 in 10 mM $MgCl_2$, 10 mM MES pH 5.6, 0.2

766 mM acetosyringone (Aldrich #D134406) and rocked at room temperature for 2-3 hrs prior to mixing and
767 infiltration of leaves on 2-3 week old *Nicotiana benthamiana* plants. For BiFC assays, Agrobacteria
768 expressing cYFP- and nYFP- fusions were combined just prior to infiltration. Fluorescence was scored 2-4
769 days later, using an Olympus AX70 microscope or a Leica SP8 Resonant Scanning Confocal microscope.
770 Confocal images were processed with Fiji (Image J) to produce maximum intensity Z-stack composites.
771
772 For stability assays of transiently transformed plants, infiltrated leaves were further infiltrated at 3d post-
773 Agrobacterium infiltration with GM supplemented with 100 µM cycloheximide (CHX) or MG132, or a
774 solvent control and incubated for 6 hrs prior to harvest.
775
776 **Immunoblots**
777 Arabidopsis seedlings or *N. benthamiana* leaf tissue were ground directly in 2x Laemmli loading buffer
778 (1.5-2 µL/mg FW), microfuged 10 min at 4°C to pellet debris, then the supernatants were boiled 5 min
779 prior to fractionation by SDS-PAGE or SuperSep™ Phos-tag™ PAGE (Fujifilm Wako Chemicals). Proteins
780 were transferred to nitrocellulose filters (Prometheus, Genesee Scientific, San Diego, CA) and stained
781 with Ponceau S, as described in (Lynch et al., 2017). Filters were blocked with Casein blocking buffer (LI-
782 COR Biosciences, Lincoln, NE), then co-incubated with anti-GFP mAb (1:10000, UBPBio, Aurora, CO)
783 and/or anti-actin mAb (A0480, Sigma) primary antibodies, followed by anti-mouse secondary IRDye 800
784 conjugated IgGs (LiCor, #926-32210), and visualized using the 800 channel of the Licor Odyssey Infrared
785 Imaging System. Mature dry Arabidopsis seeds were ground in 20 µL/mg FW 1x Laemmli loading buffer,
786 then processed as above. ABI5 was detected with anti-ABI5pAb (1:10000, Ab98831, AbCam) primary
787 antibodies, followed by anti-rabbit secondary IRDye 700 conjugated IgGs (LiCor #926-68071), and
788 visualized using the 700 channel of the Licor Odyssey Infrared Imaging System.
789
790 **Recombinant protein purification**
791
792 Fusions between His6-tags and full-length, partial and mutant AFP coding sequences were constructed by
793 CRE-lox recombination between pUNI cDNAs and the pHB3-His6 vector, as described in
794 http://signal.salk.edu/UPS_Protocols_Vectors.pdf. Primers used for subcloning and mutagenesis are
795 shown in Supplementary Table 1. Plasmids carrying fusion genes were transformed into *E.coli* BL21C+ and
796 expression was induced by growth overnight at 19-20oC in Overnight Express^{TM} Instant TB medium
797 (Novagen). Cells were harvested by microcentrifugation for 3 min at 16K rpm, resuspended in 140 µL
798 Lysis Buffer (8.3 M urea, 0.1 M NaPhosphate pH 8) per mL of initial culture. His6-fusions were affinity

799 purified in batch mode with HIS-select Nickel Affinity beads (Millipore P6611) according to the
800 manufacturer's protocol for denaturing conditions, eluting with 8 M urea, 0.1 M NaPhosphate pH 5.5.
801 The urea concentration was reduced ten-fold for use in kinase reactions.
802
803 GST fusions to full length SnRK2.6 also made use of the pUNI vector system, and induction overnight in
804 TB Express, but proteins were extracted under native conditions with CelLytic B in 1x PBS, 10 mM DTT, 83
805 units/mL Benzonase nuclease, 1 mM PMSF, 5 mg/mL lysozyme , followed by purification on glutathione-
806 agarose beads (UBP-Bio, P3060-10) and elution with 30 mM Tris pH9, 300 mM NaCl, 5 mM DTT, 0.5%
807 Triton-X100, 1 mM PMSF, 40 mM glutathione.
808
809 **In vitro kinase assays**
810
811 Purified GST-SnRK2.6 was activated by 1 hr pre-incubation in kinase buffer (25mM Tris pH 7.5, 12 mM
812 $MgCl_2$, 2 mM DTT) with 1 mM ATP, then combined with His-AFP fusions maintaining the buffer and ATP
813 concentrations for 1 additional hr of incubation. Phosphorylation was monitored in wild-type and mutant
814 constructs by incorporation of ^{32}P from gamma-labeled ATP (0.1-0.2 µCi/rxn) during the latter incubation.
815 SDS sample buffer was added to 1x final, samples were boiled 5 min., then fractionated on 13% SDS-
816 PAGE, dried and autoradiographed. Following assays with only cold ATP, gel slices containing lower
817 mobility products were excised and sent to UC Davis for mass spec analysis. Additional SnRK assays with
818 mutant AFP fusion proteins were analyzed by ProQ Diamond Phosphoprotein staining according to
819 manufacturer's instructions (Invitrogen).
820
821 **Mass Spectrometry**
822
823 Coomassie stained gel slices were processed with a standard washing, reduction/alkylation followed by
824 tryptic digestion, as described in <https://www.promega.com/-
825 /media/files/resources/protocols/technical-bulletins/101/proteasemax-surfactant-trypsin-enhancer.pdf>
826 The mass spectrometer used was a Xevo G2 QTof coupled to a nanoAcquity UPLC system (Waters,
827 Milford, MA). Samples were loaded onto a C18 Waters Trizaic nanotile of 85 um × 100 mm; 1.7 µm
828 (Waters, Milford, MA). The column temperature was set to 45°C with a flow rate of 0.45 mL/min. The
829 mobile phase consisted of A (water containing 0.1% formic acid) and B (acetonitrile containing 0.1%
830 formic acid). A linear gradient elution program was used: 0–40 min, 3–40 % (B); 40-42 min, 40–85 % (B);
831 42-46 min, 85 % (B); 46-48 min, 85-3 % (B); 48-60 min, 3% (B).

832

833 Mass spectrometry data were recorded for 60 minutes for each run and controlled by MassLynx 4.2
834 SCN990 (Waters, Milford, MA). Acquisition mode was set to positive polarity under resolution mode.
835 Mass range was set from 50 – 2000 Da. Capillary voltage was 3.5 kV, sampling cone at 25 V, and
836 extraction cone at 2.5 V. Source temperature was held at 110C. Cone gas was set to 25 L/h, nano flow
837 gas at 0.10 Bar, and desolvation gas at 1200 L/h. Leucine–enkephalin at 720 pmol/ul (Waters, Milford,
838 MA) was used as the lock mass ion at m/z 556.2771 and introduced at 1 uL/min at 45 second intervals
839 with a 3 scan average and mass window of +/- 0.5 Da. The MSe data were acquired using two scan
840 functions corresponding to low energy for function 1 and high energy for function 2. Function 1 had
841 collision energy at 6 V and function 2 had a collision energy ramp of 18 − 42 V.

842

843 Raw data was searched using Protein Lynx Global Server 3.0.3 Expression 2.0 (Waters, Milford,
844 Massachusetts). Processing parameters consisted of a low energy threshold set at 200.0 counts, an
845 elevated energy threshold set at 25.0 counts, and an intensity threshold set at 1500 counts. A dedicated
846 database was constructed containing common housekeeping proteins as well as the provided sequence
847 of the target protein. The database was randomized within PLGS. Possible structure modifications
848 included for consideration were methionine oxidation, carbamidomethylation of cysteine, deamidation
849 of asparagine or glutamine, dehydration of serine or threonine, and phosphorylation of serine, threonine,
850 or tyrosine.

851

852 **qRT-PCR analysis**

853

854 RNA was isolated from *N. benthamiana* leaf tissue or Arabidopsis seedlings as described in (Lynch et al.,
855 2017). DNA-free total RNA was prepared by incubation with RQ1 DNase (Promega) and RNAsin for 15
856 min. at room temperature, followed by inactivation of the DNase by addition of EGTA and incubation for
857 5 min. at 65°C, then clean-up over Qiagen RNeasy or Zymo-Clean columns according to manufacturers'
858 instructions. Approximately 0.5 µg of RNA was used as template for cDNA synthesis by MMLV reverse
859 transcriptase (Promega), using a 10:1 mix of random hexamers and oligo dT as primers. cDNA
860 concentrations were checked by qRT-PCR, using Forget-Me-Not master mix (Biotium) in an iQ5 or CFX
861 cycler (Bio-Rad), according to manufacturer's instructions. Primers used for normalizing were selected
862 for uniform expression in Arabidopsis seeds or young seedlings subjected to a variety of treatments:
863 AT5G46630 and At1g13320 (Czechowski et al., 2005) or a validated reference gene for *N. benthamiana*

(Pombo et al., 2019). Equal amounts of cDNA were used as templates for reactions with all other primer sets (listed in Supp. Table 1), quantified relative to a standard curve spanning the range of concentrations present in all genotypes of transgene expression.

Acknowledgements. We thank the ABRC team at Ohio State University for efficient distribution of vectors and cDNA clones, Armann Andaya at the UC Davis Campus Mass Spectrometry Facilities for MS analysis, Ben Lopez at UCSB for confocal microscopy, and Delaney O'Donnell for assistance with screening transgenic lines. This work was supported by a UCSB Academic Senate Grant to RRF, Faculty Research Assistance Program funds, and National Science Foundation Grant# IOS1558011 to RRF.

874 Table 1. AFP2 predicted phosphorylation sites.

Residue	NetPhos 2.0 score	PhosPhAt score	MUsite score	SnRK2 target	MPK target	in vitro phosphorylated
Y28	0.315	1.59				
S38	0.02	0.11	0.487			
T51	0.781	0.21	0.212			
T76	0.973	1.1	0.841		T-P	
S83	0.971		0.769			
S84	0.947		0.787			
S85	0.997	0.81	0.881	R-S-S-S		Yes
T89	0.014	0.84	0.292			
Y103	0.622	0.97				
T104	0.041	0.19	0.196			
T111	0.9		0.21			
S112	0.321	0.37	0.77	R-T-T-S		Yes!
S129	0.988		0.469			
S150	0.753	0.61	0.46	S-D		
T154	0.084	0.14	0.383			
S156	0.966	0.45	0.737			
T164	0.471	0.75	0.113			
S187	0.179	0.67	0.578	S-D		
T193	0.137	0.91	0.298			
S197	0.323	0.44	0.277	G-S?		
S198	0.725	0.52	0.227			
S199	0.063	0.21	0.154			
S200	0.992	0.65	0.539			
S202	0.996		0.274			
S213	0.572	0.03	0.249			
S215	0.916	0.8	0.402			
S221	0.772	1.13	0.654		S-P	
S232	0.844	0.46	0.47			
S234	0.745	0.56	0.536	G-S?		
T243	0.046	0.21	0.137			
S259	0.985	1.28	0.869	R-V-R-S		
S262	0.763	0.63	0.803			
S273	0.044	0.18	0.348			
S284	0.303	0.34	0.103			
Y299	0.137	0.46				
T319	0.94	0.27	0.247		T-P	
T343	0.689		0.173			

875 **Figure Legends**
876
877 Fig.1 Interactions between AFPs and PP2Cs detected by yeast two hybrid assays. Fusions were
878 combined by matings between Y187 carrying AD fusions and PJ69-4a carrying BD fusions. After
879 overnight incubation on YPD media, yeast were replica-plated onto selective media lacking leu and trp (-
880 LW) to maintain the AD- and BD- fusion plasmids, and lacking histidine and adenine (-HALW) to score
881 interactions between the fusion proteins.
882
883 Fig.2 Interactions between AFPs and kinases detected by yeast two hybrid assays. The indicated
884 fusions were combined and interactions were scored as described in Fig. 1.
885
886 Fig.3 Interactions between AFPs, receptors and GRFs detected by yeast two hybrid assays. Following
887 matings, the indicated diploid lines were grown overnight in media lacking leu and trp. After measuring
888 the OD600, cultures were diluted to the same concentration, then serially diluted 10-fold three times.
889 The diluted cultures were then replica-spotted onto selective media. The -LW plate serves as a control
890 for accuracy of the dilutions. Growth on the -HLW plate requires interaction between the AD- and BD-
891 fusions to complement the *his3-200* allele of these yeast.
892
893 Fig.4 Interactions between AFPs and SnRK2s, PP2Cs, GRFs and receptors detected by split YFP assays.
894 Low magnification images were obtained with an Infinity camera on an Olympus AX70 epifluorescence
895 microscope at 100x magnification. Insets are 400x magnification. High magnification images of individual
896 nuclei were obtained with a Leica SP8 Resonant Scanning Confocal microscope. Scale bars = 10 µm for
897 interactions with kinases, 5 µm for interactions with AHG1
898
899 Fig.5 AFP2 is a substrate for both specific kinases and PP2Cs. (A) Immunoblot of protein extracts from *N.*
900 *benthamiana* leaves with transiently expressed full-length or subdomains of AFP2 as YFP fusions,
901 detected by anti-GFP antibody; lower panel is Ponceau stain focused on Rubisco as loading control. (B)
902 Immunoblot of YFP-AFP2-AB fusion transiently co-expressed with fusions to either SnRK2.3 or AHG1. (C)
903 Transiently expressed YFP-AFP2-AB was immunoprecipitated using GFP-Trap agarose beads; upper
904 panels are immunoblots with indicated antibodies, lower panels are Ponceau stain. *In vitro* kinase
905 reactions with GST-SnRK2.6 and wt or phosphomutant His-fusions of AFP2-AB resulting in reduced
906 mobility of the fusion protein (D) detected by Coomassie stain, (E) incorporation of radioactivity, lower
907 panels are Coomassie stain of gel used in autoradiograph, or (G) reactivity with ProQDiamond stain.

908 Immunoblots of protein extracts from leaves transiently expressing YFP fusions of (F) the wild-type AB
909 and BC domains of AFP2 with Myc-MPK3 , (H) wild-type and phosphomutant AFP2-AB domain fusions, (J)
910 wild type and phosphomutant AFP2-BC domain fusions, and (K) wild type and phosphomimetic AFP2-BC
911 domain fusions, including some co-expressed with Myc-MPK3. YFP fusions were detected by anti-GFP
912 antibody, lower panels are Ponceau stain. (I) *In vitro* kinase reactions with GST-SnRK2.6 and wt or
913 mutant His6 fusions of AFP2-BC, viewed with ProQDiamond stain, lower panel is subsequent Coomassie
914 stain of same gel.
915
916 Fig.6 *In vivo* expression assays with mutant AFPs testing relative significance of specific residues for
917 ABA/stress-induced modification and stability. Transient expression in *N.benthamiana*, followed by 4 hrs
918 incubation in GM +/- 30 µM ABA (A). Stable *A. thaliana* transgenic seedlings grown 5d on GM, then
919 incubated in GM +/- 20 µM ABA for 4.5 hrs (B) or min +/- NaCl (50 - 300 mM) for 2.75 hr (C). Transient
920 expression of YFP-AFP2-AB fusions in *N.benthamiana*, followed by 6 hrs incubation in GM +/- 100 µM CHX
921 or MG132 (D). Stable *A. thaliana* transgenic seedlings grown 5d on GM, then incubated in GM +/- CHX or
922 MG132 for 6 Hrs (E).
923
924 Fig. 7 Expression assays with full-length AFP2 fusions testing relative significance of specific residues
925 for ABA-induced modification and stability. (A) Immunoblots of protein extracts from *N. benthamiana*
926 leaves transiently expressing YFP fusions of full-length AFP2 with the indicated substitutions, following
927 6 h exposure to control media (GM) +/-20 µM ABA (A20), resolved on a Phos-Tag gel. YFP-AFP2 fusions
928 were detected with anti-GFP antibody; lower panel is Ponceau stain. (B-D) Immunoblots of protein
929 extracts from stable transgenic Arabidopsis 5d old seedlings with the indicated YFP-AFP2 fusions,
930 following 6h exposure to GM, supplemented with 20 µM ABA (A20) or 100 µM cycloheximide (CHX) or
931 MG132 (MG). Proteins were resolved on 10% SDS-PAGE. (E) Accumulation of fusion protein following
932 treatment with CHX, MG132 or ABA, normalized relative to actin, expressed relative to level of that
933 fusion in seedlings incubated on GM, as shown in Figs. 7B-D. (F) Relative protein and transcript levels
934 of wild-type and mutant YFP-AFP2 fusions in 5d old seedlings of stable transgenic lines. YFP-AFP2
935 protein levels were normalized relative to actin. Transcript levels were normalized relative to the
936 geometric mean of PP2AA3 (At1g13320) and AP2M (At5g46630) of Arabidopsis. Both are expressed
937 relative to the average value for the wild-type construct. Data shown in E & F is average of at least
938 triplicate samples, error bars represent S.E.** and * indicate statistically different from control (P
939 <0.01 and P<0.05, respectively, based on two-tailed Student's t-test)

940

941 Fig. 8 Localization of YFP-fusions to wild-type and phosphomutant AFP2-AB and –BC domains, and split
942 YFP assays with GRF4, in transiently transformed *N. benthamiana*. Confocal images of nuclei: scale bars
943 = 5 μm. nYFP-GRF4/cYFP-GRF4 image: scale bar = 20 μm

944

945 Fig. 9 Physiological analysis comparing germination (A,C,D) or cotyledon greening (B,E,F) of transgenic
946 lines overexpressing wild-type (wt) vs phosphomutant or phosphomimetic AFP2 fusions in wt(Col)
947 background (A,B,C,E) or *afp2* background (A,B,D,F). Data displayed is the average of at least
948 triplicate assays for each genotype and treatment ± S.E. Bars with different letters represent
949 statistically different values using Tukey's HSD post-hoc test ($p<0.01$).

950

951 Fig. 10 Effects of phosphomutant or phosphomimetic YFP-AFP2 fusions on storage protein accumulation
952 and seed longevity. Top: comparison of dry seed protein extracts from lines either segregating a full-
953 length wild type AFP2 fusion or homozygous for S85E,S112E (S>E) or S85A,S112A (S>A) mutant full-
954 length AFP2 fusions (left) or AFP2-BC fusions with the indicated mutations (right). Upper panels show
955 immunoblots of YFP-AFP2(-BC) fusions detected by α-GFP, -ABI5, and -Actin as a loading control. Lower
956 panels show Coomassie staining of a comparably loaded higher 15% SDS-PAGE to retain and resolve the
957 storage proteins. The "old" extracts were from early generations of these lines with high transgene
958 expression and poor seed viability, while "new" extracts were from later generations with partially
959 silenced transgenes permitting better viability but still conferring ABA-resistant germination. Bottom:
960 seedlings from seed stocks of the indicated ages and genotypes, and their % germination, after 5d
961 growth on minimal medium.

962

963 Figure 11. Changing relationships in the ABA core signaling pathway during the transition from seed
964 maturation to germination. At high ABA concentrations, PP2Cs (e.g. AHG1 & AHG3) are inactive, kinases
965 (e.g. SnRK2s & MPKs) are active, bZIPs (e.g. ABI5 & ABFs) and AFPs are phosphorylated and are bound by
966 GRFs (14-3-3 proteins). When the bZIP:AFP ratio is high, ABA-regulated gene expression proceeds and
967 germination is blocked (Garcia et al, 2008). As ABA levels decrease, ABA induces repressors including AFPs
968 and PP2Cs in a feedback mechanism, the bZIP:AFP ratio decreases and seed-expressed gene expression
969 declines. Interaction between AFPs and co-repressors (e.g. TPL/TPR and HDAC components) leads to
970 inactivation of seed-expressed genes (Lynch et al. 2016). At low ABA levels, the PP2Cs are active and
971 inactivate the SnRK2s, bZIPs (Lynch et al. 2012) and AFPs, and the latter two classes are proteasomally

972 degraded. Many additional interactors are not included due to space constraints. The figure was created
973 with BioRender.com.
974
975 **Supplementary Figures**
976
977 Supp. Fig. 1. Alphafold prediction of AFP2 structure (Model AF-Q9LMX5-F1) with locations of predicted
978 SnRK2 or MPK phosphorylation sites labeled.
979
980 Supp Fig. 2. Interactions between MPK6, AFPs and their subdomains detected by yeast two-hybrid assays.
981 Following matings between haploid lines carrying the BD-MPK6 or AD-AFP fusions, the indicated diploid
982 lines were grown overnight in media lacking leu and trp. After measuring the OD600, cultures were diluted
983 to the same concentration, then serially diluted 10-fold three times. The diluted cultures were then
984 replica-spotted onto selective media. The -LW plate serves as a control for accuracy of the dilutions.
985 Growth on the -HALW plate requires interaction between the AD- and BD- fusions to activate the reporter
986 genes complementing the his3- and ade2- mutations of these yeast.
987
988 Supp Fig. 3 Expression of MPKs in dry seeds and either 24 h post-2d-stratification (top) or after 24h
989 imbibition in water or 3 uM ABA following 2-4 months after-ripening (bottom). Data from (Narsai et al.,
990 2011; Nakabayashi et al., 2005) displayed as "Absolute" units on http://bar.utoronto.ca/efp//cgi-
991 bin/efpWeb.cgi (Winter et al., 2007).
992
993 Supp. Fig. 4. Yeast two-hybrid test of interactions between ABA receptors and AFPs, presented as GAL4BD-
994 PYR/PYL and GAL4AD-AFP fusions. The AD fusion to the PP2C HAB1 is included as a positive control, and
995 pACT is a negative control. Fusions were combined by matings between Y187 carrying AD fusions and PJ69-
996 4a carrying BD fusions. After overnight incubation on YPD media, yeast were replica plated onto selective
997 media lacking leu and trp (-LW) to maintain the AD- and BD-fusion plasmids, then replica plated again to
998 media lacking histidine (-HLW) and supplemented with ABA to score interactions between the fusion
999 proteins. Lower panel: test of potential positives by dilution assay, as in Fig.3.
1000
1001 Supp. Fig. 5 Expression of PYLs, GRFs and AFPs in maturing embryos (top), dry seeds and either 24 h
1002 post-2d- stratification (middle) or after 24h imbibition in water following 2-4 months after-ripening
1003 (bottom). Data from (Narsai et al., 2011; Nakabayashi et al., 2005; Hofmann et al., 2019) displayed as
1004 "Absolute" units on http://bar.utoronto.ca/efp//cgi-bin/efpWeb.cgi (Winter et al., 2007)

1005

1006 Supp. Fig. 6 Interactions between 14-3-3 proteins (GRFs) and ABA core signaling elements. Top: Yeast
1007 two-hybrid assays combining AD-fusions to 14-3-3 proteins with BD-fusions to wild-type and mutant
1008 AFP2, PP2Cs, SnRK2.3 and ABI5 by matings, as described for Supp.Fig. 4.
1009 Bottom: BiFC assays testing GRF interactions with kinases and phosphatases. Scale bars = 10 µm
1010

1011 Supp Fig. 7 Potential dimerization domains of AFP2
1012 Top: Mapping interacting domains of AFP2 by yeast two hybrid assays, as in Supp. Fig. 2. The AFP2-AB
1013 domain includes aa 1-149 and the C domain includes aa 150-348. Bottom: Alphafold prediction of AFP2
1014 dimer structure.
1015

1016 Supp. Fig. 8 Biomolecular fluorescence complementation of full length AFP2 (middle) and AFP1 (bottom)
1017 and subdomains versus ABA core signaling components in *N. benthamiana* leaves (100X magnification).
1018 Top panel shows localization of YFP-fused phosphatase and kinase for reference. Color differences are
1019 due to different versions of image capture software. Inset images show examples of nuclear speckles
1020 observed at 200X or 400X magnification (Erickson McNally, 2016)
1021

1022 Supp. Fig. 9 Predicted phosphorylated residues in AFP1 and AFP2. Top: PhosPhAt shows possible
1023 phosphorylation sites of AFP1 highlighted in green, with documented sites identified by black letters.
1024 Middle: Alignment of AFP1 and AFP2. A, B and C domains are underlined in blue, green and red,
1025 respectively. Residues fitting consensus for MAPK phosphorylation are in blue, those fitting SnRK2
1026 consensus are in red. Bottom: Disordered regions (score <8) in AFP2 predicted by Attention based
1027 DisOrder PredicTor (ADOPT) (Redl et al., 2023).
1028

1029 Supp. Fig. 10 *In vitro* kinase reaction of His-AFP2-AB incubated with GST-SnRK2.6 used for mass
1030 spectrometric analysis of phosphorylation site(s). Top: Coomassie-stained SDS-PAGE; the replicate
1031 phosphorylated substrate bands were excised from the gel, and sent to the UC Davis Mass
1032 Spectrometry Facility for analysis following tryptic digestion. Bottom: Summary of Mass Spec analysis
1033 by Scaffold software, including Fragmentation Table for the only peptide showing phosphorylation.
1034 The initiating Met of AFP2, at position 44 of the fusion protein, is circled in the sequence.
1035

1036 Supp. Fig. 11 Tests of potential phosphorylation sites by kinase reactions with mutant AFP substrates.
1037 (A) *In vitro* kinase assay comparing phosphorylation of wild-type AFP2-AB domain with phosphomutants

1038 or AFP2-C domain. Top two panels are autoradiographs of the Coomassie-stained gel shown in the
1039 bottom panel. Affinity-purified GST-SnRK2.6 was pre-activated, then reactions set up as pool before
1040 aliquoting for combination with His-AFP2 substrates. Coomassie shows loading of AB fusions and SnRK.
1041 "4xA" = (S85,T111,S112,S129)A; as shown in Fig. 5E, (S85,S112)A gives the same result as the 4xA
1042 mutant. (B) Comparison of wild type and phosphomutant YFP-AFP2-AB domain mobility when
1043 transiently expressed in *N. benthamiana*, either alone or in combination with either Myc-SnRK2.3 or
1044 Myc-MPK3. "3xA" = (T76,S85,S112)A
1045
1046 Supp. Fig. 12 Comparison of phosphorylation status of AFP2-BC domain by Phos-tag gels. YFP-AFP2-BC
1047 fusions were expressed transiently in *N.benthamiana* (A,B,C) or stably in *A.thaliana* (C). Fusions were
1048 expressed alone or in combination with Myc-SnRK2.3 (A), Myc-MPK3 (B) or Myc-AHG1 (C). ABA or GM
1049 incubations were as described in Fig. 6AB. The "3xD" mutant is altered at S112, S221, and T319. The
1050 unphosphorylated AFP2-BC domain is identified by the arrows. Full-length AFP2 fusions were
1051 expressed transiently alone or in combination with Myc-AHG1 or Myc-SnRK2.3 in *N.benthamiana* (D).
1052
1053 Supp. Fig. 13 Effects of ABA, mutations and genetic background on expression and mobility of YFP-AFP2-
1054 BC transgenes in stably transformed *A. thaliana*. (A) Time course of changes in mobility of wild-type
1055 AFP2- BC in response to 20 µM ABA. (B) Dose response of ABA-induced changes in mobility of wild-type
1056 AFP2- BC domain in stably transformed *A. thaliana* incubated for 6 hrs in GM with or without ABA
1057 ranging from 1-20 µM. (C) Expression of wild-type (wt) YFP-AFP2-BC and transgenes with the indicated
1058 mutations in wt and *afp2* seedlings following germination and 7d growth on minimal media
1059 supplemented with 3 µM ABA. Upper panels are immunoblots probed with anti-GFP. Lower panels in B
1060 and C are the RbcL bands seen on Ponceau stained filters
1061
1062 Supp. Fig. 14 Comparison of protein and transcript levels for AFP2-AB or AFP2-BC domain fusions.
1063 Transient expression in *N. benthamiana* (A-C) or stable transformants in *A. thaliana* (D,E). The standard
1064 series of wt AFP2-AB shows the volume of extract loaded for the standard curve. Amounts of YFP fusion
1065 protein were normalized relative to actin. YFP-fusion transcripts were normalized relative to these stably
1066 expressed endogenous genes: PP2A (Niben101Scf09716g01002.1) of *N.benthamiana* and the geometric
1067 mean of PP2AA3 (At1g13320) and AP2M (At5g46630) of Arabidopsis.
1068

1069 Supp. Fig. 15. Comparison of stability and accumulation of transiently expressed wild type, double
1070 (S112A,S259A or S221A,T319A) or triple (3xA=S112A,S221A,T319A) mutant AFP2-BC domain fusions to
1071 YFP. Following infiltration, *N. benthamiana* leaf discs were infiltrated with GM (0.5x MS medium) with or
1072 without 100 µM cycloheximide (CHX) or MG132(MG), and incubated 6 hrs prior to harvest for extraction.
1073 Immunoblots were probed with anti-GFP (top panels) after staining with Ponceau (lower panels) (A,B).
1074 Micrographs of *N. benthamiana* leaves used for assay in B, taken with 10x objective on an Olympus AX70
1075 epifluorescence microscope (C). Gain was set at 11.9 for 3xA mutant vs. 2.0 for wild-type. Inset is wild-type
1076 nucleus taken with 40x objective. Scale bars = 10 µm for wild-type, 20 µm for 3xA mutant
1077
1078 Supp. Fig. 16. Germination phenotypes of wild type (Col) and transgenic seeds expressing the
1079 indicated YFP-AFP2 fusions after 7d incubation on either 10 or 50 µM ABA.
1080
1081 Supp. Fig. 17. Transgenic line hemizygous for 35S-YFP-AFP2(S85,S112,S221,T319)A fails to complete seed
1082 maturation. (A) Maturing silique segregating green seeds. (B) Dry seeds with green embryos are
1083 desiccation intolerant and shrunken. (C) Comparison of seedlings from wild type siblings (left) and green
1084 seeds (right) removed from maturing siliques prior to desiccation. (D) Some green seeds fail to develop
1085 roots on minimal media. (E) Transgenic seeds are highly resistant to ABA-inhibition of germination. (F)
1086 Immunoblot comparing accumulation of wild type and mutant AFP2 fusions in seedlings following 6h
1087 incubation in GM with or without 100 µM CHX or MG132 or 20 µM ABA. Dry seed protein extracts of the
1088 indicated genotypes were separated on 10% SDS-PAGE for immunoblots (G) or 15% SDS-PAGE to resolve
1089 storage proteins (cruciferins) (H). "4xA" = 35S-YFP-AFP2(S85,S112,S221,T319)A. Scale bars = 0.5 mm
1090
1091 Supp. Fig. 18. Effects of phosphomutant or phosphomimetic YFP-AFP2 fusions on storage protein
1092 accumulation and seed longevity. Dry seed protein extracts of the indicated genotypes and ages were
1093 separated on 10% SDS-PAGE for immunoblot or 15% SDS-PAGE for resolution of storage proteins.
1094 Germination was scored at 4d post-stratification incubation on minimal nutrient media.
1095
1096 Supp. Fig. 19. Effect of ABA on accumulation and phosphorylation of ABI5 in seeds with wild type or
1097 mutant YFP-AFP2-BC fusions in an *afp2* mutant background. Protein extracts were separated on 10%
1098 SDS-PAGE (upper panels) or a 7.5% Phos-tag gel, then transferred to filters for immunoblots.
1099 Germination on minimal media supplemented with 3 µM ABA (A3) was scored just prior to harvest.
1100

1101 **Supp. Fig. 20.** Alphafold predictions of AFP2 dimer structure when phosphorylated, or blocked from
1102 phosphorylation, at residues tested in this work.

1103 **REFERENCES**
1104

1105 Ali A, Pardo JM, Yun D-J (2020) Desensitization of ABA-Signaling: The Swing From Activation to
1106 Degradation. *Frontiers in Plant Science* 11
1107 Alonso JM, Stepanova AN, Leisse TJ, Kim CJ, Chen H, Shinn P, Stevenson DK, Zimmerman J, Barajas P, Cheuk
1108 R, Gadrinab C, Heller C, Jeske A, Koesema E, Meyers CC, Parker H, Prednis L, Ansari Y, Choy N, Deen
1109 H, Geralt M, Hazari N, Hom E, Karnes M, Mulholland C, Ndubaku R, Schmidt I, Guzman P, Aguilar-
1110 Henonin L, Schmid M, Weigel D, Carter DE, Marchand T, Risseeuw E, Brogden D, Zeko A, Crosby
1111 WL, Berry CC, Ecker JR (2003) Genome-Wide Insertional Mutagenesis of Arabidopsis thaliana.
1112 *Science* 301**:** 653-657
1113 Bhagat PK, Verma D, Verma N, Sinha AK (2021) A novel positive feedback mechanism of ABI5
1114 phosphorylation by mitogen activated protein kinase-3 regulates ABA signaling in *Arabidopsis*.
1115 *bioRxiv***:** 2021.02.02.429361
1116 Bohn L, Huang J, Weidig S, Yang Z, Heidersberger C, Genty B, Falter-Braun P, Christmann A, Grill E (2024)
1117 The temperature sensor TWA1 is required for thermotolerance in Arabidopsis. *Nature* 629**:** 1126-
1118 1132
1119 Camoni L, Visconti S, Aducci P, Marra M (2018) 14-3-3 Proteins in Plant Hormone Signaling: Doing
1120 Several Things at Once. *Frontiers in Plant Science* 9
1121 Chang G, Yang W, Zhang Q, Huang J, Yang Y, Hu X (2019) ABI5-BINDING PROTEIN2 Coordinates
1122 CONSTANS to Delay Flowering by Recruiting the Transcriptional Corepressor TPR2. *Plant*
1123 *Physiology* 179**:** 477-490
1124 Chen K, Li G-J, Bressan RA, Song C-P, Zhu J-K, Zhao Y (2020) Abscisic acid dynamics, signaling, and functions
1125 in plants. *Journal of Integrative Plant Biology* 62**:** 25-54
1126 Chen X, Li Q, Ding L, Zhang S, Shan S, Xiong X, Jiang W, Zhao B, Zhang L, Luo Y, Lian Y, Kong X, Ding X, Zhang
1127 J, Li C, Soppe WJJ, Xiang Y (2023) The MKK3-MPK7 cascade phosphorylates ERF4 and promotes its
1128 rapid degradation to release seed dormancy in Arabidopsis. *Mol Plant* 16**:** 1743-1758
1129 Cutler SR, Rodriguez PL, Finkelstein RR, Abrams SR (2010) Abscisic Acid: Emergence of a Core Signaling
1130 Network. *Ann Rev of Plant Biology* 61**:** 651-679
1131 Czechowski T, Stitt M, Altmann T, Udvardi MK, Scheible W-RD (2005) Genome-Wide Identification and
1132 Testing of Superior Reference Genes for Transcript Normalization in Arabidopsis. *Plant Physiol*
1133 139**:** 5-17
1134 Danquah A, De Zélicourt A, Boudsocq M, Neubauer J, Frei Dit Frey N, Leonhardt N, Pateyron S, Gwinner F,
1135 Tamby J-P, Ortiz-Masia D, Marcote MJ, Hirt H, Colcombet J (2015) Identification and
1136 characterization of an ABA-activated MAP kinase cascade in Arabidopsis thaliana. *The Plant Journal*
1137 82**:** 232-244
1138 Deng G, Sun H, Hu Y, Yang Y, Li P, Chen Y, Zhu Y, Zhou Y, Huang J, Neill SJ, Hu X (2023) A transcription
1139 factor WRKY36 interacts with AFP2 to break primary seed dormancy by progressively silencing
1140 DOG1 in Arabidopsis. *New Phytologist* 238**:** 688-704
1141 Dephoure N, Gould KL, Gygi SP, Kellogg DR (2013) Mapping and analysis of phosphorylation sites: a quick
1142 guide for cell biologists. *Molecular Biology of the Cell* 24**:** 535-542
1143 De Zelicourt A, Colcombet J, Hirt H (2016) The Role of MAPK Modules and ABA during Abiotic Stress
1144 Signaling. *Trends in Plant Science* 21**:** 677-685
1145 Dorone Y, Boeynaems S, Flores E, Jin B, Hateley S, Bossi F, Lazarus E, Pennington JG, Michiels E, De
1146 Decker M, Vints K, Baatsen P, Bassel GW, Otegui MS, Holehouse AS, Exposito-Alonso M, Sukenik
1147 S, Gitler AD, Rhee SY (2021) A prion-like protein regulator of seed germination undergoes
1148 hydration-dependent phase separation. *Cell* 184**:** 4284-4298.e27
1149 Earley K, Haag J, Pontes O, Opper K, Juehne T, Song K, Pikaard C (2006) Gateway-compatible vectors for
1150 plant functional genomics and proteomics. *Plant J* 45**:** 616-629
1151 Eisner N, Maymon T, Sanchez EC, Bar-Zvi D, Brodsky S, Finkelstein R, Bar-Zvi D (2021) Phosphorylation of

1152 Serine 114 of the transcription factor ABSCISIC ACID INSENSITIVE 4 is essential for activity. *Plant*
1153 *science : an international journal of experimental plant biology* 305**:** 110847
1154 Emenecker RJ, Holehouse AS, Strader LC (2021) Biological Phase Separation and Biomolecular
1155 Condensates in Plants. *Annual Review of Plant Biology* 72**:** 17-46
1156 Erickson McNally BJ-A. 2016. *Expression patterns of legume-specific cell wall proteins and their genomic*
1157 *organization in Medicago truncatula and Investigating the relationship between post-translational*
1158 *modification and AFP2 function.* 10194236 Ph.D., University of California, Santa Barbara.
1159 Finkelstein R (2013) Abscisic Acid Synthesis and Response. *The Arabidopsis Book***:** e0166
1160 Finkelstein RR, Lynch TJ (2022) Overexpression of ABI5 Binding Proteins Suppresses
1161 Inhibition of Germination Due to Overaccumulation of DELLA Proteins. *Int J Mol Sci* 23**:**
1162 5537
1163 Fujii H, Zhu J-K (2009) Arabidopsis mutant deficient in 3 abscisic acid-activated protein kinases reveals
1164 critical roles in growth, reproduction, and stress. *Proc Natl Acad Sci USA* 106**:** 8380-8385
1165 Fujita Y, Nakashima K, Yoshida T, Katagiri T, Kidokoro S, Kanamori N, Umezawa T, Fujita M, Maruyama K,
1166 Ishiyama K, Kobayashi M, Nakasone S, Yamada K, Ito T, Shinozaki K, Yamaguchi-Shinozaki K (2009)
1167 Three SnRK2 Protein Kinases are the Main Positive Regulators of Abscisic Acid Signaling in
1168 Response to Water Stress in Arabidopsis. *Plant Cell Physiol* 50**:** 2123-2132
1169 Galletti R, Ferrari S, De Lorenzo G (2011) Arabidopsis MPK3 and MPK6 play different roles in basal and
1170 oligogalacturonide- or flagellin-induced resistance against Botrytis cinerea. *Plant Physiol* 157**:** 804-
1171 14
1172 Garcia M, Lynch T, Peeters J, Snowden C, Finkelstein R (2008) A small plant-specific protein family of ABI
1173 five binding proteins (AFPs) regulates stress response in germinating *Arabidopsis* seeds and
1174 seedlings. *Plant Molecular Biology* 67**:** 643-658
1175 Group M, Ichimura K, Shinozaki K, Tena G, Sheen J, Henry Y, Champion A, Kreis M, Zhang S, Hirt H, Wilson
1176 C, Heberle-Bors E, Ellis BE, Morris PC, Innes RW, Ecker JR, Scheel D, Klessig DF, Machida Y, Mundy J,
1177 Ohashi Y, Walker JC (2002) Mitogen-activated protein kinase cascades in plants: a new
1178 nomenclature. *Trends in Plant Science* 7**:** 301-308
1179 Guan Y, Lu J, Xu J, Mcclure B, Zhang S (2014) Two Mitogen-Activated Protein Kinases, MPK3 and MPK6, Are
1180 Required for Funicular Guidance of Pollen Tubes in Arabidopsis *Plant Physiology* 165**:** 528-533
1181 Guo H, Feng P, Chi W, Sun X, Xu X, Li Y, Ren D, Lu C, David Rochaix J, Leister D, Zhang L (2016) Plastid-
1182 nucleus communication involves calcium-modulated MAPK signalling. *Nature Communications*
1183 7**:** 12173
1184 Hofmann F, Schon MA, Nodine MD (2019) The embryonic transcriptome of *Arabidopsis thaliana*. *Plant*
1185 *reproduction* 32**:** 77-91
1186 Hong S-Y, Sun B, Straub D, Blaakmeer A, Mineri L, Koch J, Brinch-Pedersen H, Holme IB, Burow M, Lyngs
1187 Jørgensen HJ, Albà MM, Wenkel S (2020) Heterologous microProtein expression identifies LITTLE
1188 NINJA, a dominant regulator of jasmonic acid signaling. *Proc Natl Acad Sci USA* 117: 26197-26205
1189 Jagodzik P, Tajdel-Zielinska M, Ciesla A, Marczak M, Ludwikow A (2018) Mitogen-Activated Protein
1190 Kinase Cascades in Plant Hormone Signaling. *Frontiers in Plant Science* 9
1191 Jang G-J, Yang J-Y, Hsieh H-L, Wu S-H (2019) Processing bodies control the selective translation for
1192 optimal development of Arabidopsis young seedlings. *Proceedings of the National Academy of*
1193 *Sciences* 116**:** 6451-6456
1194 Jaspert N, Throm C, Oecking C (2011) Arabidopsis 14-3-3 Proteins: Fascinating and Less Fascinating
1195 Aspects. *Frontiers in Plant Science* 2
1196 Ko DK, Brandizzi F (2020) Network-based approaches for understanding gene regulation and function in
1197 plants. *The Plant journal : for cell and molecular biology* 104**:** 302-317
1198 Kobayashi Y, Yamamoto S, Minami H, Kagaya Y, Hattori T (2004) Differential activation of the rice sucrose
1199 nonfermenting1-related protein kinase2 family by hyperosmotic stress and abscisic acid. *Plant Cell*

1200 16: 1163-77
1201 Koornneef M, Reuling G, Karssen C (1984) The isolation and characterization of abscisic acid-insensitive
1202 mutants of *Arabidopsis thaliana*. *Physiol Plant* 61: 377-383
1203 Kozeleková A, Náplavová A, Brom T, Gašparik N, Šimek J, Houser J, Hritz J (2022) Phosphorylated and
1204 Phosphomimicking Variants May Differ—A Case Study of 14-3-3 Protein. *Frontiers in Chemistry*
1205 10
1206 Krüger T, Brandt D, Sodenkamp J, Gasper M, Romera-Branchat M, Ahloumessou F, Gehring E, Drotleff J,
1207 Bell C, Kramer K, Eirich J, Soppe WJJ, Finkemeier I, Née G (2025) DOG1 controls dormancy
1208 independently of ABA core signaling kinases regulation by preventing AFP dephosphorylation
1209 through AHG1. *Science Advances* 11: eadr8502
1210 Kulik A, Wawer I, Krzywińska E, Bucholc M, Dobrowolska G (2011) SnRK2 protein kinases--key regulators
1211 of plant response to abiotic stresses. *Omics : a journal of integrative biology* 15: 859-72
1212 Lee S-J, Lee MH, Kim J-I, Kim SY (2014) Arabidopsis Putative MAP Kinase Kinase Kinases Raf10 and Raf11
1213 are Positive Regulators of Seed Dormancy and ABA Response. *Plant and Cell Physiology* 56: 84-
1214 97
1215 Lim J, Lim CW, Lee SC (2022) Core Components of Abscisic Acid Signaling and Their Post-translational
1216 Modification. *Frontiers in Plant Science* 13
1217 Liu Q, Li MZ, Leibham D, Cortez D, Elledge SJ (1998) The univector plasmid-fusion system, a method for
1218 rapid construction of recombinant DNA without restriction enzymes. *Current Biology* 8: 1300–
1219 1309
1220 Liu Q, Liu W, Niu Y, Wang T, Dong J (2023) Liquid–liquid phase separation in plants: Advances and
1221 perspectives from model species to crops. *Plant Communications*: 100663
1222 Lopez-Molina L, Mongrand S, Kinoshita N, Chua N-H (2003) AFP is a novel negative regulator of ABA
1223 signaling that promotes ABI5 protein degradation. *Genes Dev* 17: 410-418
1224 Lumba S, Toh S, Handfield L-F, Swan M, Liu R, Youn J-Y, Cutler Sean r, Subramaniam R, Provart N, Moses
1225 A, Desveaux D, Mccourt P (2014) A Mesoscale Abscisic Acid Hormone Interactome Reveals a
1226 Dynamic Signaling Landscape in Arabidopsis. *Developmental Cell* 29: 360-372
1227 Lynch T, Erickson B, Finkelstein R (2012) Direct interactions of ABA-insensitive (ABI)-clade protein
1228 phosphatase (PP)2Cs with calcium-dependent protein kinases and ABA response element-
1229 binding bZIPs may contribute to turning off ABA response. *Plant Molecular Biology* 80: 647-658
1230 Lynch T, Nee G, Chu A, Kruger T, Finkemeier I, Finkelstein RR (2022) ABI5 binding protein2 inhibits ABA
1231 responses during germination without ABA-INSENSITIVE5 degradation. *Plant Physiol* 189: 666-
1232 678
1233 Lynch TJ, Erickson BJ, Miller DR, Finkelstein RR (2017) ABI5-binding proteins (AFPs) alter transcription of
1234 ABA-induced genes via a variety of interactions with chromatin modifiers. *Plant Molecular*
1235 *Biology* 93: 403-418
1236 Lyzenga WJ, Liu H, Schofield A, Muise-Hennessey A, Stone SL (2013) Arabidopsis CIPK26 interacts with KEG,
1237 components of the ABA signalling network and is degraded by the ubiquitin-proteasome system. *J*
1238 *Exp Bot* 64: 2779-91
1239 Madeira F, Tinti M, Murugesan G, Berrett E, Stafford M, Toth R, Cole C, Mackintosh C, Barton GJ (2015)
1240 14-3-3-Pred: improved methods to predict 14-3-3-binding phosphopeptides. *Bioinformatics* 31:
1241 2276-2283
1242 Maszkowska J, Szymańska KP, Kasztelan A, Krzywińska E, Sztatelman O, Dobrowolska G (2021) The
1243 Multifaceted Regulation of SnRK2 Kinases. *Cells* 10
1244 Maymon T, Eisner N, Bar-Zvi D (2022) The ABCISIC ACID INSENSITIVE (ABI) 4 Transcription Factor Is
1245 Stabilized by Stress, ABA and Phosphorylation. *Plants* 11: 2179
1246 Miller CJ, Turk BE (2018) Homing in: Mechanisms of Substrate Targeting by Protein Kinases. *Trends in*
1247 *biochemical sciences* 43: 380-394

1248 Nakabayashi K, Okamoto M, Koshiba T, Kamiya Y, Nambara E (2005) Genome-wide profiling of stored
1249 mRNA in *Arabidopsis thaliana* seed germination: epigenetic and genetic regulation of
1250 transcription in seed. *Plant J* 41**:** 697-709
1251 Nakashima K, Fujita Y, Kanamori N, Katagiri T, Umezawa T, Kidokoro S, Maruyama K, Yoshida T, Ishiyama K,
1252 Kobayashi M, Shinozaki K, Yamaguchi-Shinozaki K (2009) Three Arabidopsis SnRK2 Protein Kinases,
1253 SRK2D/SnRK2.2, SRK2E/SnRK2.6/OST1 and SRK2I/SnRK2.3, Involved in ABA Signaling are Essential
1254 for the Control of Seed Development and Dormancy. *Plant Cell Physiol* 50**:** 1345-1363
1255 Narsai R, Law SR, Carrie C, Xu L, Whelan J (2011) In-Depth Temporal Transcriptome Profiling Reveals a
1256 Crucial Developmental Switch with Roles for RNA Processing and Organelle Metabolism That Are
1257 Essential for Germination in Arabidopsis. *Plant Physiology* 157**:** 1342-1362
1258 Née G, Krüger T (2023) Dry side of the core: a meta-analysis addressing the original nature of the ABA
1259 signalosome at the onset of seed imbibition. *Frontiers in Plant Science* 14
1260 Nguyen T-P, Cueff G, Hegedus DD, Rajjou L, Bentsink L (2015) A role for seed storage proteins in
1261 Arabidopsis seed longevity. *Journal of experimental botany* 66**:** 6399-6413
1262 Nishimura N, Yoshida T, Kitahata N, Asami T, Shinozaki K, Hirayama T (2007) *ABA-Hypersensitive*
1263 *Germination1* encodes a protein phosphatase 2C, an essential component of abscisic acid
1264 signaling in Arabidopsis seed. *Plant J* 50**:** 935-49
1265 Park S-Y, Fung P, Nishimura N, Jensen DR, Fujii H, Zhao Y, Lumba S, Santiago J, Rodrigues A, Chow T-FF,
1266 Alfred SE, Bonetta D, Finkelstein R, Provart NJ, Desveaux D, Rodriguez PL, Mccourt P, Zhu J-K,
1267 Schroeder JI, Volkman BF, Cutler SR (2009) Abscisic Acid Inhibits Type 2C Protein Phosphatases via
1268 the PYR/PYL Family of START Proteins. *Science* 324**:** 1068-1071
1269 Pauwels L, Barbero GF, Geerinck J, Tilleman S, Grunewald W, Perez AC, Chico JM, Bossche RV, Sewell J,
1270 Gil E, Garcia-Casado G, Witters E, Inze D, Long JA, De Jaeger G, Solano R, Goossens A (2010)
1271 NINJA connects the co-repressor TOPLESS to jasmonate signalling. *Nature* 464**:** 788-791
1272 Peng J, Wang M, Wang X, Qi L, Guo C, Li H, Li C, Yan Y, Zhou Y, Terzaghi W, Li Z, Song C-P, Qin F, Gong Z, Li J
1273 (2022) COP1 positively regulates ABA signaling during Arabidopsis seedling growth in darkness by
1274 mediating ABA-induced ABI5 accumulation. *The Plant Cell* 34**:** 2286-2308
1275 Pombo MA, Ramos RN, Zheng Y, Fei Z, Martin GB, Rosli HG (2019) Transcriptome-based identification
1276 and validation of reference genes for plant-bacteria interaction studies using Nicotiana
1277 benthamiana. *Sci Rep* 9**:** 1632
1278 Powers SK, Holehouse AS, Korasick DA, Schreiber KH, Clark NM, Jing H, Emenecker R, Han S, Tycksen E,
1279 Hwang I, Sozzani R, Jez JM, Pappu RV, Strader LC (2019) Nucleo-cytoplasmic Partitioning of ARF
1280 Proteins Controls Auxin Responses in *Arabidopsis thaliana*. *Molecular Cell* 76**:** 177- 190.e5
1281 Redl I, Fisicaro C, Dutton O, Hoffmann F, Henderson L, Owens Benjamin M J, Heberling M, Paci E,
1282 Tamiola K (2023) ADOPT: intrinsic protein disorder prediction through deep bidirectional
1283 transformers. *NAR Genomics and Bioinformatics* 5
1284 Roitinger E, Hofer M, Köc her T, Pichler P, Novatchkova M, Yang J, Schlög elhofer P, Mechtler K
1285 (2015) Quantitative Phosphoproteomics of the Ataxia Telangiectasia-Mutated (ATM) and Ataxia
1286 Telangiectasia-Mutated and Rad3-related (ATR) Dependent DNA Damage Response in
1287 *Arabidopsis thaliana*. *Molec Cell Proteomics* 14**:** 556-571
1288 Schoonheim PJ, Sinnige MP, Casaretto JA, Veiga H, Bunney TD, Quatrano RS, De Boer AH (2007) 14-3-3
1289 adaptor proteins are intermediates in ABA signal transduction during barley seed germination
1290 *Plant J* 49**:** 289-301
1291 Seger R, Krebs E (1995) The MAPK signaling cascade. *FASEB J* 9**:** 726-735
1292 Shao Y, Yu X, Xu X, Li Y, Yuan W, Xu Y, Mao C, Zhang S, Xu J (2020) The YDA-MKK4/MKK5-MPK3/MPK6
1293 Cascade Functions Downstream of the RGF1-RGI Ligand–Receptor Pair in Regulating Mitotic
1294 Activity in Root Apical Meristem. *Molecular Plant* 13**:** 1608-1623
1295 Sutherland C (2011) What Are the bona fide GSK3 Substrates? *International Journal of Alzheimer's*

1296 *Disease* 2011: Article ID 505607
1297 Takahashi Y, Zhang J, Hsu P-K, Ceciliato PHO, Zhang L, Dubeaux G, Munemasa S, Ge C, Zhao Y, Hauser F,
1298 Schroeder JI (2020) MAP3Kinase-dependent SnRK2-kinase activation is required for abscisic acid
1299 signal transduction and rapid osmotic stress response. *Nature Communications* 11: 12
1300 Tischer SV, Wunschel C, Papacek M, Kleigrewe K, Hofmann T, Christmann A, Grill E (2017) Combinatorial
1301 interaction network of abscisic acid receptors and coreceptors from *Arabidopsis thaliana* .
1302 *Proceedings of the National Academy of Sciences* 114: 10280-10285
1303 Umezawa T, Sugiyama N, Takahashi F, Anderson JC, Ishihama Y, Peck SC, Shinozaki K (2013) Genetics and
1304 Phosphoproteomics Reveal a Protein Phosphorylation Network in the Abscisic Acid Signaling
1305 Pathway in Arabidopsis thaliana. *Sci Signal* 6: rs8-
1306 Varadi M, Bertoni D, Magana P, Paramval U, Pidruchna I, Radhakrishnan M, Tsenkov M, Nair S, Mirdita M,
1307 Yeo J, Kovalevskiy O, Tunyasuvunakool K, Laydon A, Žídek A, Tomlinson H, Hariharan D,
1308 Abrahamson J, Green T, Jumper J, Birney E, Steinegger M, Hassabis D, Velankar S (2023)
1309 AlphaFold Protein Structure Database in 2024: providing structure coverage for over 214 million
1310 protein sequences. *Nucleic Acids Research* 52: D368-D375
1311 Voinnet O, Rivas S, Mestre P, Baulcombe D (2003) An enhanced transient expression system in plants
1312 based on suppression of gene silencing by the p19 protein of tomato bushy stunt virus. *Plant*
1313 *Journal* 33: 949-956
1314 Wang C, Wen J, Liu Y, Yu B, Yang S (2024) SOS2-AFP2 module regulates seed germination by inducing ABI5
1315 degradation in response to salt stress in Arabidopsis. *Biochemical and Biophysical Research*
1316 *Communications* 723: 150190
1317 Wang H, Ngwenyama N, Liu Y, Walker JC, Zhang S (2007) Stomatal Development and Patterning Are
1318 Regulated by Environmentally Responsive Mitogen-Activated Protein Kinases in Arabidopsis. *The*
1319 *Plant Cell* 19: 63-73
1320 Wang P, Xue L, Batelli G, Lee S, Hou Y-J, Van Oosten MJ, Zhang H, Tao WA, Zhu J-K (2013) Quantitative
1321 phosphoproteomics identifies SnRK2 protein kinase substrates and reveals the effectors of
1322 abscisic acid action. *Proceedings of the National Academy of Sciences* 110: 11205-11210
1323 Wang X, Guo C, Peng J, Li C, Wan F, Zhang S, Zhou Y, Yan Y, Qi L, Sun K, Yang S, Gong Z, Li J (2019) ABRE-
1324 BINDING FACTORS play a role in the feedback regulation of ABA signaling by mediating rapid ABA
1325 induction of ABA co-receptor genes. *New Phytologist* 221: 341-355
1326 Wei J, Li X, Song P, Wang Y, Ma J (2022) Studies on the interactions of AFPs and bZIP transcription factor
1327 ABI5. *Biochem Biophys Res Commun* 590: 75-81
1328 Winter D, Vinegar B, Nahal H, Ammar R, Wilson G, Provart N (2007) An "Electronic Fluorescent
1329 Pictograph" Browser for Exploring and Analyzing Large-Scale Biological Data Sets. *PLoS ONE* 2:
1330 e718
1331 Xie D, Chen M, Niu J, Wang L, Li Y, Fang X, Li P, Qi Y (2021) Phase separation of SERRATE drives dicing
1332 body assembly and promotes miRNA processing in Arabidopsis. *Nature Cell Biology* 23: 32-39
1333 Yilmaz M, Paulic M, Seidel T (2022) Interactome of Arabidopsis Thaliana. *Plants* 11: 350
1334 Yoshida T, Nishimura N, Kitahata N, Kuromori T, Ito T, Asami T, Shinozaki K, Hirayama T (2006) *ABA-*
1335 *hypersensitive germination3* encodes a protein phosphatase 2C (AtPP2CA) that strongly
1336 regulates abscisic acid signaling during germination among Arabidopsis protein phosphatase
1337 2Cs. *Plant Physiol* 140: 115-26
1338 Yu F, Wu Y, Xie Q (2015) Precise protein post-translational modifications modulate ABI5 activity. *Trends*
1339 *in Plant Science* 20: 569-575
1340 Zhao H, Nie K, Zhou H, Yan X, Zhan Q, Zheng Y, Song C-P (2020) ABI5 modulates seed germination via
1341 feedback regulation of the expression of the PYR/PYL/RCAR ABA receptor genes. *New Phytologist*
1342 228: 596-608
1343 Zhou X, Hao H, Zhang Y, Bai Y, Zhu W, Qin Y, Yuan F, Zhao F, Wang M, Hu J, Xu H, Guo A, Zhao H, Zhao Y,
1344 Cao C, Yang Y, Schumaker KS, Guo Y, Xie CG (2015) SOS2-LIKE PROTEIN KINASE5, an SNF1-RELATED

1345 PROTEIN KINASE3-Type Protein Kinase, Is Important for Abscisic Acid Responses in Arabidopsis
1346 through Phosphorylation of ABSCISIC ACID-INSENSITIVE5. *Plant Physiol* 168**:** 659-76
1347 Zou M, Guo M, Zhou Z, Wang B, Pan Q, Li J, Zhou J-M, Li J (2021) MPK3- and MPK6-mediated VLN3
1348 phosphorylation regulates actin dynamics during stomatal immunity in Arabidopsis. *Nature*
1349 *Communications* 12**:** 6474
1350 Zulawski M, Braginets R, Schulze WX (2012) PhosPhAt goes kinases—searchable protein kinase target
1351 information in the plant phosphorylation site database PhosPhAt. *Nucleic Acids Research* 41**:**
1352 D1176-D1184

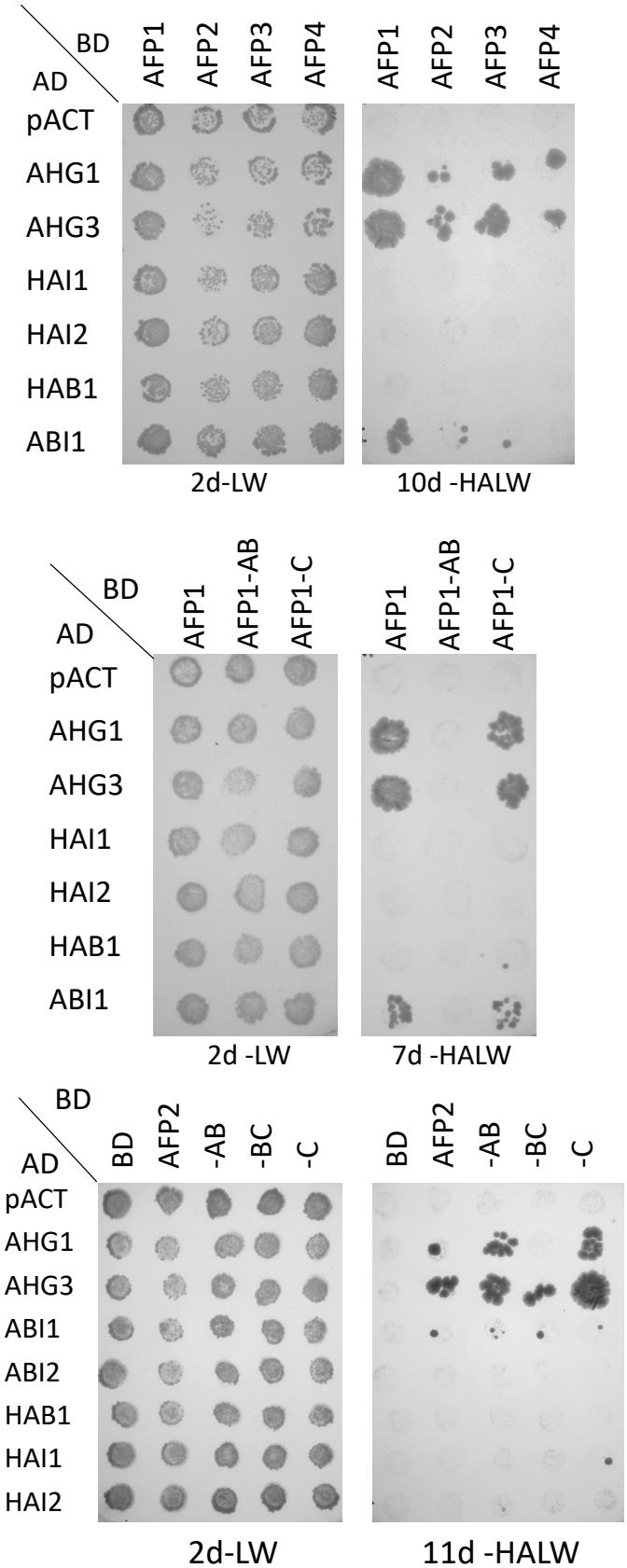

Figure 1 interactions between AFPs and PP2Cs detected by yeast two hybrid assays. Fusions were combined by matings between Y187 carrying AD fusions and PJ69-4a carrying BD fusions. After overnight incubation on YPD media, yeast were replica plated onto selective media lacking leu and trp (-LW) to maintain the AD- and BD-fusion plasmids, and lacking histidine and adenine (-HALW) to score interactions between the fusion proteins.

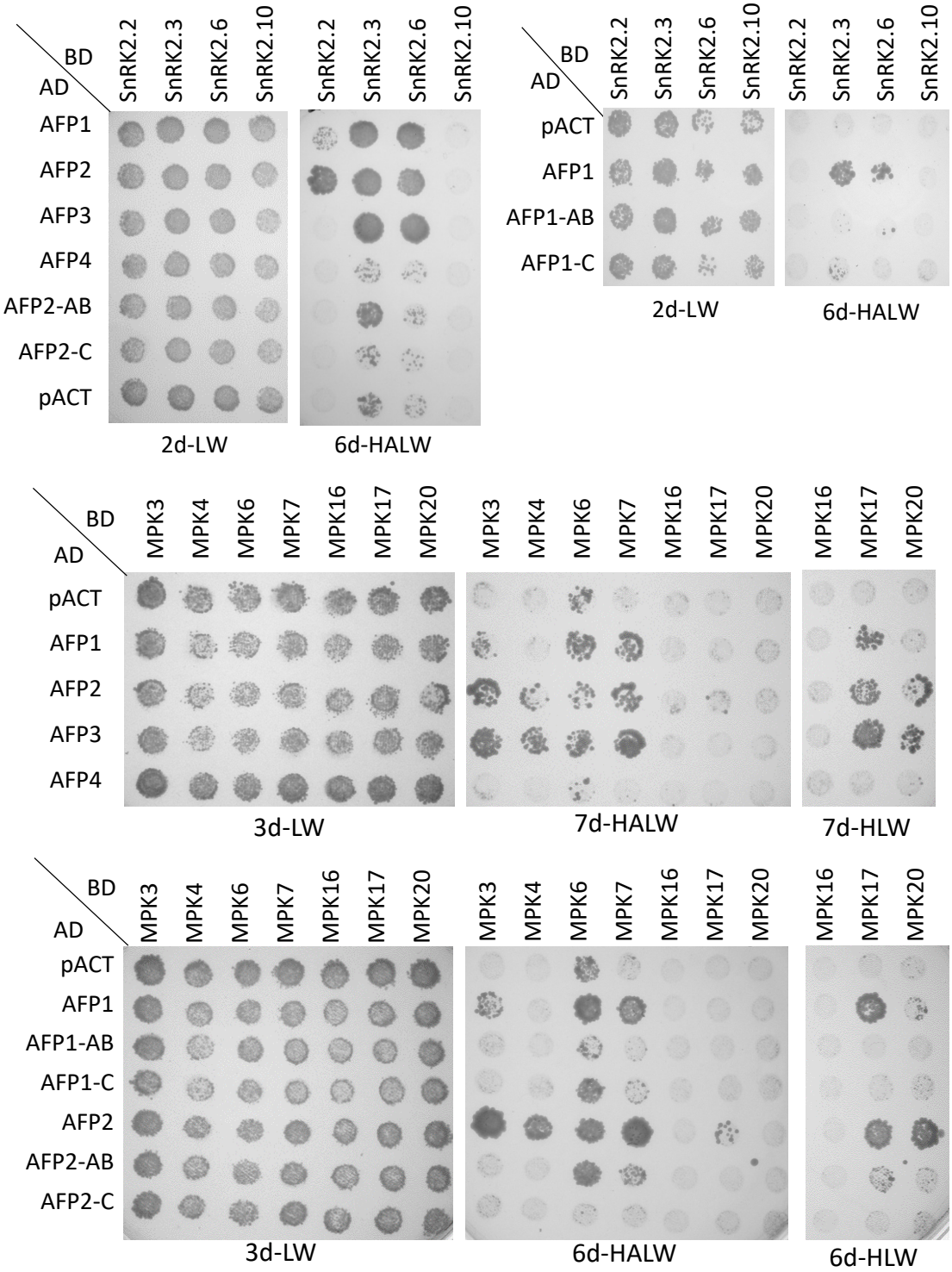

Figure 2 Interactions between AFPs and kinases detected by yeast two hybrid assays. The indicated fusions were combined and interactions were scored as described in Fig. 1.

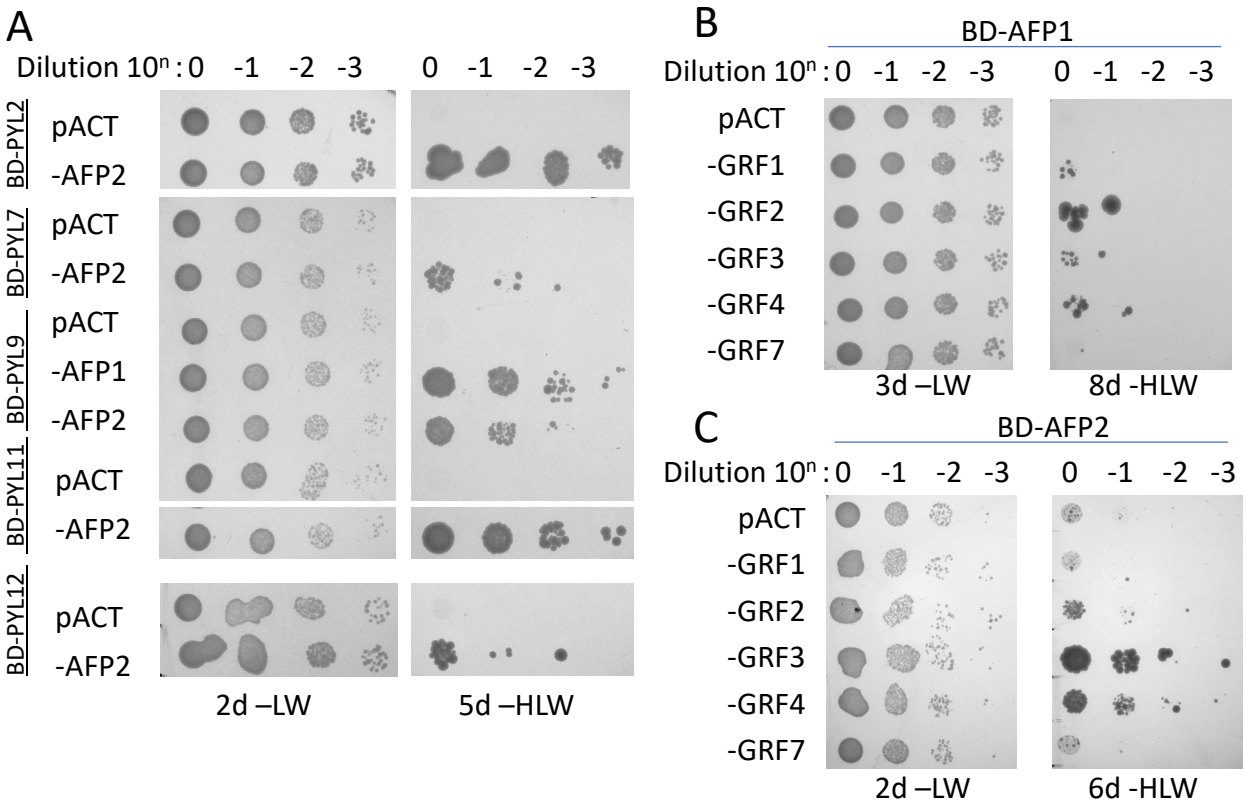

Figure 3. Interactions between AFPs, receptors and GRFs detected by yeast two hybrid assays. Following matings, the indicated diploid lines were grown overnight in media lacking leu and trp. After measuring the OD600, cultures were diluted to the same concentration, then serially diluted 10-fold three times. The diluted cultures were then replica-spotted onto selective media. The -LW plate serves as a control for accuracy of the dilutions. Growth on the -HLW plate requires interaction between the AD- and BD- fusions to complement the *his3*- of these yeast.

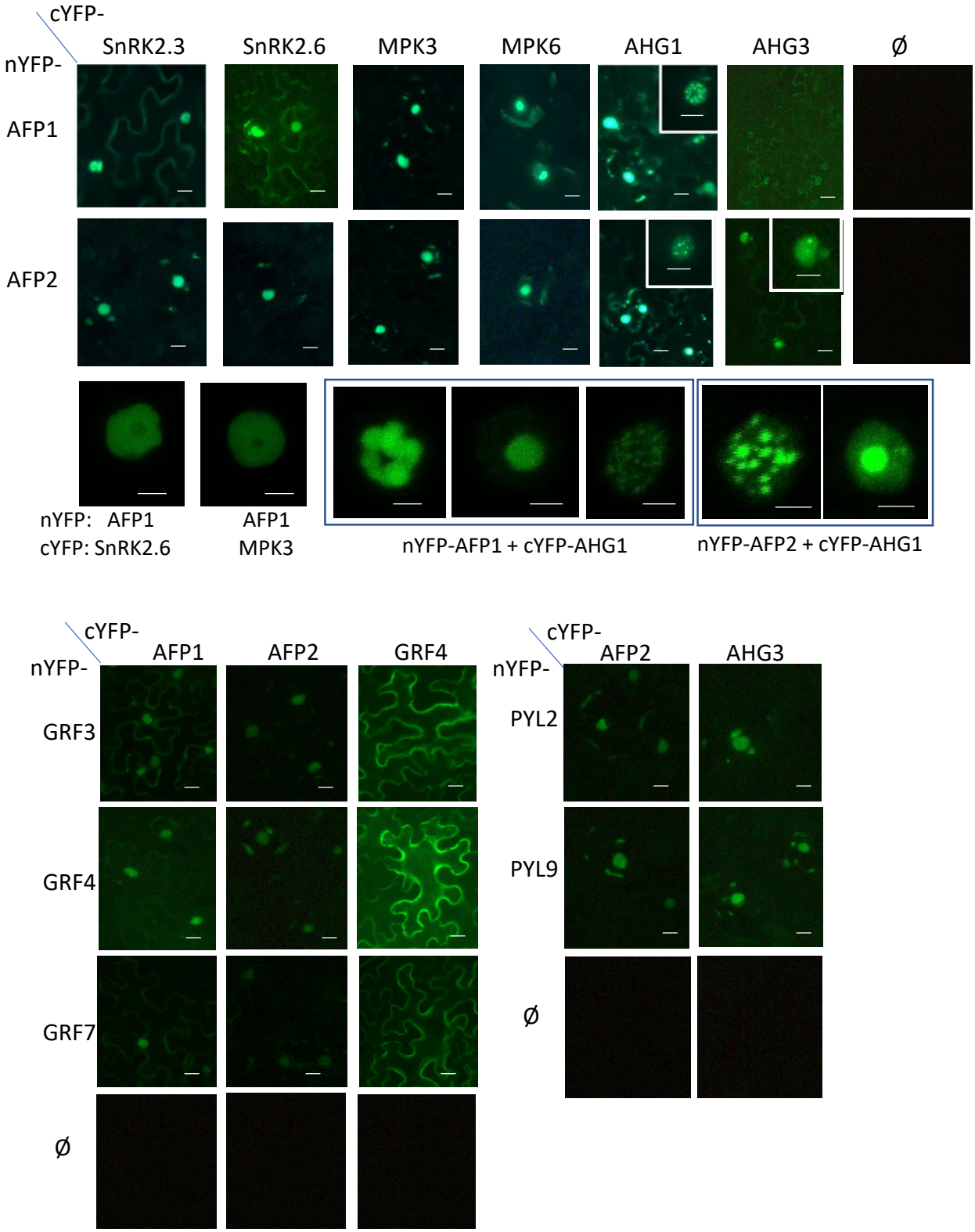

Figure 4. Interactions between AFPs and SnRK2s , PP2Cs, GRFs and receptors detected by split YFP assays. Ø indicates empty vector control. Low magnification images were obtained with an Infinity camera on an Olympus AX70 epifluorescence microscope at 100x magnification. Scale bars = 10 μm. Insets are 400x magnification. High magnification images of individual nuclei were obtained with a Leica SP8 Resonant Scanning Confocal microscope. Scale bars = 10 μm for interactions with kinases, 5 μm for interactions with AHG1

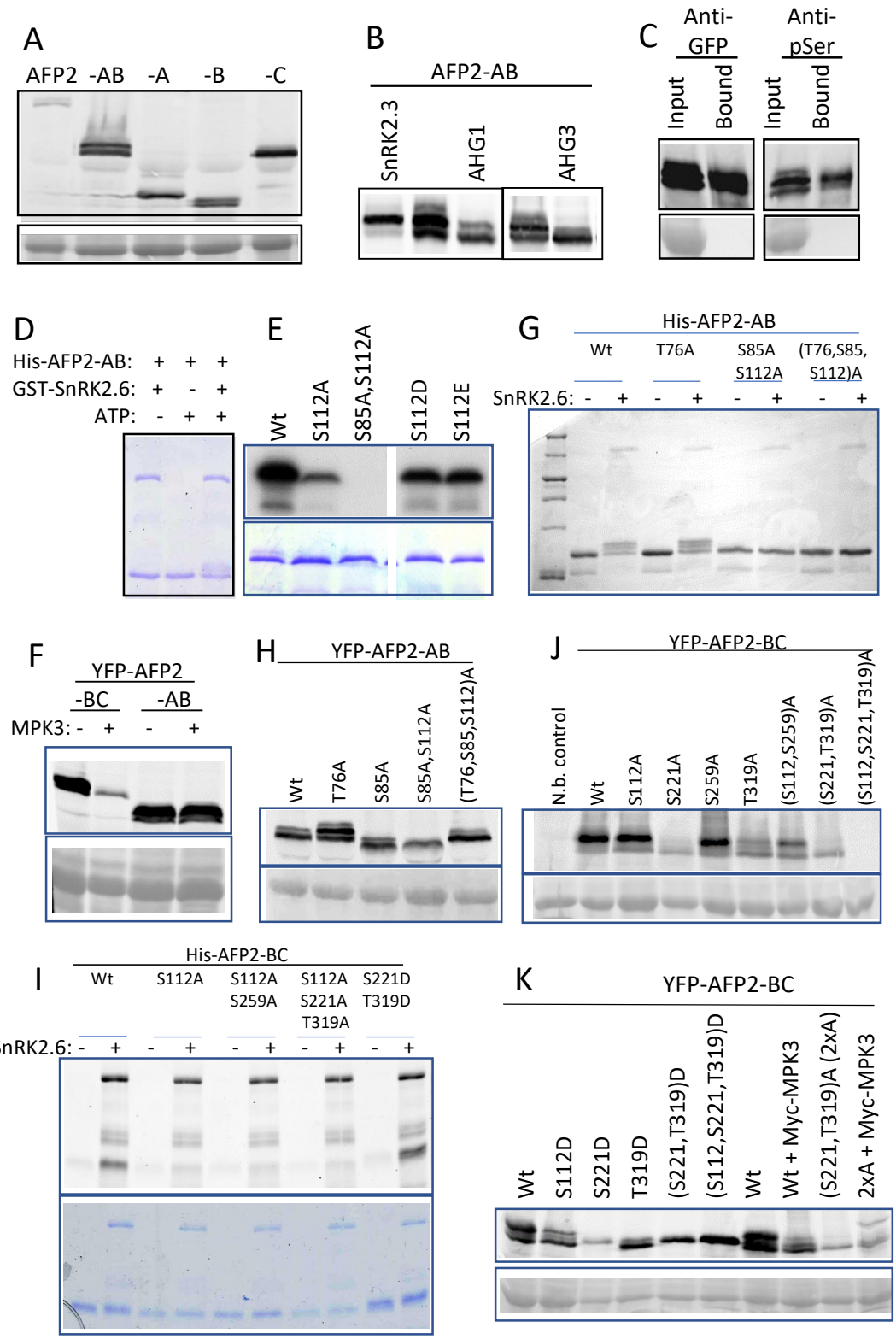
A
AFP2 -AB -A -B -C
B
AFP2-AB
SnRK2.3
AHG1
AHG3
C
Anti-GFP
Anti-pSer
Input
Bound
Input
Bound
D
His-AFP2-AB: + + +
GST-SnRK2.6: + - +
ATP: - + +
E
Wt
S112A
S85A,S112A
S112D
S112E
G
His-AFP2-AB
Wt
T76A
S85A S112A
(T76,S85, S112)A
SnRK2.6: - + - + - + - +
F
YFP-AFP2
-BC
-AB
MPK3: - + - +
H
YFP-AFP2-AB
Wt
T76A
S85A
S85A,S112A
(T76,S85,S112)A
J
YFP-AFP2-BC
N.b. control
Wt
S112A
S221A
S259A
T319A
(S112,S259)A
(S221,T319)A
(S112,S221,T319)A
I
His-AFP2-BC
Wt
S112A
S112A S259A
S112A S221A T319A
S221D T319D
SnRK2.6: - + - + - + - + - +
K
YFP-AFP2-BC
Wt
S112D
S221D
T319D
(S221,T319)D
(S112,S221,T319)D
Wt
Wt + Myc-MPK3
(S221,T319)A (2xA)
2xA + Myc-MPK3

Fig.5 AFP2 is a substrate for both specific kinases and PP2Cs. (A) Immunoblot of protein extracts from *N. benthamiana* leaves with transiently expressed full-length or subdomains of AFP2 as YFP fusions, detected by anti-GFP antibody; lower panel is Ponceau stain focused on Rubisco as loading control. (B) Immunoblot of YFP-AFP2-AB fusion transiently co-expressed with fusions to either SnRK2.3 or AHG1. (C) Transiently expressed YFP-AFP2-AB was immunoprecipitated using GFP-Trap agarose beads; upper panels are immunoblots with indicated antibodies, lower panels are Ponceau stain. *In vitro* kinase reactions with GST-SnRK2.6 and wt or phosphomutant His-fusions of AFP2-AB resulting in reduced mobility of the fusion protein (D) detected by Coomassie stain, (E) incorporation of radioactivity, lower panels are Coomassie stain of gel used in autoradiograph, or (G) reactivity with ProQDiamond stain. Immunoblots of protein extracts from leaves transiently expressing YFP fusions of (F) the wild-type AB and BC domains of AFP2 with Myc-MPK3 , (H) wild-type and phosphomutant AFP2-AB domain fusions,(J) wild type and phosphomutant AFP2-BC domain fusions, and (K) wild type and phosphomimetic AFP2-BC domain fusions, including some co-expressed with Myc-MPK3. YFP fusions were detected by anti-GFP antibody, lower panels are Ponceau stain. (I) In vitro kinase reactions with GST-SnRK2.6 and wt or mutant His fusions of AFP2-BC, viewed with ProQDiamond stain, lower panel is subsequent Coomassie stain of same gel.

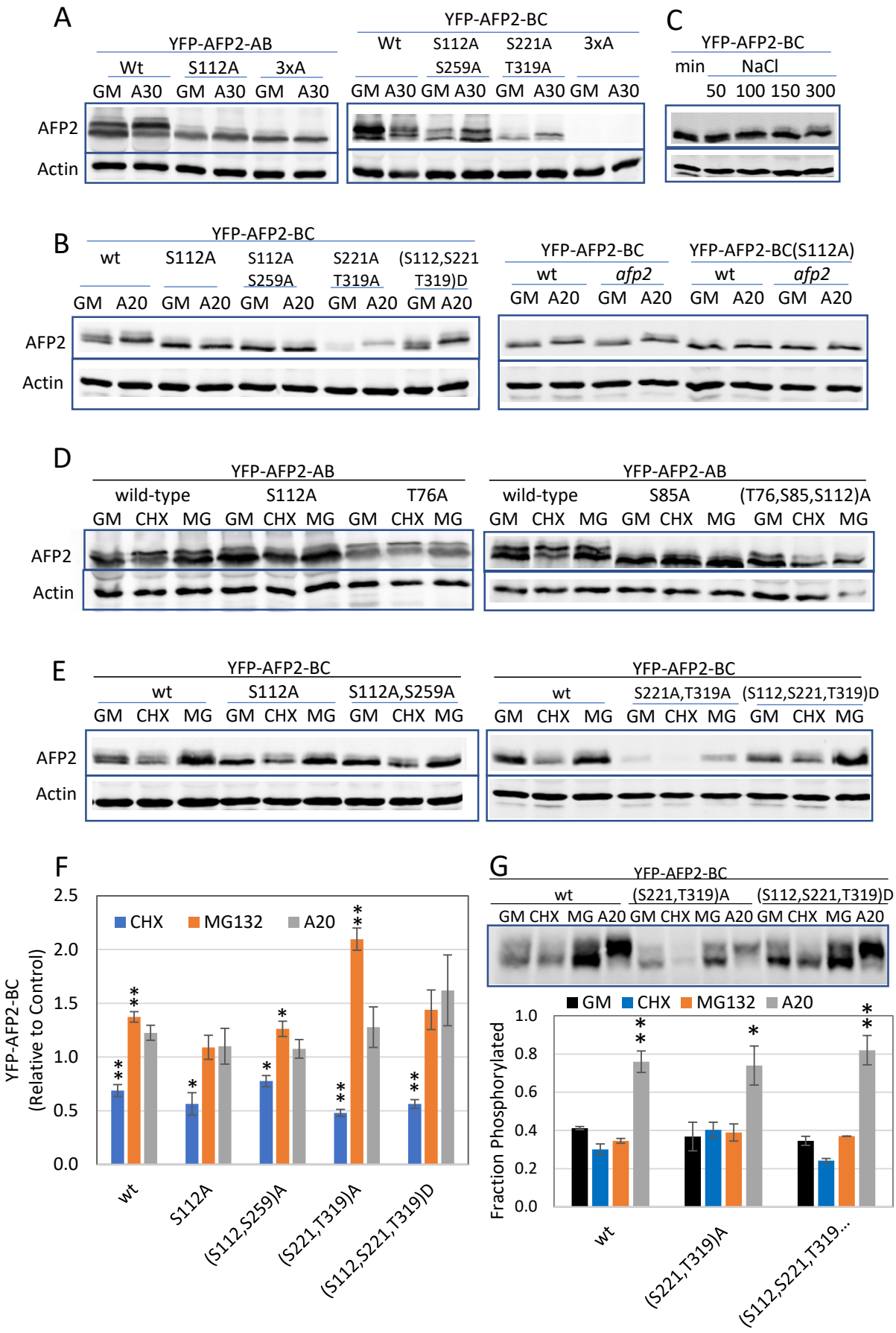
A
YFP-AFP2-AB
Wt
S112A
3xA
GM A30 GM A30 GM A30
AFP2
Actin
YFP-AFP2-BC
Wt
S112A
S259A
S221A
T319A
3xA
GM A30 GM A30 GM A30 GM A30
C
YFP-AFP2-BC
min
NaCl
50 100 150 300
B
YFP-AFP2-BC
wt
S112A
S112A S259A
S221A T319A
(S112,S221 T319)D
GM A20 GM A20 GM A20 GM A20 GM A20
AFP2
Actin
YFP-AFP2-BC
wt
afp2
GM A20 GM A20
YFP-AFP2-BC(S112A)
wt
afp2
GM A20 GM A20
D
YFP-AFP2-AB
wild-type
S112A
T76A
GM CHX MG GM CHX MG GM CHX MG
AFP2
Actin
YFP-AFP2-AB
wild-type
S85A
(T76,S85,S112)A
GM CHX MG GM CHX MG GM CHX MG
E
YFP-AFP2-BC
wt
S112A
S112A,S259A
GM CHX MG GM CHX MG GM CHX MG
AFP2
Actin
YFP-AFP2-BC
wt
S221A,T319A
(S112,S221,T319)D
GM CHX MG GM CHX MG GM CHX MG
F
CHX
MG132
A20
YFP-AFP2-BC (Relative to Control)
2.5
2.0
1.5
1.0
0.5
0.0
wt
S112A
(S112,S259)A
(S221,T319)A
(S112,S221,T319)D
G
YFP-AFP2-BC
wt
(S221,T319)A
(S112,S221,T319)D
GM CHX MG A20 GM CHX MG A20 GM CHX MG A20
GM
CHX
MG132
A20
Fraction Phosphorylated
1.0
0.8
0.6
0.4
0.2
0.0
wt
(S221,T319)A
(S112,S221,T319...

Figure 6. *In vivo* expression assays with AFP2 domain fusions testing relative significance of specific residues for ABA/stress-induced modification and stability. Immunoblots of extracts from (A) the indicated YFP-AFP fusions transiently expressed in *N.benthamiana*, followed by 4 hrs incubation in GM +/- 30 μM ABA; (B,C) *A. thaliana* transgenic seedlings grown 5d on GM, then incubated in (B) GM +/- 20 μM ABA for 4.5 hrs or (C) min +/- NaCl (50 - 300 mM) for 2.75 hrs; (D) YFP-AFP2-AB fusions transiently expressed in *N.benthamiana*, followed by 6 hrs incubation in GM +/- 20 μM CHX or MG132; (E) *A. thaliana* transgenic seedlings grown 5d on GM, then incubated in GM +/- 20 μM CHX or MG132 for 6 Hrs. All upper panels were probed with anti-GFP. Lower panels show either anti-actin reactivity or Ponceau stain (pink).(F) Quantification of YFP-AFP2-BC protein with the indicated mutations from stable *A. thaliana* transgenic seedlings incubated in GM + 20 μM CHX, MG132 or ABA as shown in panels B and E, normalized relative to actin as loading control and expressed relative to the levels of each fusion protein following incubation in GM. Data displayed is the average of triplicate samples ± s.e. ** and * indicate statistically different from level in GM ($P < 0.01$ and $P < 0.05$, respectively, based on two-tailed Student's t-test). (G) Immunoblot of PhosTag gel separating YFP-AFP2-BC from a subset of the extracts shown in panels B and E. The fraction phosphorylated was calculated as the intensity of the upper band(s) relative to the sum of upper and lower band intensities. The average shown is based on quantification of replicate gels ± s.d. ** and * indicate statistically different from all other treatments ($P < 0.01$ and $P < 0.05$, respectively, based on ANOVA with post-hoc Tukey HSD test)

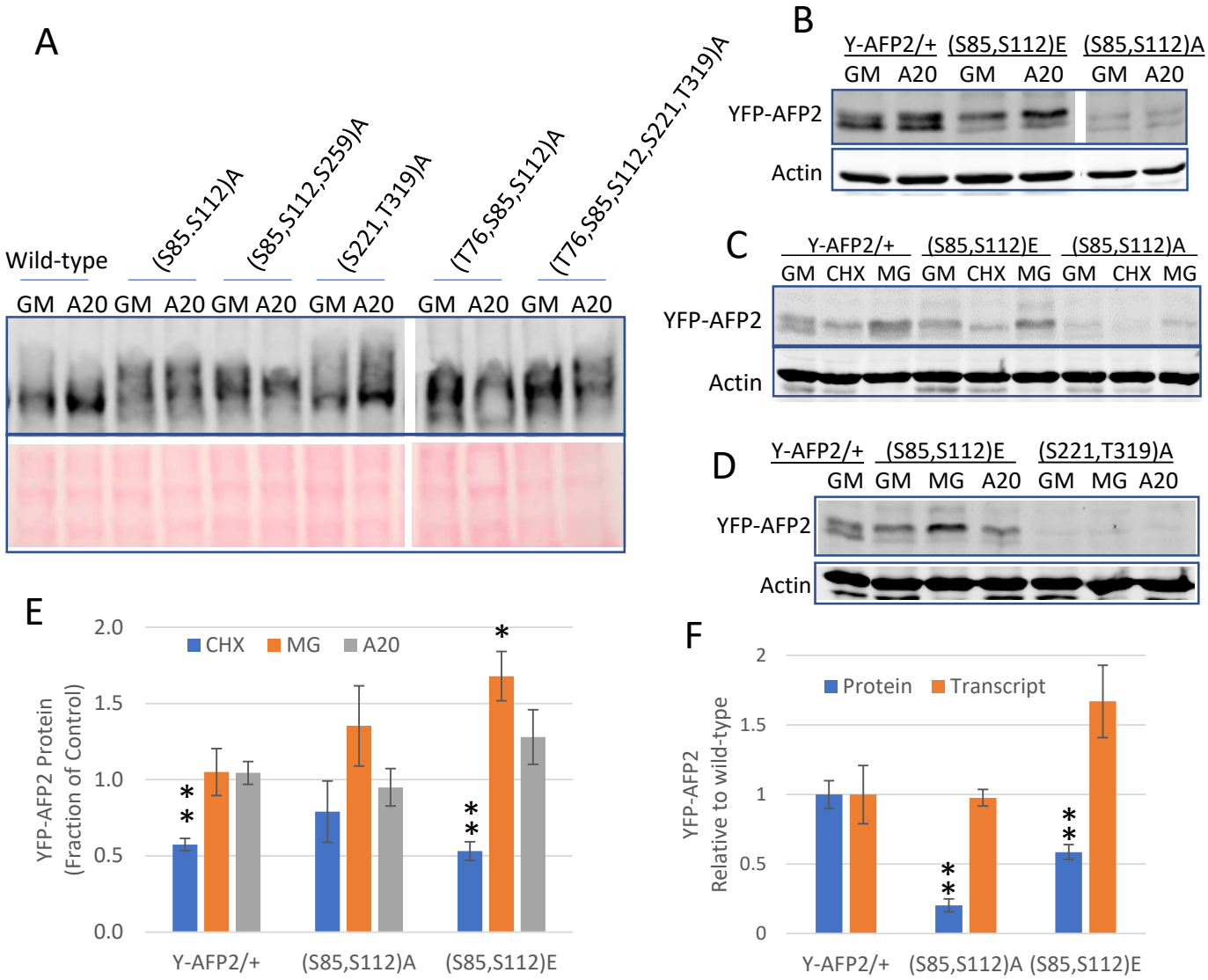

Figure 7. Expression assays with full-length AFP2 fusions testing relative significance of specific residues for ABA-induced modification and stability. (A) Immunoblots of protein extracts from *N. benthamiana* leaves transiently expressing YFP fusions of full-length AFP2 with the indicated substitutions, following 6 h exposure to control media (GM) +/- 20 uM ABA (A20), resolved on a Phos-Tag gel. YFP-AFP2 fusions were detected with anti-GFP antibody; lower panel is Ponceau stain.(B-D) Immunoblots of protein extracts from stable transgenic Arabidopsis 5d old seedlings with the indicated YFP-AFP2 fusions, following 6h exposure to GM, supplemented with 20 uM ABA (A20) or 100 uM cycloheximide (CHX) or MG132 (MG). Proteins were resolved on 10% SDS-PAGE. (E) Accumulation of fusion protein following treatment with CHX, MG132 or ABA, normalized relative to actin, expressed relative to level of that fusion in seedlings incubated on GM, as shown in Figs. 7B-D. (F) Relative protein and transcript levels of wild-type and mutant YFP-AFP2 fusions in 5d old seedlings of stable transgenic lines. YFP-AFP2 protein levels were normalized relative to actin. Transcript levels were normalized relative to the geometric mean of PP2AA3 (At1g13320) and AP2M (At5g46630) of Arabidopsis. Both are expressed relative to the average value for the wild-type construct. Data shown in E & F is average of at least triplicate samples, error bars represent s.e. ** and * indicate statistically different from control (P <0.01 and P<0.05, respectively, based on two-tailed Student's t-test)

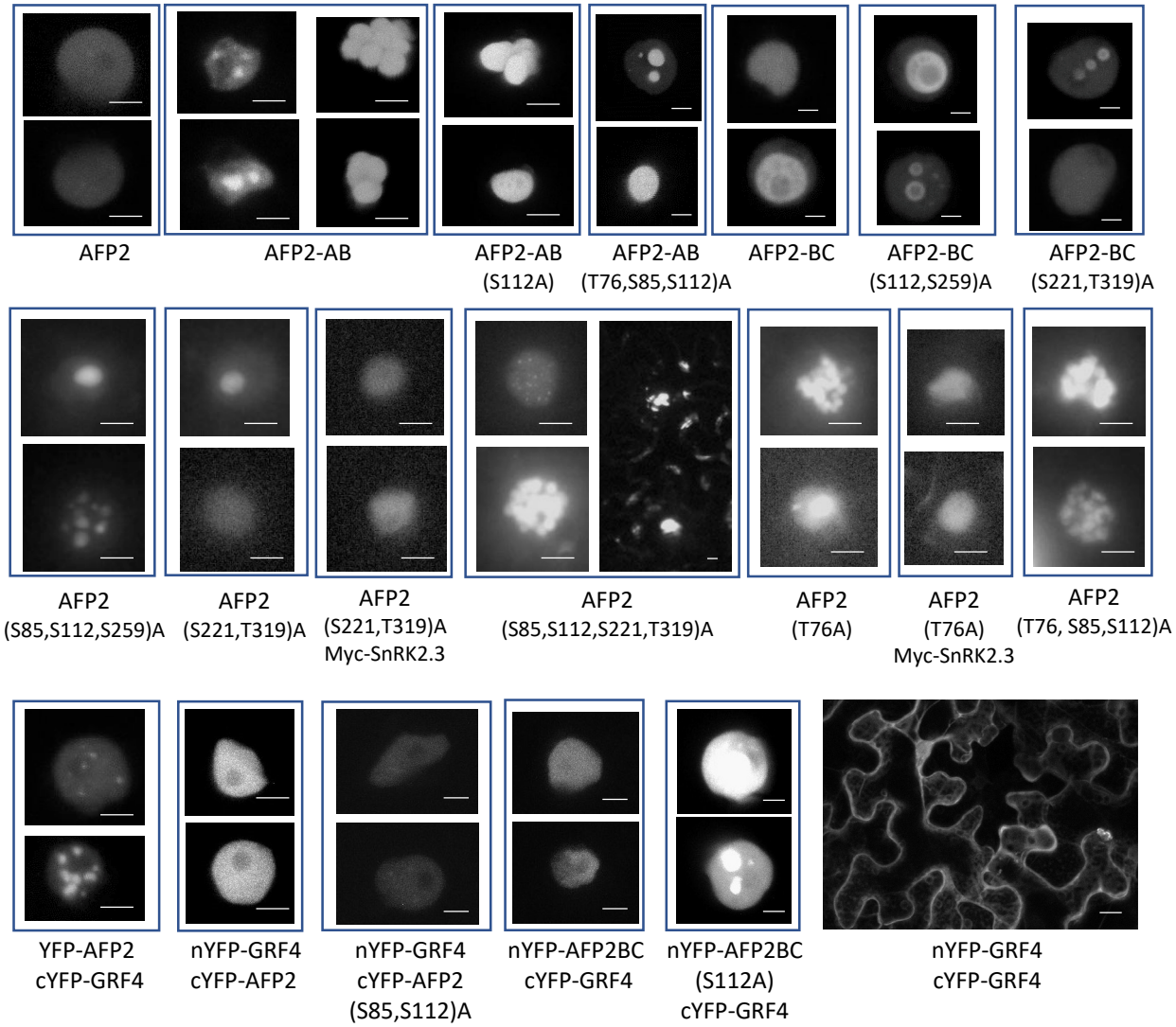

Figure 8. Localization of YFP-fusions to wild-type and phosphomutant AFP2 and its -AB and –BC domains, and split YFP assays with GRF4, in transiently transformed *N. benthamiana*. Confocal images of nuclei: scale bars = 5 μm. nYFP-GRF4/cYFP-GRF4 image: scale bar = 20 μm

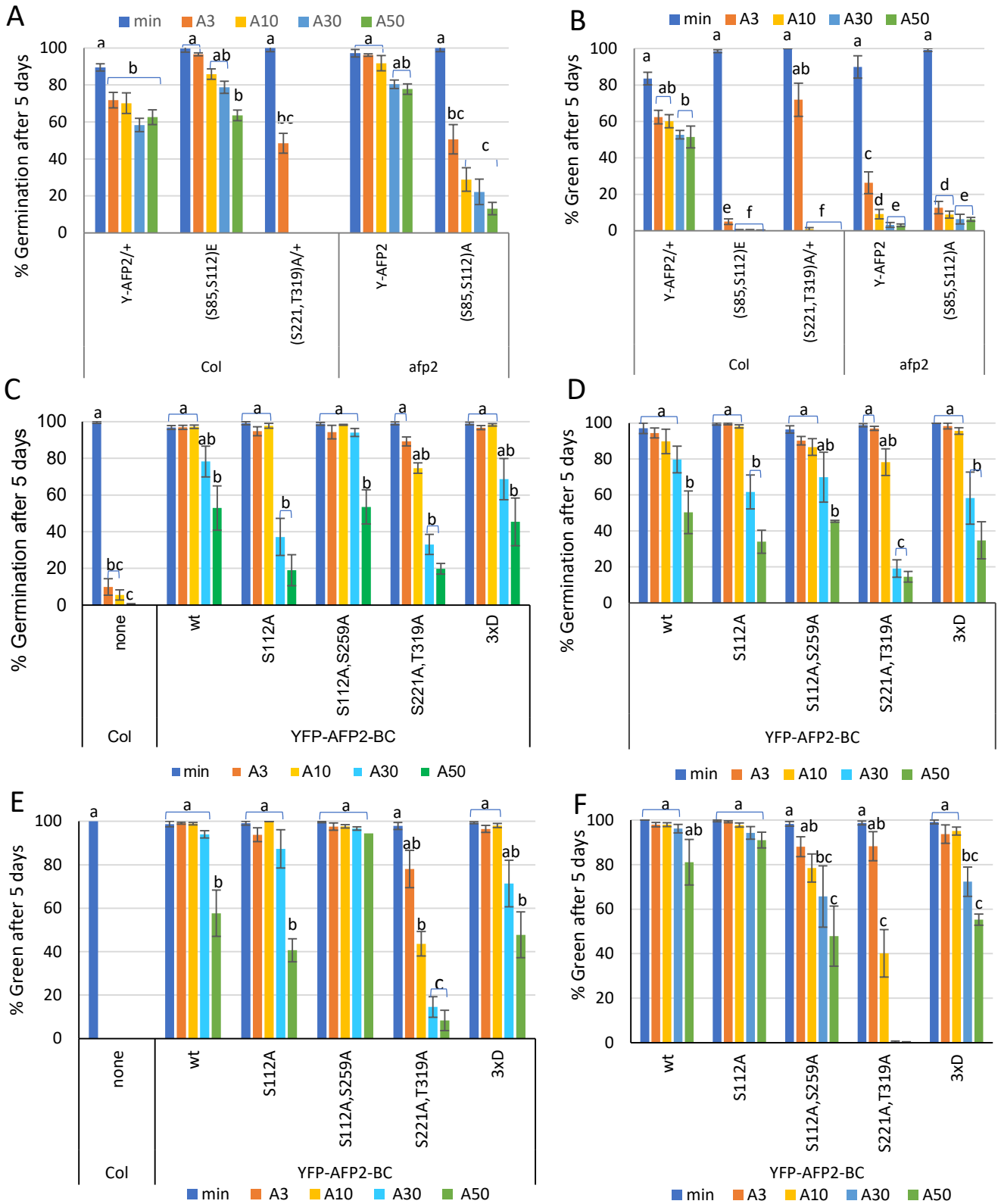

Figure 9. Physiological analysis comparing germination (A,C,D) or cotyledon greening (B,E,F) of transgenic lines overexpressing wild-type (wt) vs phosphomutant or phosphomimic AFP2 fusions in wt(Col) background (A,B,C,E) or *afp2* background (A,B,D,F). Data displayed is the average of at least triplicate assays for each genotype and treatment ± S.E. Bars with different letters represent statistically different values using Tukey's HSD post-hoc test ($p<0.01$).

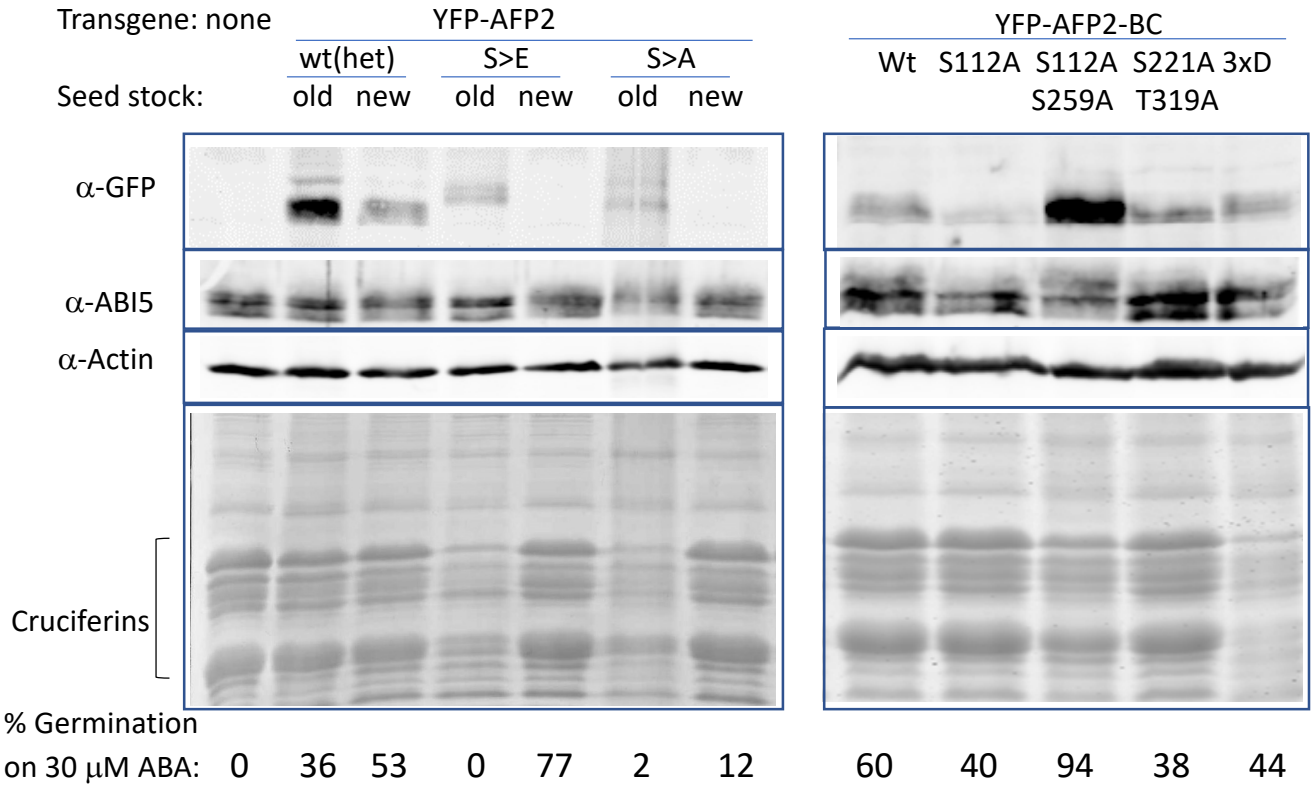

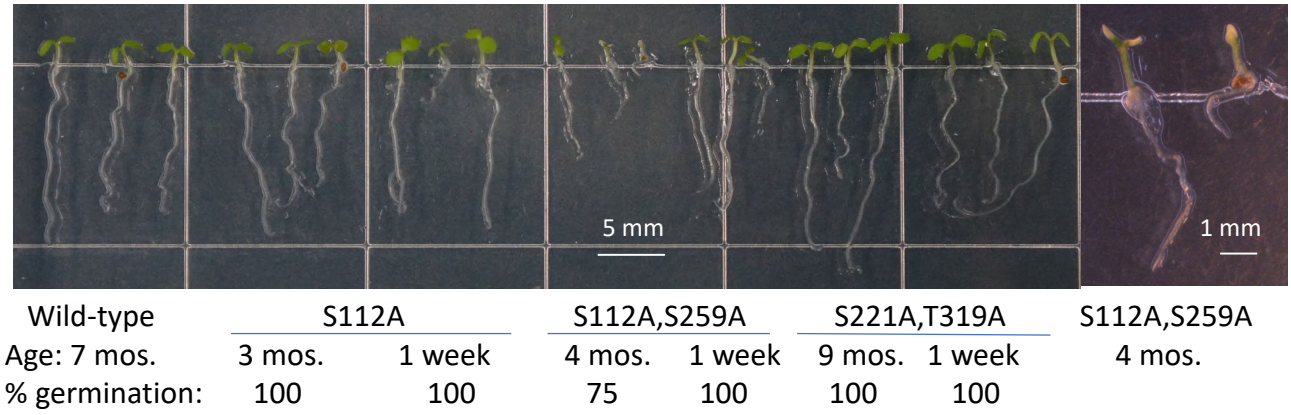

Figure 10. Effects of phosphomutant or phosphomimetic YFP-AFP2 fusions on storage protein accumulation and seed longevity. Top: comparison of dry seed protein extracts from lines either segregating a full-length wild type AFP2 fusion or homozygous for S85E,S112E (S>E) or S85A,S112A (S>A) mutant full-length AFP2 fusions (left) or AFP2-BC fusions with the indicated mutations (right). Upper panels show immunoblots of YFP-AFP2(-BC) fusions detected by α-GFP, ABI5, and Actin as a loading control. Lower panels show Coomassie staining of a comparably loaded higher (15%) SDS-PAGE to retain and resolve the storage proteins. The "old" extracts were from early generations of these lines with high transgene expression and poor seed viability, while "new" extracts were from later generations with partially silenced transgenes permitting better viability but still conferring ABA-resistant germination. Bottom: YFP-AFP2-BC seedlings from seed stocks of the indicated ages and genotypes, and their % germination, after 5d growth on minimal medium.

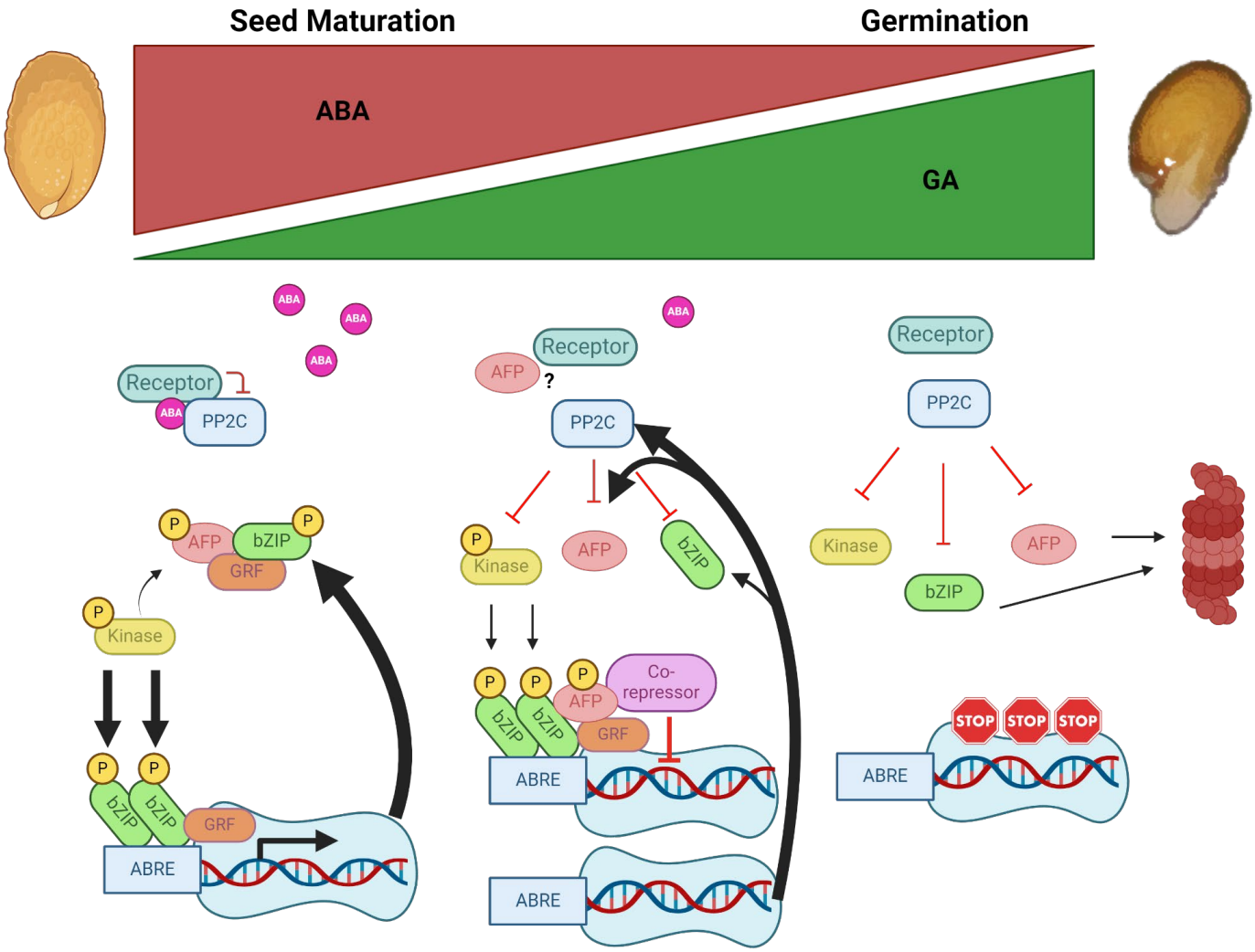

Figure 11. Changing relationships in the ABA core signaling pathway during the transition from seed maturation to germination. At high ABA concentrations, PP2Cs (e.g. AHG1 & AHG3) are inactive, kinases (e.g. SnRK2s & MPKs) are active, bZIPs (e.g. ABI5 & ABFs) and AFPs are phosphorylated and are bound by GRFs (14-3-3 proteins). When the bZIP:AFP ratio is high, ABA-regulated gene expression proceeds and germination is blocked (Garcia et al, 2008). As ABA levels decrease, ABA induces repressors including AFPs and PP2Cs in a feedback mechanism, the bZIP:AFP ratio decreases and seed-expressed gene expression declines. Interaction between AFPs and co-repressors (e.g. TPL/TPR and HDAC components) leads to inactivation of seed-expressed genes (Lynch et al. 2016). At low ABA levels, the PP2Cs are active and inactivate the SnRK2s, bZIPs (Lynch et al. 2012) and AFPs, and the latter two classes are proteasomally degraded. Many additional interactors are not included due to space constraints. The figure was created with BioRender.com.

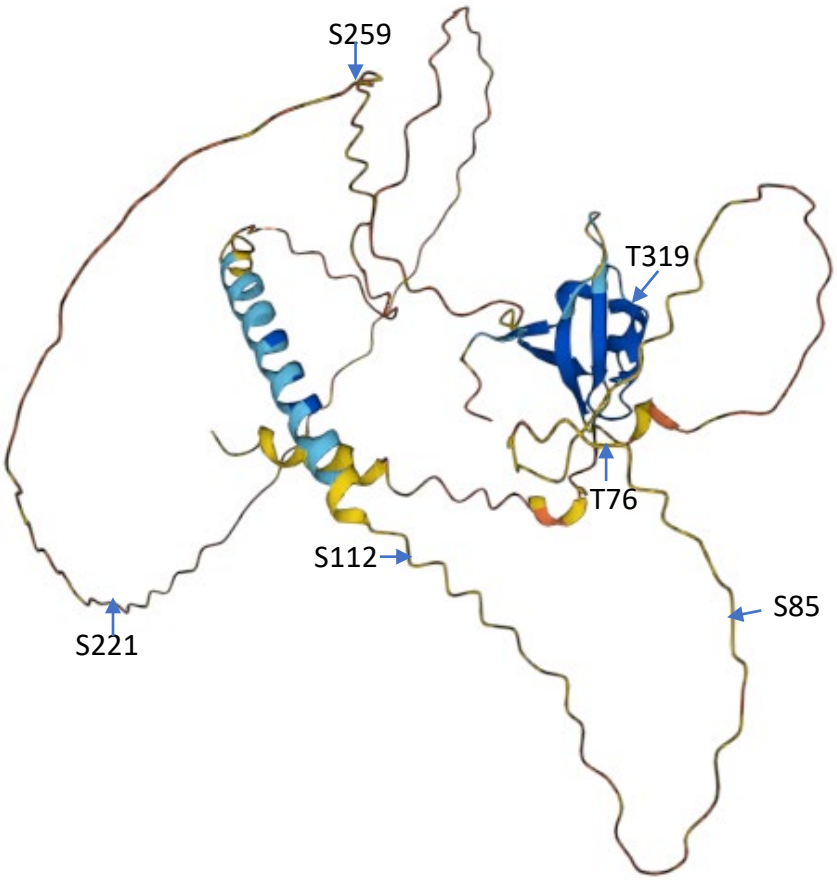

Supp. Fig. 1. Alphafold prediction of AFP2 structure (Model AF-Q9LMX5-F1) with locations of predicted SnRK2 or MPK phosphorylation sites labeled.

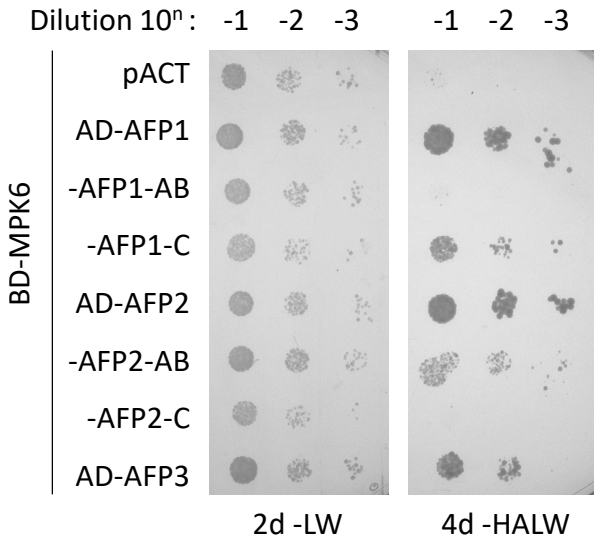

Supp Fig. 2. Interactions between MPK6, AFPs and their subdomains detected by yeast two-hybrid assays. Following matings between haploid lines carrying the BD-MPK6 or AD-AFP fusions, the indicated diploid lines were grown overnight in media lacking leu and trp. After measuring the OD600, cultures were diluted to the same concentration, then serially diluted 10-fold three times. The diluted cultures were then replica-spotted onto selective media. The -LW plate serves as a control for accuracy of the dilutions. Growth on the -HALW plate requires interaction between the AD- and BD- fusions to activate the reporter genes complementing the *his3*- and *ade2*- mutations of these yeast.

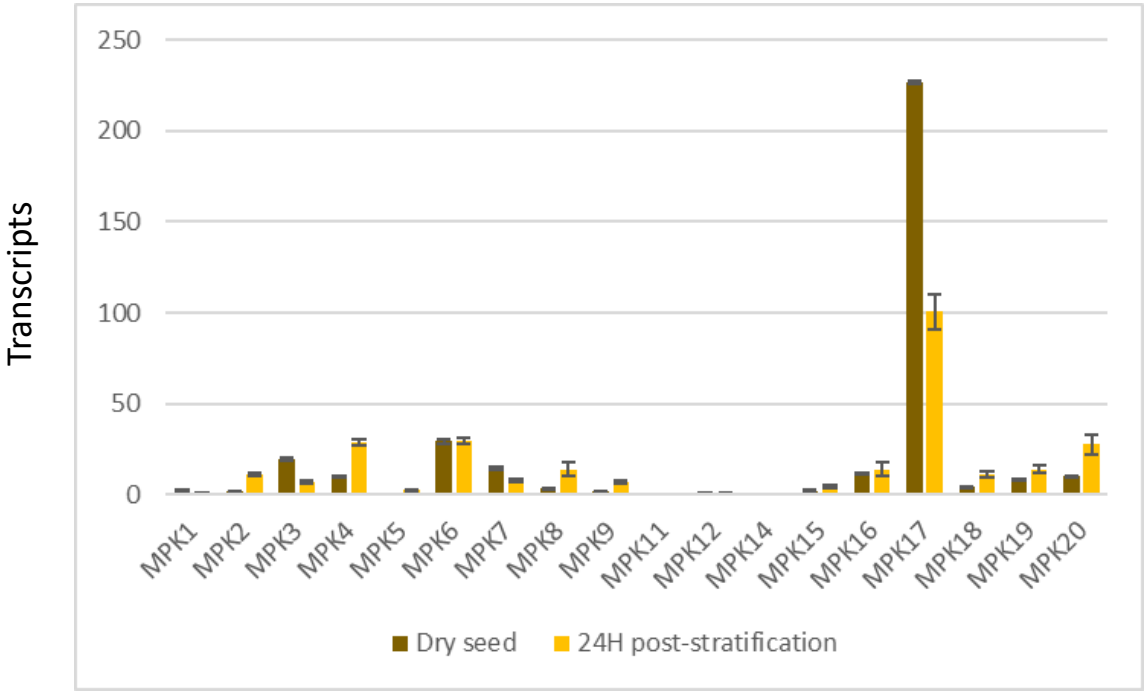

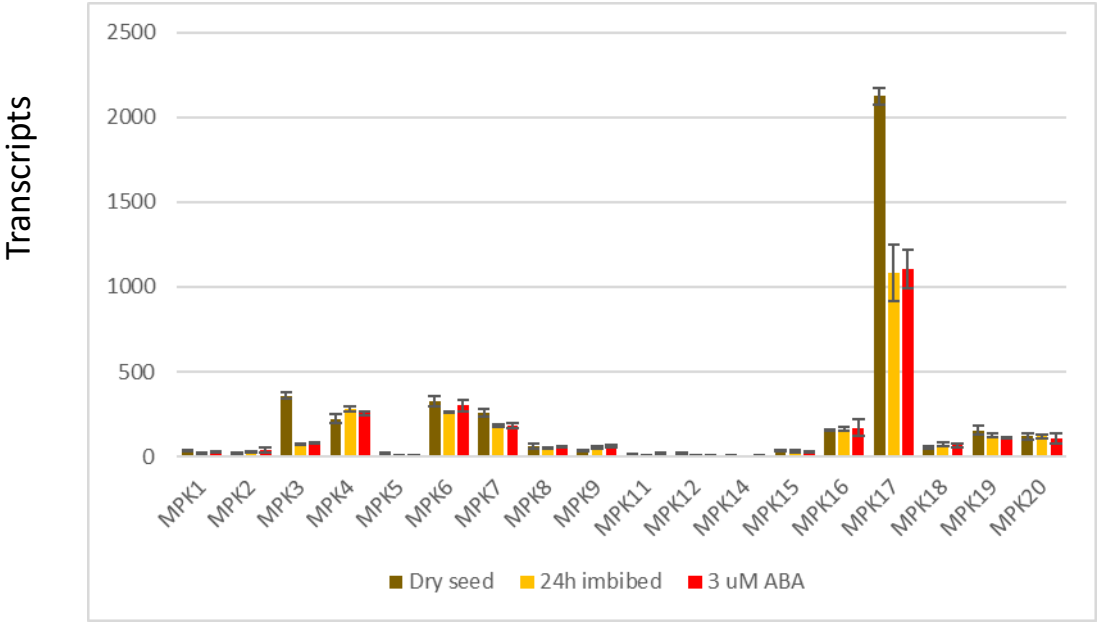

Supp Fig. 3 Expression of MPKs in dry seeds and either 24 h post-2d-stratification (top) or after 24h imbibition in water or 3 uM ABA following 2-4 months after-ripening (bottom). Data from (Narsai et al., 2011; Nakabayashi et al., 2005) displayed as "Absolute" units on http://bar.utoronto.ca/efp//cgi-bin/efpWeb.cgi (Winter et al., 2007).

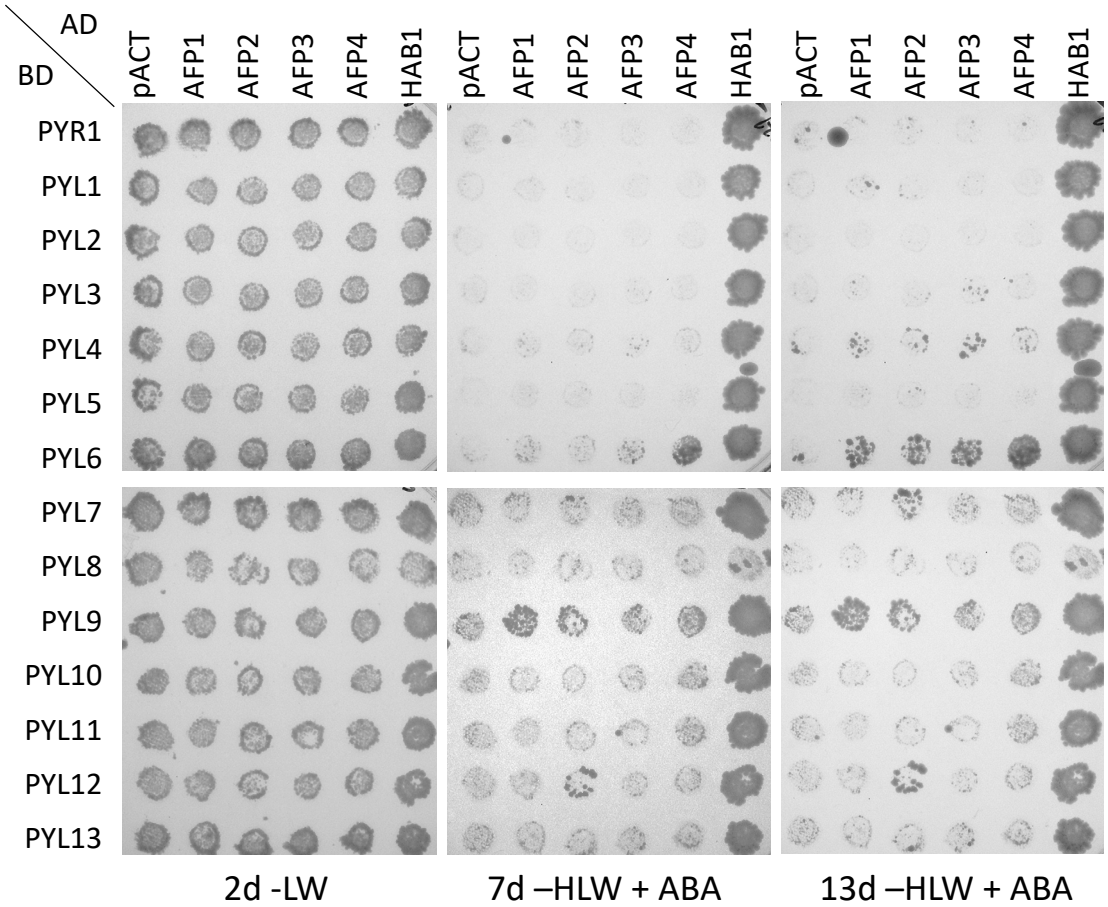

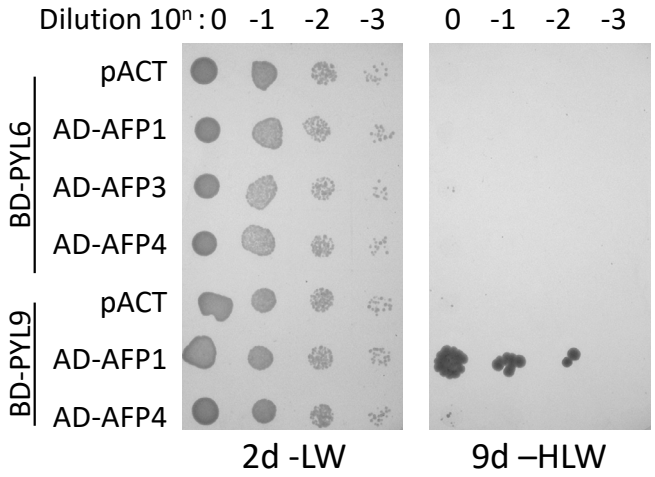

Supp. Fig. 4. Yeast two-hybrid test of interactions between ABA receptors and AFPs, presented as GAL4BD-PYR/PYL and GAL4AD-AFP fusions. The AD fusion to the PP2C HAB1 is included as a positive control, and pACT is a negative control. Fusions were combined by matings between Y187 carrying AD fusions and PJ69-4a carrying BD fusions. After overnight incubation on YPD media, yeast were replica plated onto selective media lacking leu and trp (-LW) to maintain the AD- and BD-fusion plasmids, then replica plated again to media lacking histidine (-HLW) and supplemented with ABA to score interactions between the fusion proteins. Lower panel: test of potential positives by dilution assay, as in Fig.3.

Supp Fig. 5 Expression of PYLs, GRFs and AFPs in maturing embryos (top), dry seeds and either 24 h post-2d-stratification (middle) or after 24h imbibition in water following 2-4 months after-ripening (bottom). Data from (Narsai et al., 2011; Nakabayashi et al., 2005; Hofmann et al.,2019) displayed as "Absolute" units on http://bar.utoronto.ca/efp//cgi-bin/efpWeb.cgi (Winter et al., 2007).

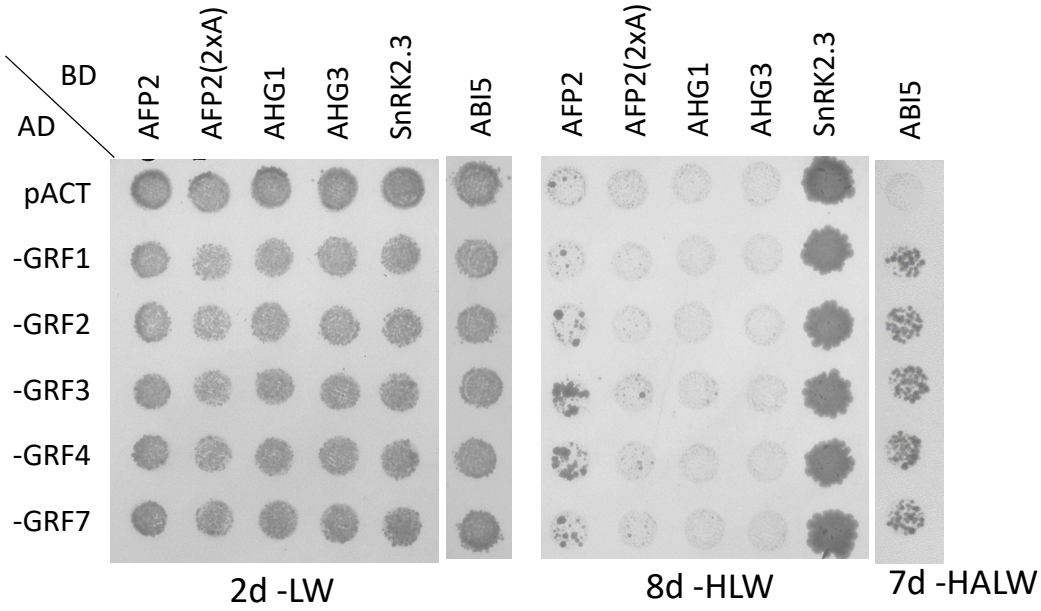

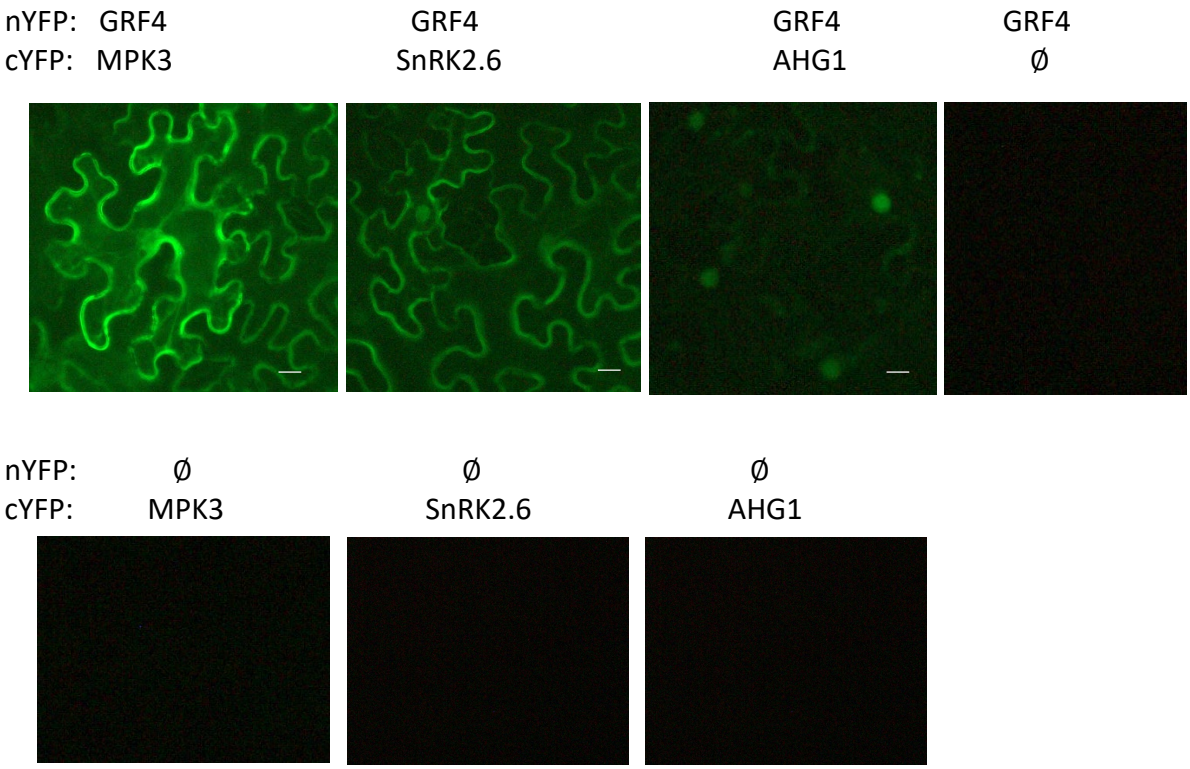

Supp Fig. 6. Interactions between 14-3-3 proteins (GRFs) and ABA core signaling elements. Top: Yeast two-hybrid assays combining AD-fusions to 14-3-3 proteins with BD-fusions to wild-type and mutant AFP2, PP2Cs, SnRK2.3 and ABI5 by matings, as described for Supp.Fig.4.
Bottom: BiFC assays testing GRF interactions with kinases and phosphatases. Scale bars = 10 μm

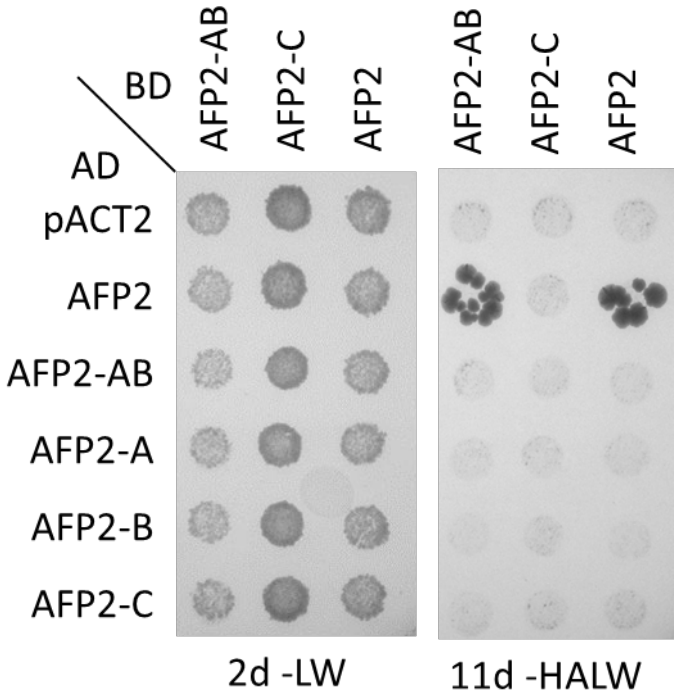

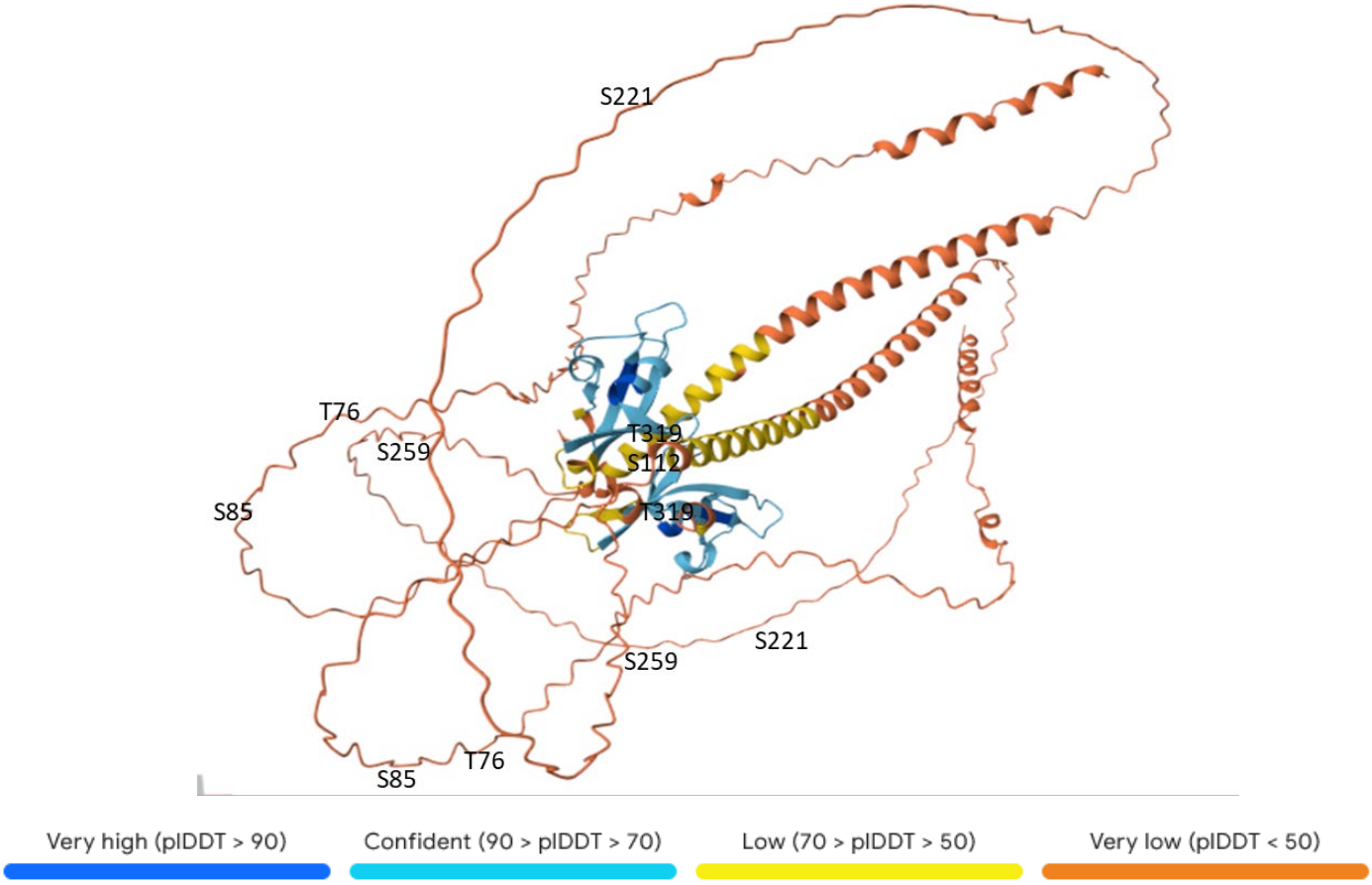

Supp Fig. 7 Potential dimerization domains of AFP2
Top: Mapping interacting domains of AFP2 by yeast two hybrid assays, as in Supp. Fig. 2. The AFP2-AB domain includes aa 1-149 and the C domain includes aa 150-348. Bottom: Alphafold prediction of AFP2 dimer structure.

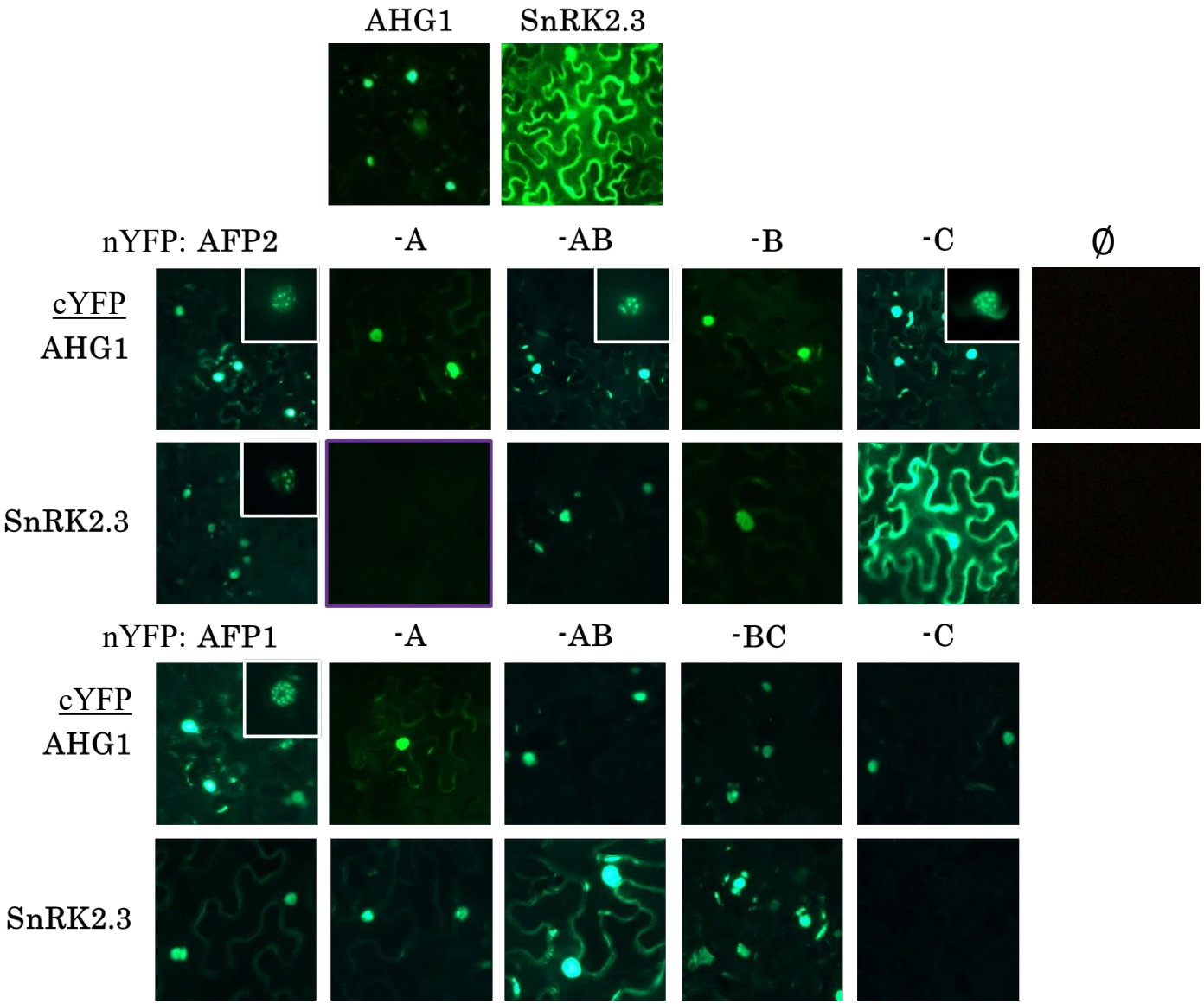

Supp Fig.8. Biomolecular fluorescence complementation of full length AFP2 (middle) and AFP1 (bottom) and subdomains versus ABA core signaling components in *N. benthamiana* leaves (100X magnification). Top panel shows localization of YFP-fused phosphatase and kinase for reference. Color differences are due to different versions of image capture software. Inset images show examples of nuclear speckles observed at 200X or 400X magnification. (Erickson McNally, 2016)

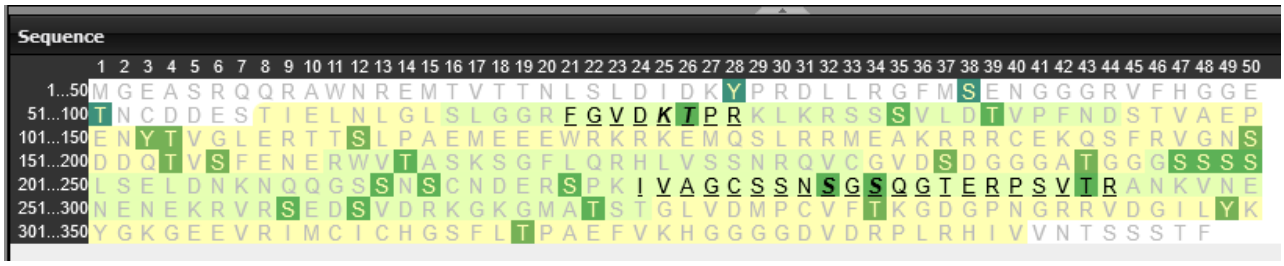


```
AFP2 :    28 YPRDLLRGFMSENGGGRVFHGGETNCDDESTIELNLGLSLGGRFGVDKTPRKLKRSSSVL 87
             +PRDLL+ F+S +   G       E    DDE   IELNLGLSLGGRFGVDK+   KL RSSSV+
AFP1 :    19 FPRDLLQRFISNSVEGE--DDDEEEDDDE--IELNLGLSLGGRFGVDKS-NKLVRSSSVV 73

AFP2 :    88 DTVP-FNDS-----------------TVAEPENYTVGLERTTSLPAEMEEEWRKRKEMQS 129
              T+P F +                  TVA      T GL RTTSLPAE EEEWRKRKEMQ+
AFP1 :    74 VTMPLFREDHHHHQAAAMITTKVSTETVAGATRGT-GLMRTTSLPAESEEEWRKRKEMQT 132

AFP2 :   130 LRRMEAKRRRCEKQSFRVGNSDDQTVSFENERWVTASKSGFLQRHLVSSNRQVCGVDSDG 189
             LRRM AKRRR EK     VG  +       E      TAS+     +R    SS        ++
AFP1 :   133 LRRMAAKRRRSEKLRTGVGGGNSNNP--EEAATATASR----RRGRPSSGLPRWSATANK 186

AFP2 :   190 GGATGGGSSSSLSELDNKNQQ-GSSNSCNDERSPKIVAGCSSNSGSQGTERPSVTRANKV 248
              G       S+ L  L     +  G    +      S    +    +  S  +     PS T+  +
AFP1 :   187 SGLLRQ-HSAGLDSLQVSGESLGGGRAAGSSSSVSELE--TKASSDEARSLPSTTQPQQE 243

AFP2 :   249 NENENEKRVRSEDSVDRKGKGMATSTGLVDMPCVFTKGDGPNGRRVDGILYKYGKGEEVR 308
                +   R+R    SVD    K       G  +MPCVFTKGDGPNG+RVDGILY+YG GEEVR
AFP1 :   244 TTTKPTNRLRRLSSVDMNMKMEPQGKGKSEMPCVFTKGDGPNGKRVDGILYRYGSGEEVR 303

AFP2 :   309 IMCICHGSFLTPAEFVKHGGGGDVDRPLRHIVVNTSS 345
             IMC+CHG FL+PA+FVKH GG  VD PLRHIVVNTSS
AFP1 :   304 IMCVCHGDFLSPADFVKHAGGPHVDHPLRHIVVNTSS 340
```

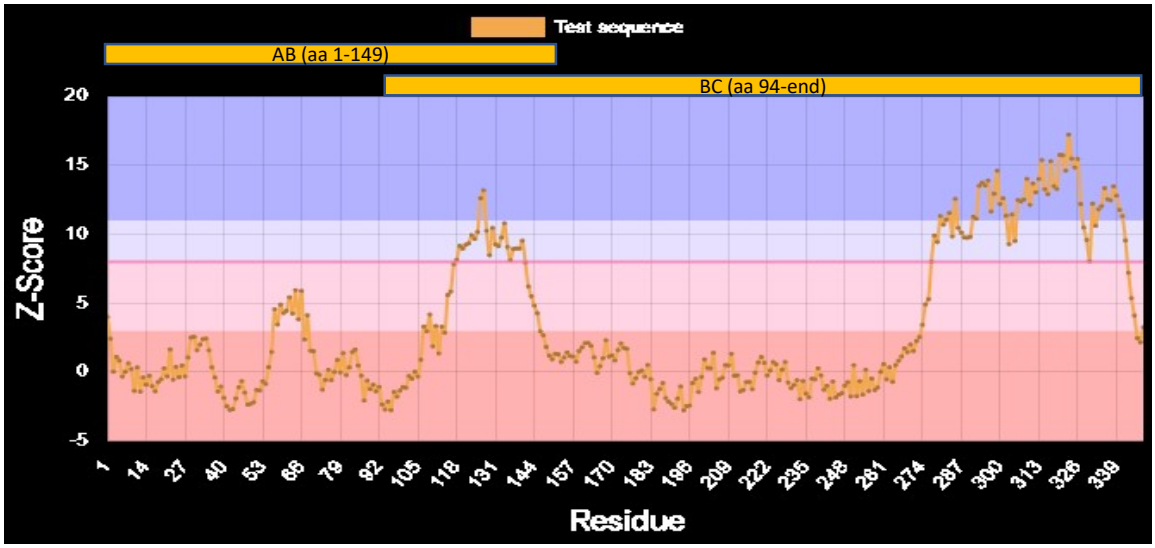

Supp Fig. 9 Predicted phosphorylated residues in AFP1 and AFP2. Top: PhosPhAt shows possible phosphorylation sites of AFP1 highlighted in green, with documented sites identified by black letters. Middle: Alignment of AFP1 and AFP2. A, B and C domains are underlined in blue, green and red, respectively. Residues fitting consensus for MAPK phosphorylation are in blue, those fitting SnRK2 consensus are in red. Bottom: Disordered regions (score <8) in AFP2 predicted by Attention based DisOrder PredicTor (ADOPT) (Redl et al. 2023), with extent of the subdomain constructs shown above the disorder plot.

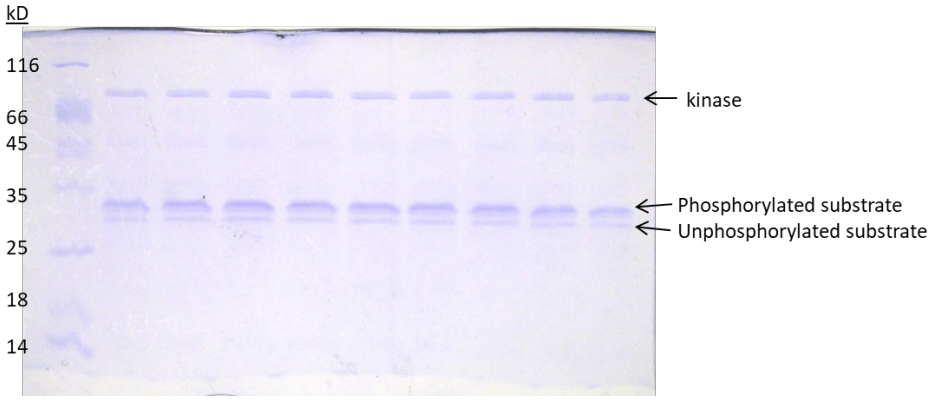

10 exclusive unique peptides, 10 exclusive unique spectra, 10 total spectra, 113/192 amino acids (59% coverage)

M G S S H H H H H H S S G L V P R **G S H** **M I T S Y S I H Y T** **K L S G I R P S R P** **Q D P M G E A S R** Q
Q R A W N R **E M T V** **T T N L S L D I D K** **Y P R D L L R G F M** **S E N G G G R** V F H G G E T N C D D E S
T I E L N L G L S L G G R **F G V D K T P** **R** K L K R **S S S V L** **D T V P F N D S T V** **A E P E N Y T V G L**
E R T T S L P A E M **E E E W R K R** K E M Q S L R R M E A K R R R C E K Q S F R V G N

Valid	Weight	Sequence	Prob	Identity Score	NTT	Modifications
☑	1.0	(R)GSHMITSYSIHYTK(L)	100%	8.7	2	
☑	1.0	(K)LSGIRPSRPQDPMGEASR(Q)	100%	8.6	2	
☑	1.0	(R)EMTVTTNLSLDIDKYPR(D)	99%	7.8	2	Oxidation (+16)
☑	1.0	(R)DLLRGFMSENGGGR(V)	97%	7.1	2	Oxidation (+16)
☑	1.0	(R)GFMSENGGGR(V)	99%	8.0	2	Deamidated (+1)
☑	1.0	(R)FGVDKTPR(K)	98%	7.5	2	
☑	1.0	(R)SSSVLDTVPFNDSTVAEPENYTVGLER(T)	99%	7.7	2	
☑	1.0	(R)TTSLPAEMEEEWR(K)	100%	8.3	2	
☑	1.0	(R)TTSLPAEMEEEWRK(R)	99%	8.1	2	
☑	1.0	(R)TTSLPAEMEEEWRKR(K)	98%	7.6	2	Phosphoryl+STY (+80)

Protein Sequence | Similar Proteins | Spectrum | Spectrum/Model Error | Fragmentation Table

B	B Ions	B+2H	B-NH3	B-H2O	AA	Y Ions	Y+2H	Y-NH3	Y-H2O	Y
1	102.1	51.5		84.0	T	1,942.9	971.9	1,925.8	1,924.9	15
2	203.1	102.1		185.1	T	1,841.8	921.4	1,824.8	1,823.8	14
3	370.1	185.6		352.1	S+80	1,740.8	870.9	1,723.8	1,722.8	13
4	483.2	242.1		465.2	L	1,573.8	787.4	1,556.8	1,555.8	12
5	580.2	290.6		562.2	P	1,460.7	730.9	1,443.7	1,442.7	11
6	651.3	326.1		633.3	A	1,363.6	682.3	1,346.6	1,345.6	10
7	780.3	390.7		762.3	E	1,292.6	646.8	1,275.6	1,274.6	9
8	911.4	456.2		893.3	M	1,163.6	582.3	1,146.5	1,145.6	8
9	1,040.4	520.7		1,022.4	E	1,032.5	516.8	1,015.5	1,014.5	7
10	1,169.4	585.2		1,151.4	E	903.5	452.2	886.5	885.5	6
11	1,298.5	649.7		1,280.5	E	774.4	387.7	757.4	756.4	5
12	1,484.6	742.8		1,466.6	W	645.4	323.2	628.4		4
13	1,640.7	820.8	1,623.6	1,622.7	R	459.3	230.2	442.3		3
14	1,768.8	884.9	1,751.7	1,750.8	K	303.2	152.1	286.2		2
15	1,942.9	971.9	1,925.8	1,924.9	R	175.1	88.1	158.1		1

Supp. Fig. 10 *In vitro* kinase reaction of His-AFP2-AB incubated with GST-SnRK2.6 used for mass spectrometric analysis of phosphorylation site(s). Top: Coomassie-stained SDS-PAGE; the replicate phosphorylated substrate bands were excised from the gel, and sent to the UC Davis Mass Spectrometry Facility for analysis following tryptic digestion. Bottom: Summary of Mass Spec analysis by Scaffold software, including Fragmentation Table for the only peptide showing phosphorylation. The initiating Met of AFP2, at position 44 of the fusion protein, is circled in the sequence.

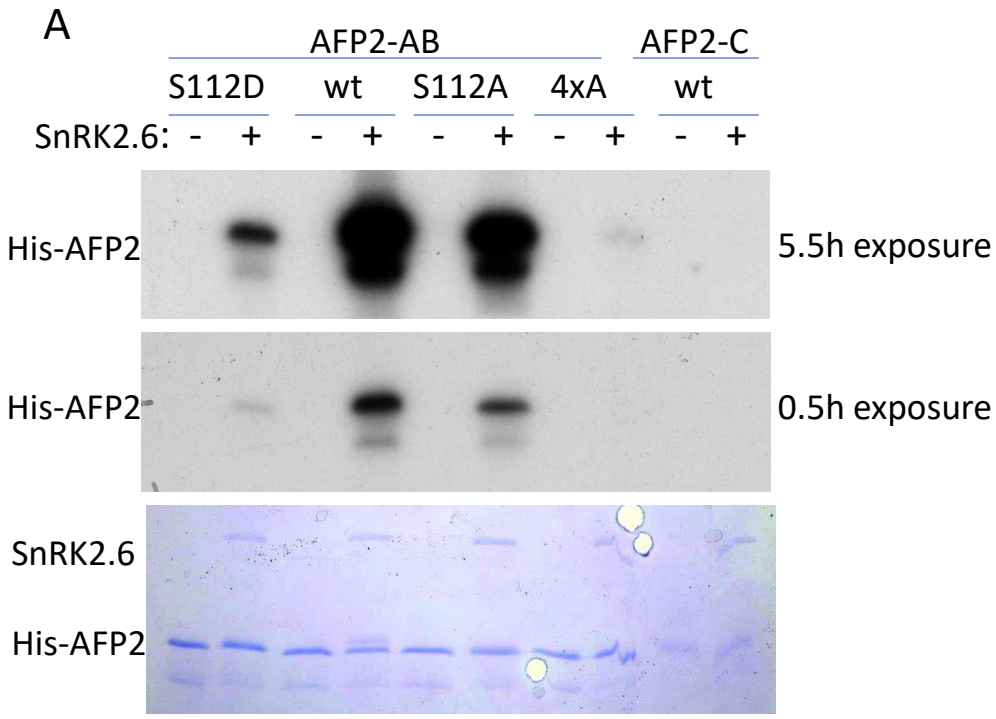

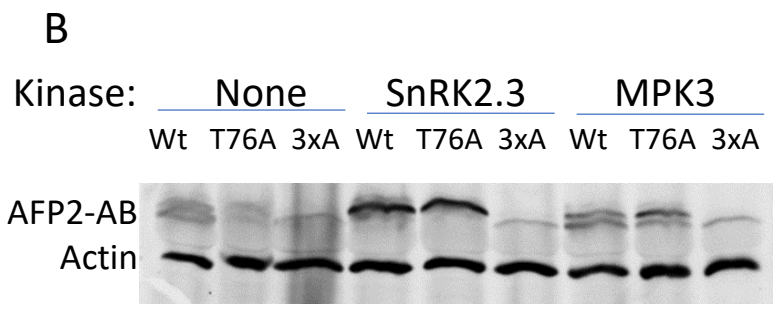

Supp. Fig. 11 Tests of potential phosphorylation sites by kinase reactions with mutant AFP substrates. In vitro kinase assay comparing phosphorylation of wild-type AFP2-AB domain with phosphomutants or AFP2-C domain (A). Top two panels are autoradiographs of the Coomassie-stained gel shown in the bottom panel. Affinity-purified GST-SnRK2.6 was pre-activated, then reactions set up as pool before aliquoting for combination with His-AFP2 substrates. Coomassie shows loading of AB fusions and SnRK. “4xA” = (S85,T111,S112,S129)A; as shown in Fig. 5E, (S85,S112)A gives the same result as the 4xA mutant.
Comparison of wild type and phosphomutant YFP-AFP2-AB domain mobility when transiently expressed in *N. benthamiana*, either alone or in combination with either Myc-SnRK2.3 or Myc-MPK3 (B). “3xA” = (T76,S85,S112)A

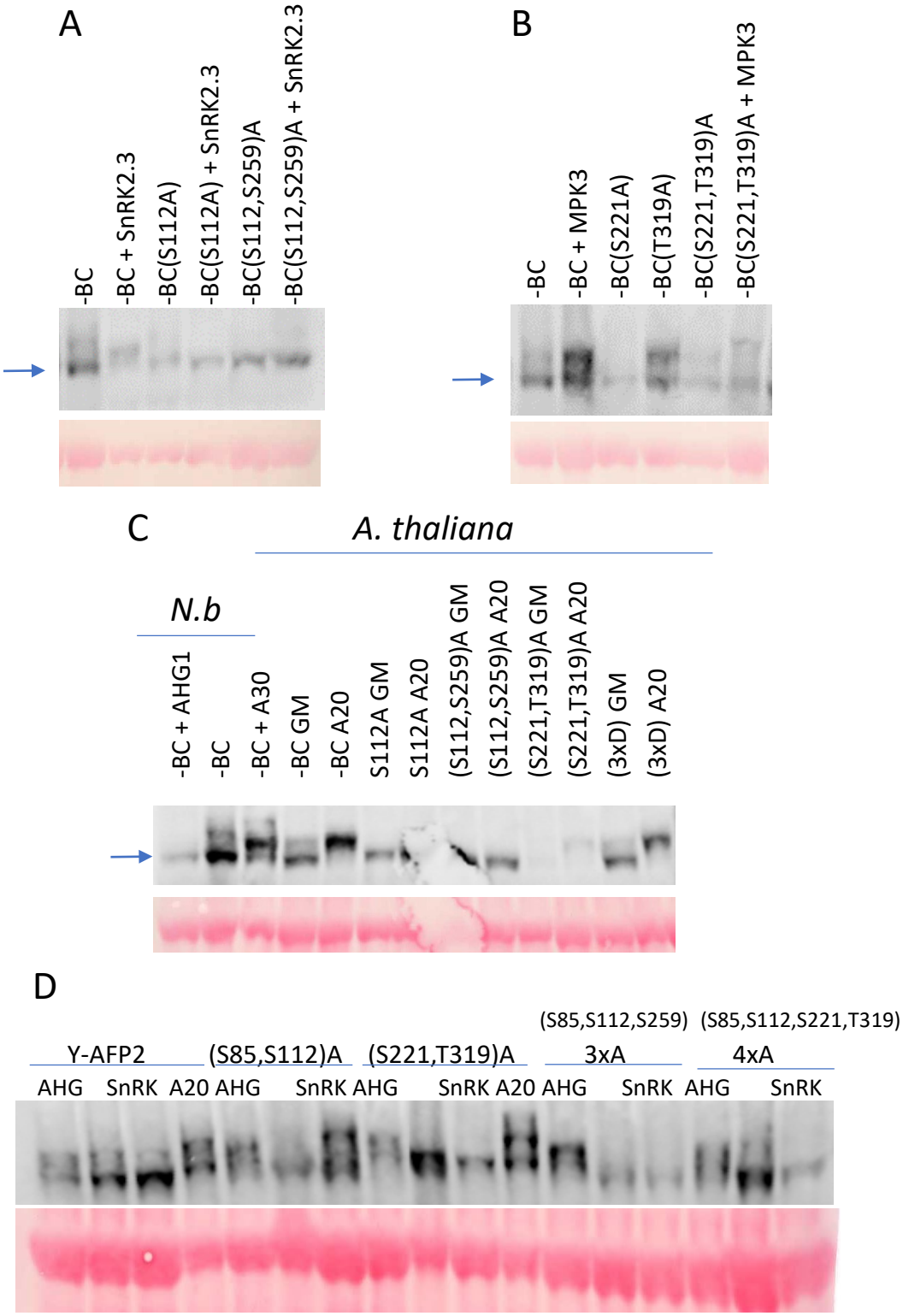

Supp. Fig 12 Comparison of phosphorylation status of AFP2-BC domain and full-length AFP2 by Phos-tag gels. YFP-AFP2-BC fusions were expressed transiently in *N.benthamiana* (A,B,C) or stably in *A.thaliana* (C) Fusions were expressed alone or in combination with Myc-SnRK2.3 (A), Myc-MPK3 (B) or Myc-AHG1 (C). ABA or GM incubations were as described in Fig. 6AB. The "3xD" mutant is altered at S112, S221, and T319. The unphosphorylated AFP2-BC domain is identified by the arrows. Full-length AFP2 fusions were expressed transiently alone or in combination with Myc-AHG1 or Myc-SnRK2.3 in *N.benthamiana* (D).

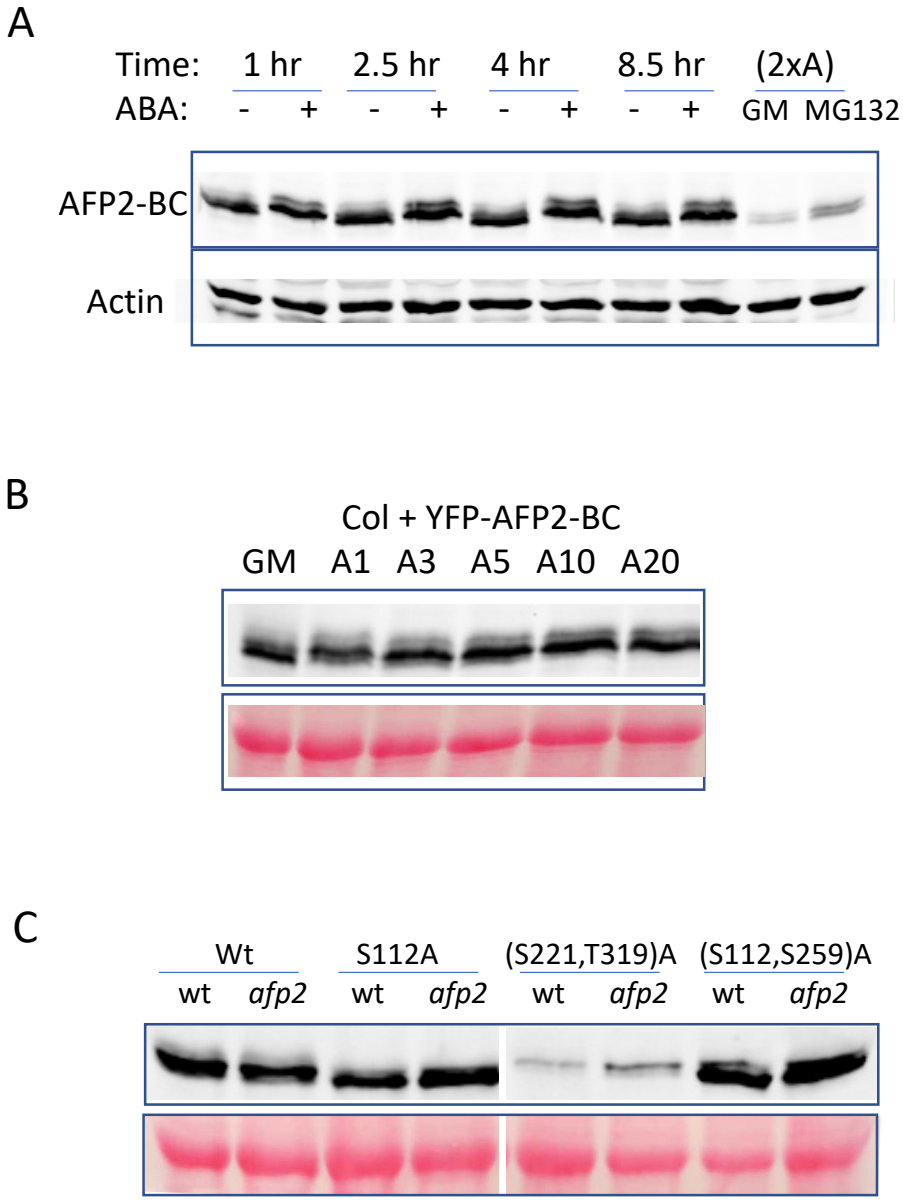

Supp. Fig. 13. Effects of ABA, mutations and genetic background on expression and mobility of YFP-AFP2-BC transgenes in stably transformed *A. thaliana.* Time course of changes in mobility of wild-type AFP2-BC in response to 20 μM ABA (A). Dose response of ABA-induced changes in mobility of wild-type AFP2-BC domain in stably transformed *A. thaliana* incubated for 6 hrs in GM with or without ABA ranging from 1-20 μM (B). Expression of wild-type (wt) YFP-AFP2-BC and transgenes with the indicated mutations in wt and *afp2* seedlings following germination and 7d growth on minimal media supplemented with 3 μM ABA (C). Upper panels are immunoblots probed with anti-GFP. Lower panels in B and C are the RbcL bands seen on Ponceau stained filters.

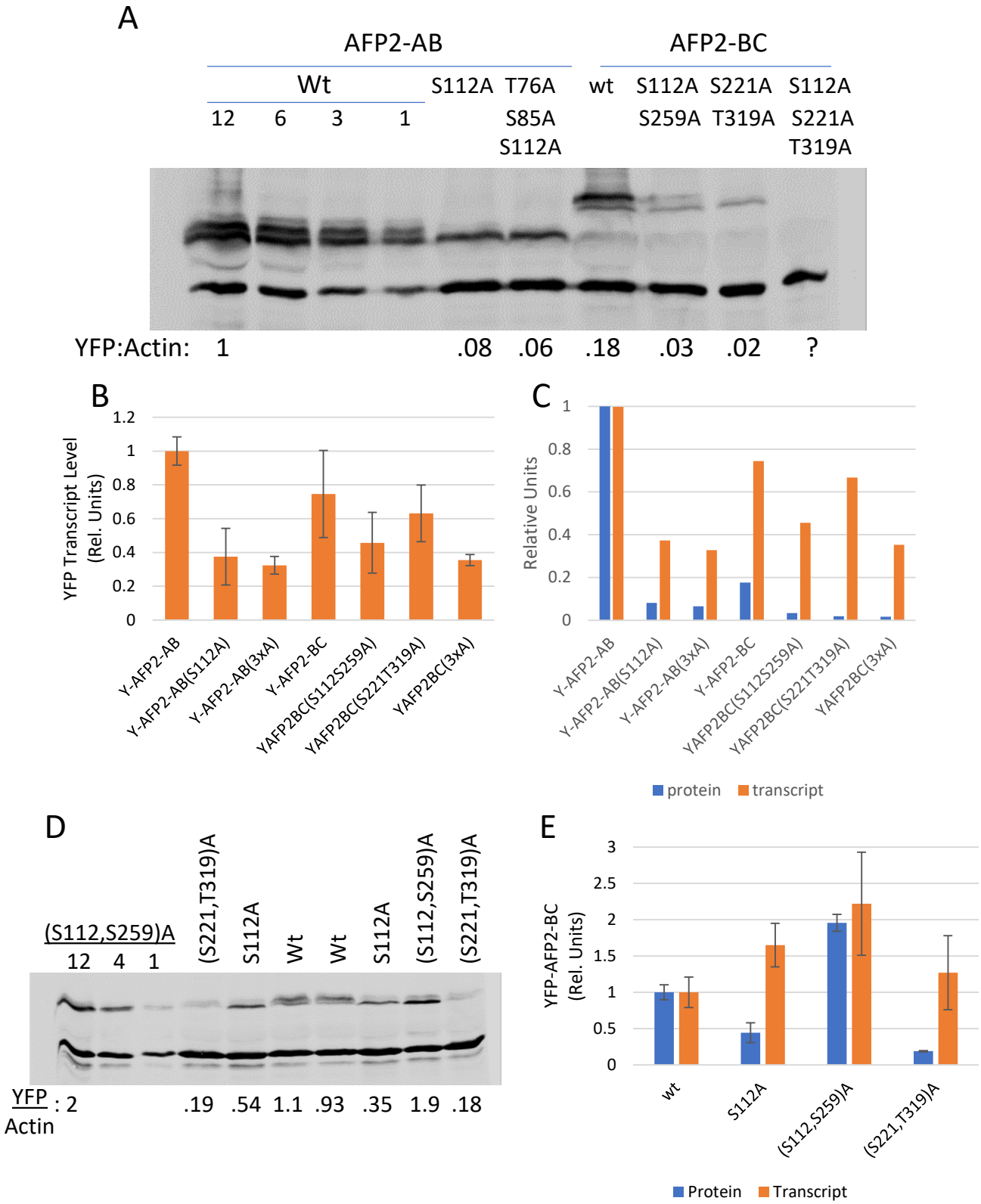

Supp. Fig. 14. Comparison of protein and transcript levels for AFP2-AB or AFP2-BC domain fusions. Transient expression in *N. benthamiana* (A-C) or stable transformants in *A. thaliana* (D,E). The standard series of wt AFP2-AB shows the volume of extract loaded for the standard curve. Amounts of YFP fusion protein were normalized relative to actin. YFP-fusion transcripts were normalized relative to these stably expressed endogenous genes: PP2A (Niben101Scf09716g01002.1) of *N.benthamiana* and the geometric mean of PP2AA3 (At1g13320) and AP2M (At5g46630) of Arabidopsis.

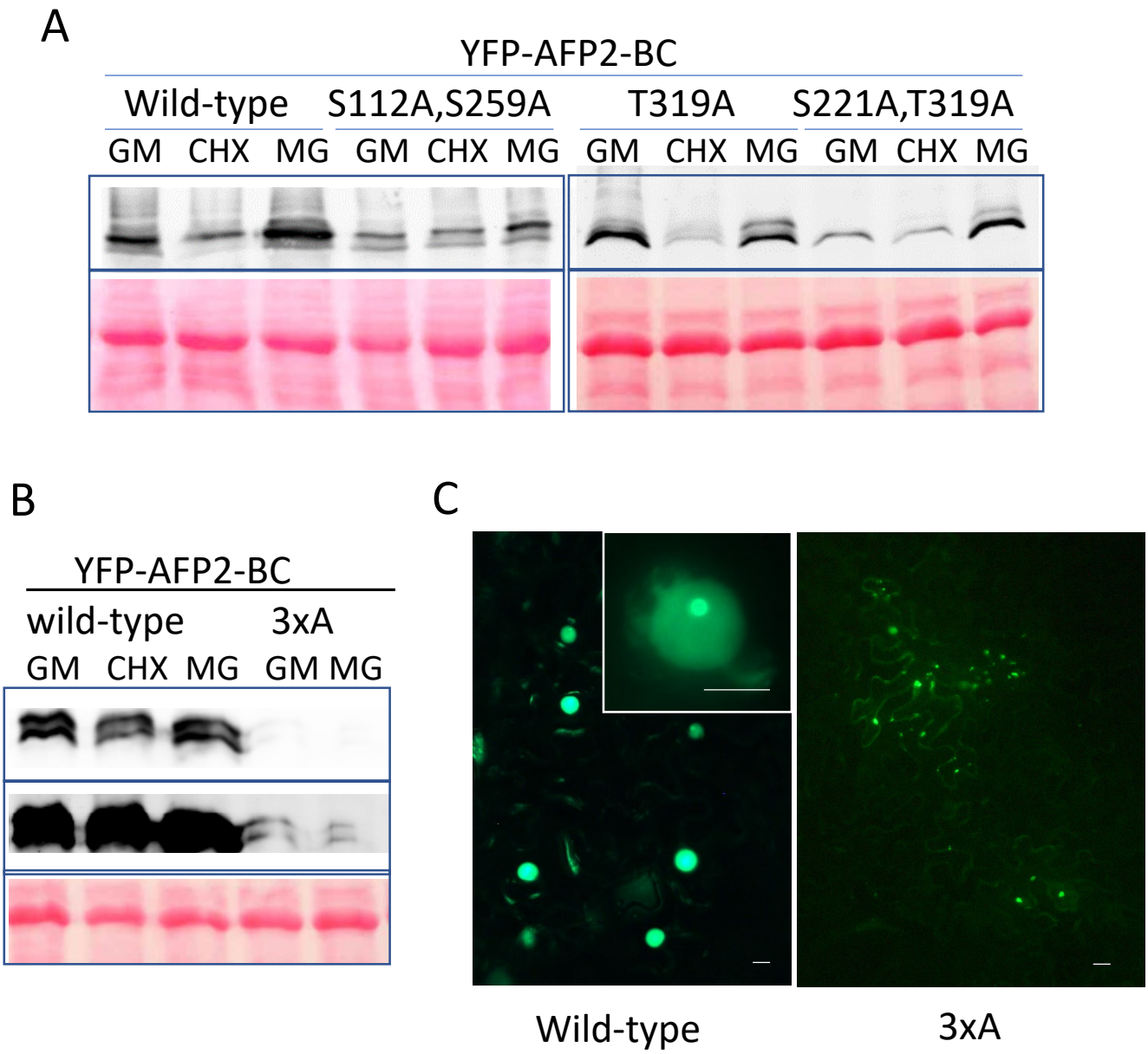

Supp. Fig. 15. Comparison of stability and accumulation of transiently expressed wild type, double (S112A,S259A or S221A,T319A) or triple (3xA=S112A,S221A,T319A) mutant AFP2-BC domain fusions to YFP. Following infiltration, *N. benthamiana* leaf discs were infiltrated with GM (0.5x MS medium) with or without 20 uM cycloheximide (CHX) or MG132(MG), and incubated 6 hrs prior to harvest for extraction. Immunoblots were probed with anti-GFP (top panels) after staining with Ponceau (lower panels) (A,B). Micrographs of *N. benthamiana* leaves used for assay in B, taken with 10x objective on an Olympus AX70 epifluorescence microscope (C). Gain was set at 11.9 for 3xA mutant vs. 2.0 for wild-type. Inset is wild-type nucleus taken with 40x objective. Scale bars = 10 μm for wild-type, 20 μm for 3xA mutant

Supp. Fig. 16. Germination phenotypes of wild type (Col) and transgenic seeds expressing the indicated YFP-AFP2 fusions after 7d incubation on either 10 or 50 µM ABA.

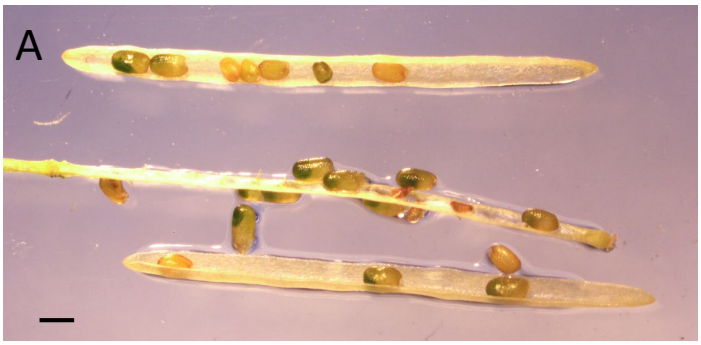
A

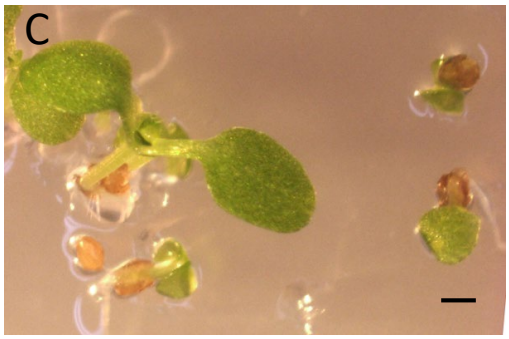
C

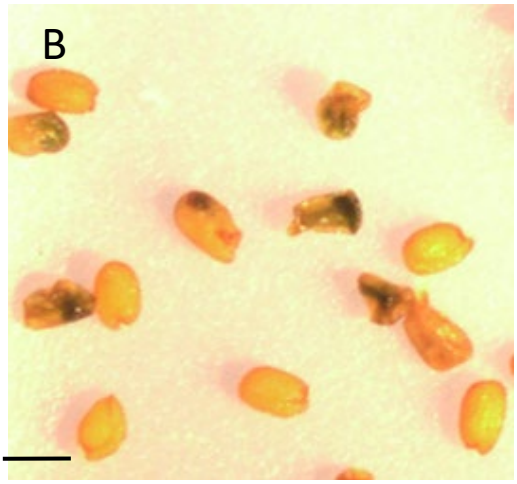
B

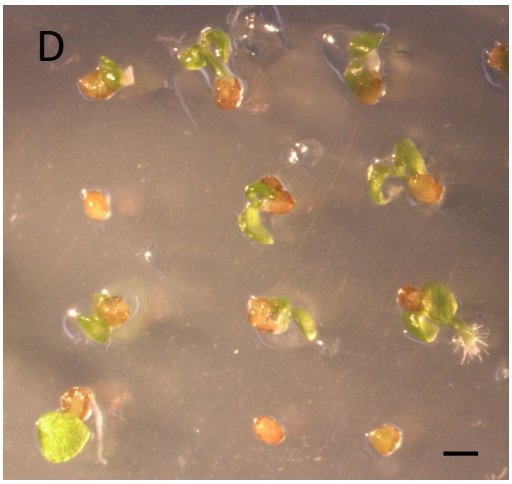
D

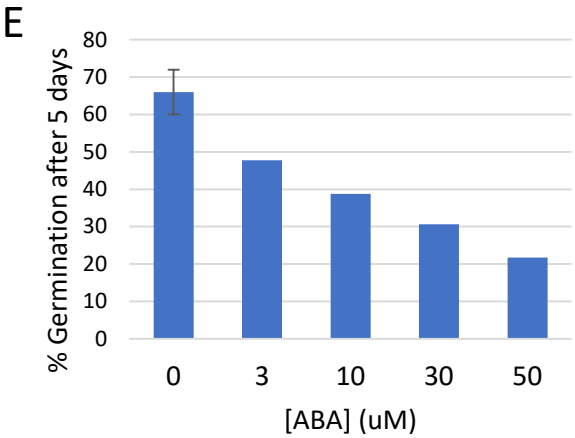
E
% Germination after 5 days
80
70
60
50
40
30
20
10
0
0
3
10
30
50
[ABA] (uM)

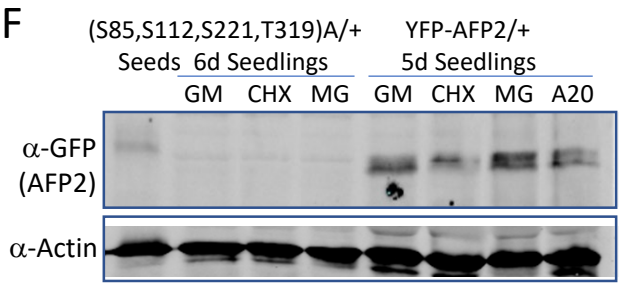
F
(S85,S112,S221,T319)A/+
YFP-AFP2/+
Seeds
6d Seedlings
5d Seedlings
GM
CHX
MG
GM
CHX
MG
A20
α-GFP
(AFP2)
α-Actin

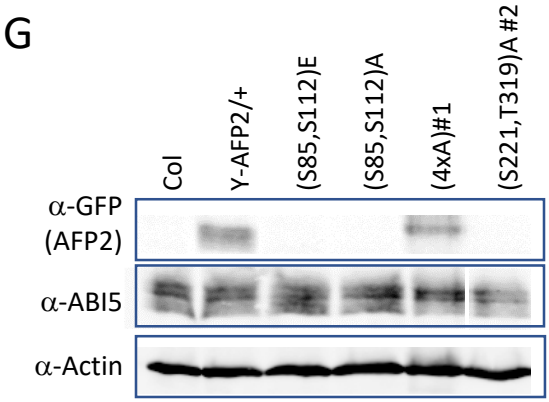
G
Col
Y-AFP2/+
(S85,S112)E
(S85,S112)A
(4xA)#1
(S221,T319)A #2
α-GFP
(AFP2)
α-ABI5
α-Actin

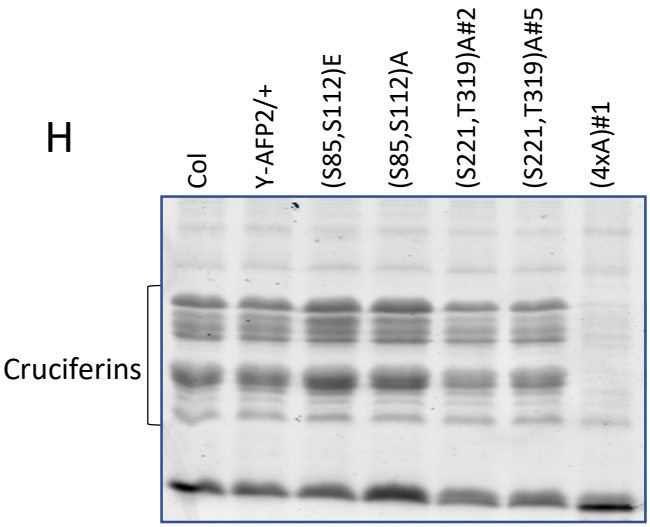
H
Col
Y-AFP2/+
(S85,S112)E
(S85,S112)A
(S221,T319)A#2
(S221,T319)A#5
(4xA)#1
Cruciferins

Supp. Fig. 17. Transgenic line hemizygous for 35S-YFP-AFP2(S85,S112,S221,T319)A fails to complete seed maturation. (A) Maturing silique segregating green seeds. (B) Dry seeds with green embryos are desiccation intolerant and shrunken. (C) Comparison of seedlings from wild type siblings (left) and green seeds (right) removed from maturing siliques prior to desiccation. (D) Some green seeds fail to develop roots on minimal media. (E) Transgenic seeds are highly resistant to ABA-inhibition of germination. (F) Immunoblot comparing accumulation of wild type and mutant AFP2 fusions in seedlings following 6h incubation in GM with or without 100 uM CHX or MG132, or 20 uM ABA. Dry seed protein extracts of the indicated genotypes were separated on 10% SDS-PAGE for immunoblots (G) or 15% SDS-PAGE to resolve storage proteins (cruciferins) (H). “4xA” = 35S-YFP-AFP2(S85,S112,S221,T319)A. Scale bars = 0.5 mm

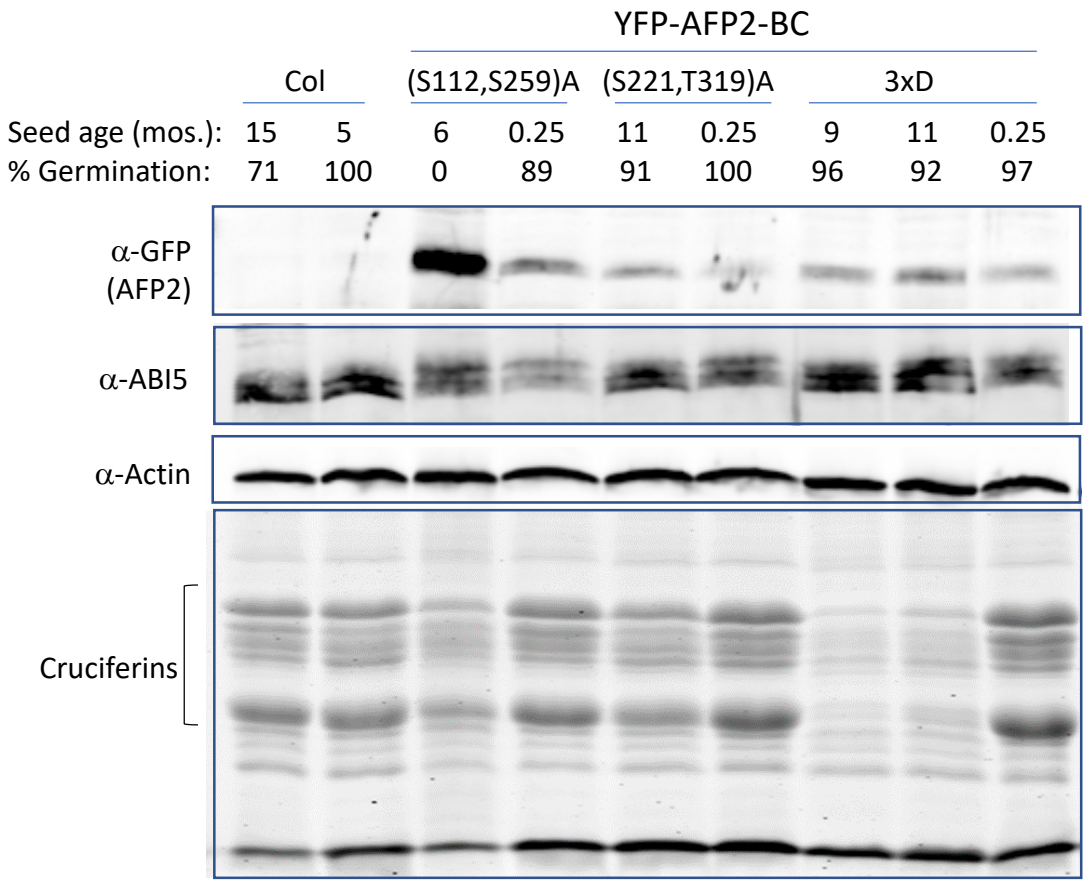

Supp. Fig. 18. Effects of phosphomutant or phosphomimetic YFP-AFP2 fusions on storage protein accumulation and seed longevity. Dry seed protein extracts of the indicated genotypes and ages were separated on 10% SDS-PAGE for immunoblot or 15% SDS-PAGE for resolution of storage proteins. Germination was scored at 4d post-stratification incubation on minimal nutrient media.

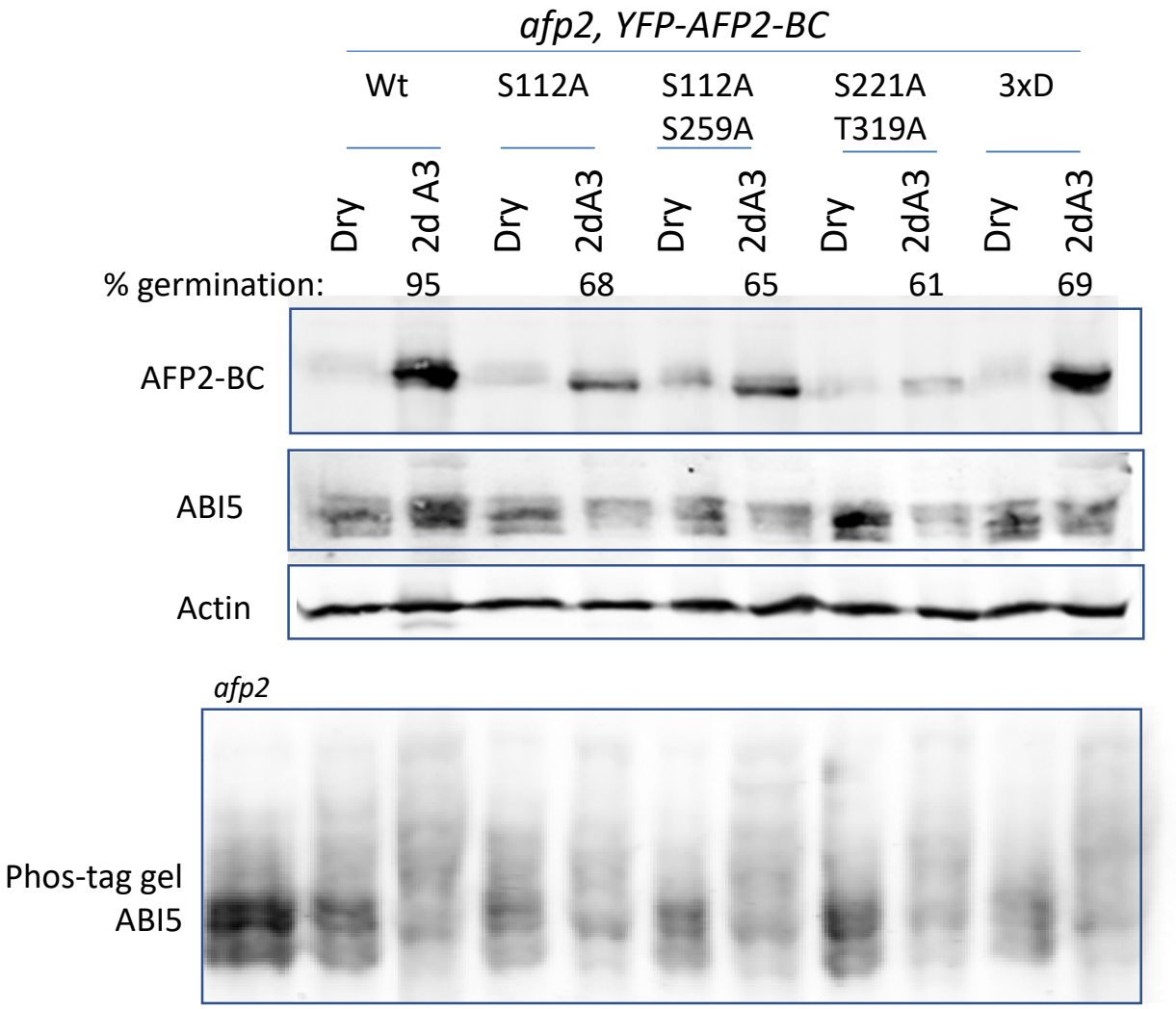

Supp. Fig. 19. Effect of ABA on accumulation and phosphorylation of ABI5 in seeds with wild type or mutant YFP-AFP2-BC fusions in an *afp2* mutant background. Protein extracts were separated on 10% SDS-PAGE (upper panels) or a 7.5% Phos-tag gel, then transferred to filters for immunoblots. Germination on minimal media supplemented with 3 μM ABA (A3) was scored just prior to harvest.

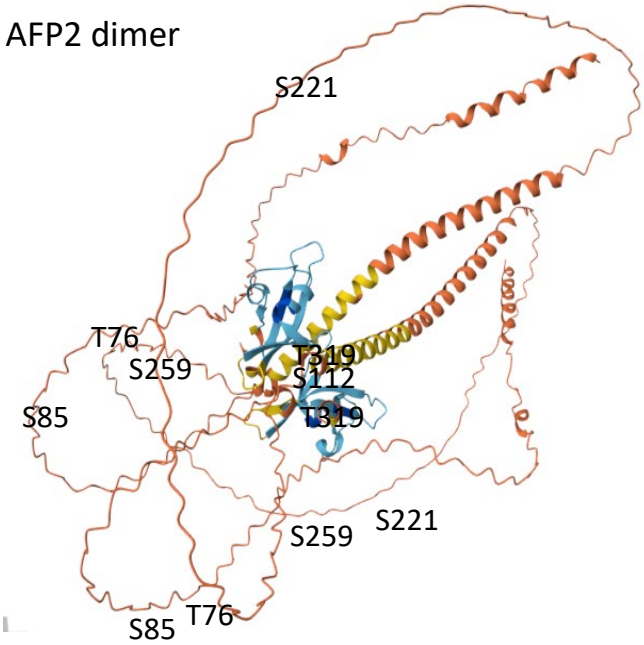

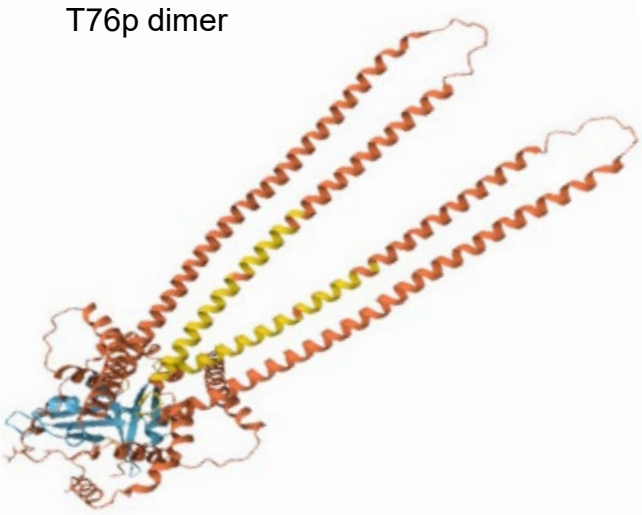

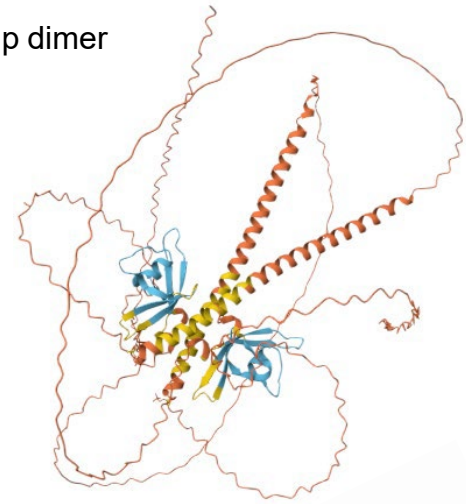

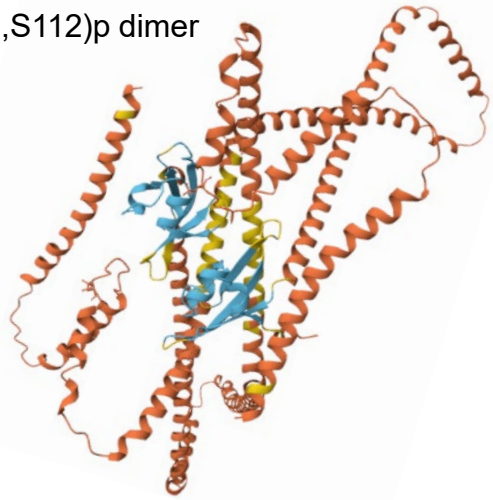

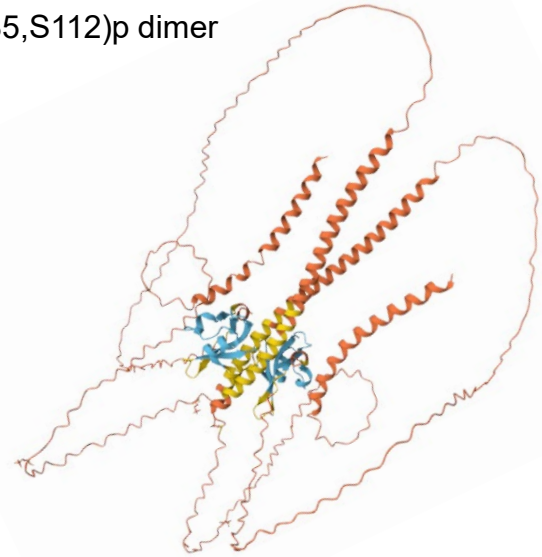

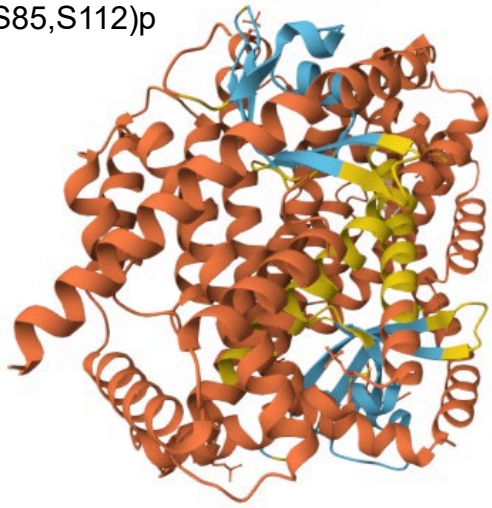

Supp. Fig. 20. Alphafold predictions of AFP2 dimer structure when phosphorylated, or blocked from phosphorylation, at residues tested in this work.

(S85,S112,S259)p dimer

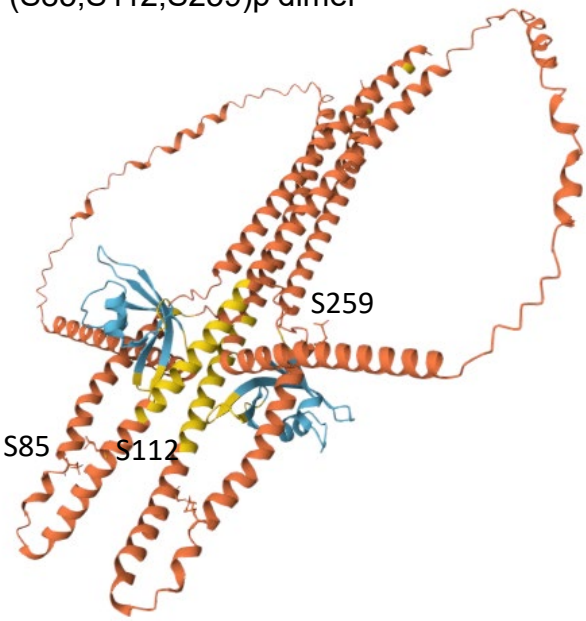

(T76,S85,S112,S259)p dimer

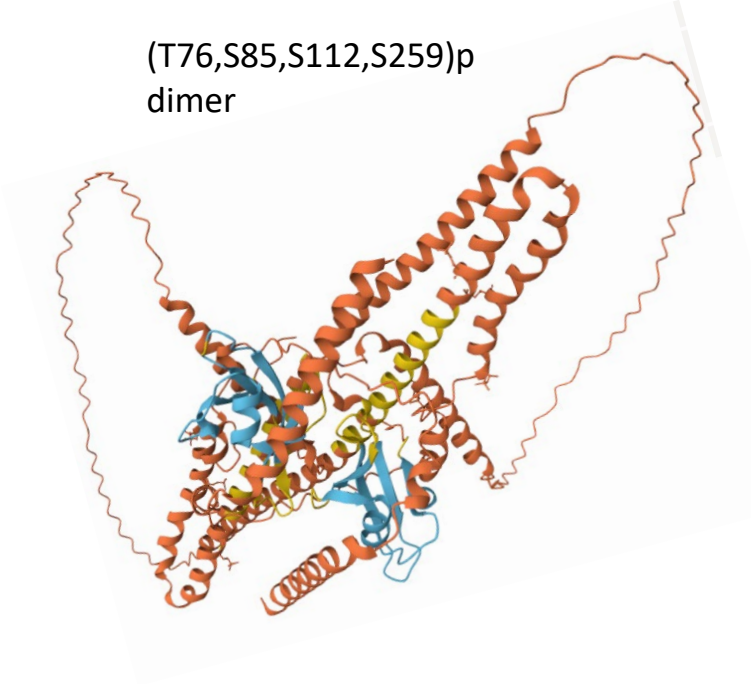

(S221,T319)p dimer

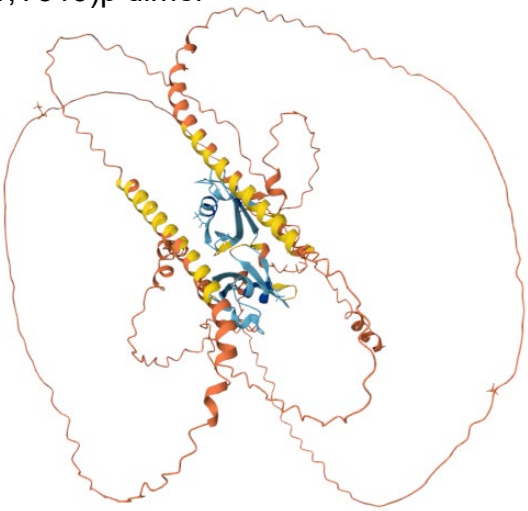

(T76, S221,T319)p dimer

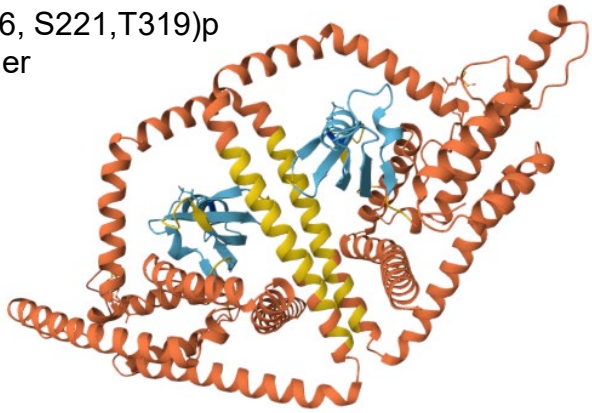

(S85,S112,S221,T319)p dimer

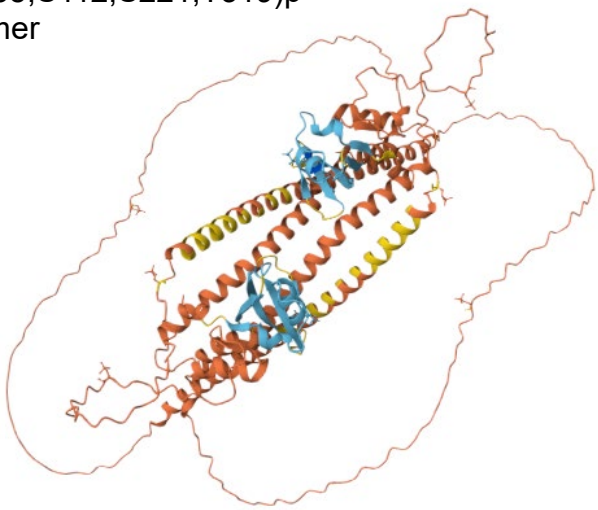

(T76,S85,S112,S221,T319)p dimer

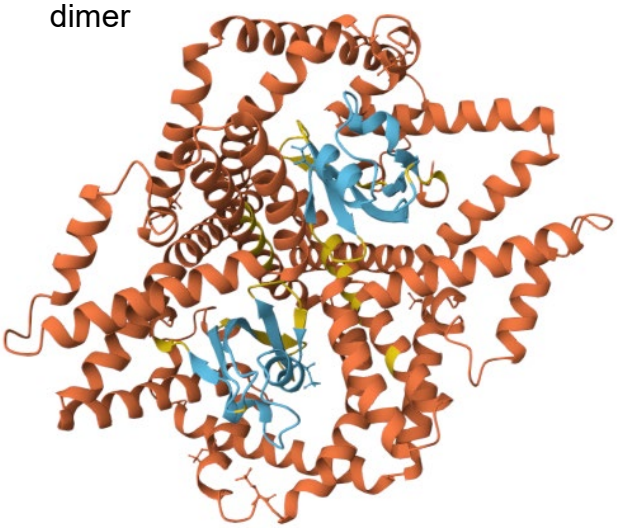

AFP2(S85,S112)A dimer

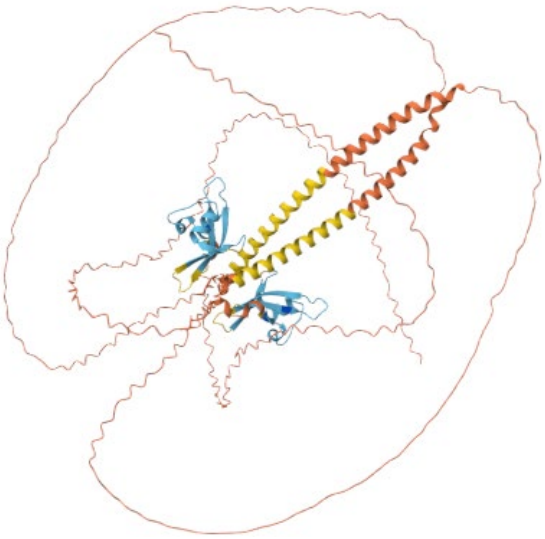

AFP2(T76,S85,S112)A dimer

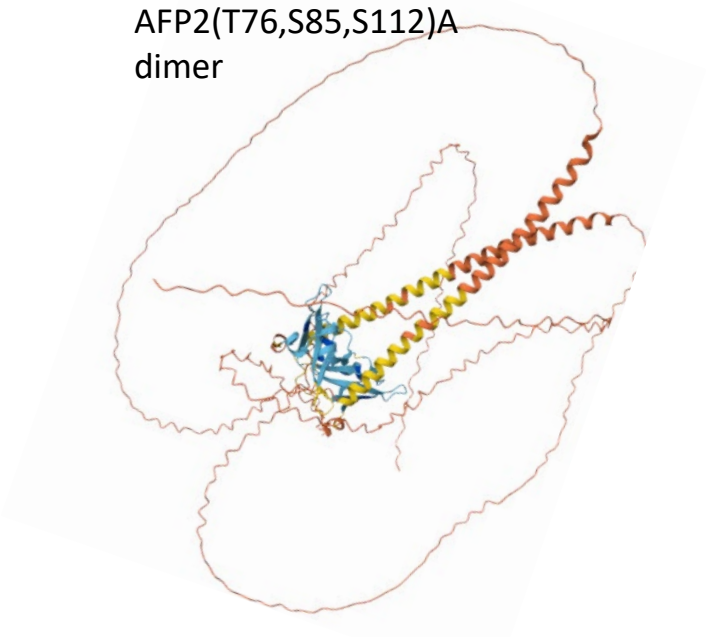

AFP2(S85,S112,S259)A dimer

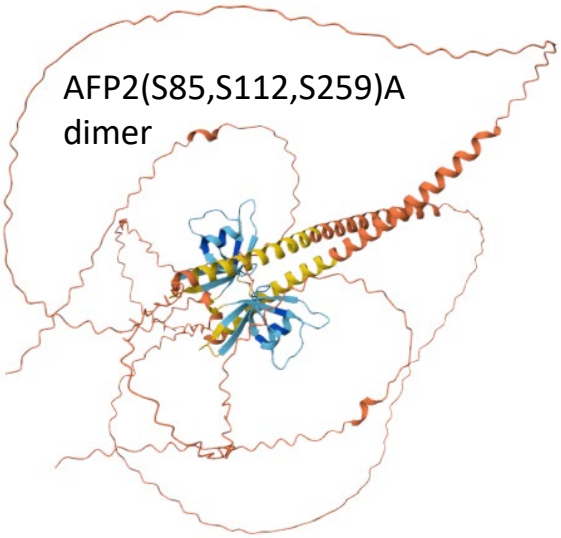

AFP2(S85,S112,S221,T319)A dimer

AFP2_T76p(S85,S112,S259)A dimer

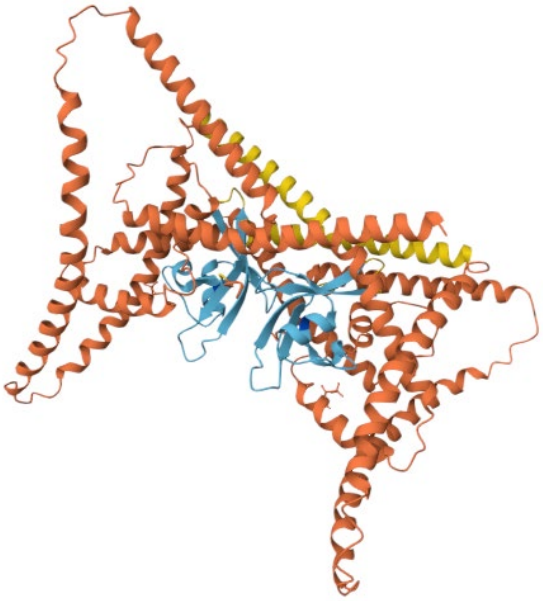
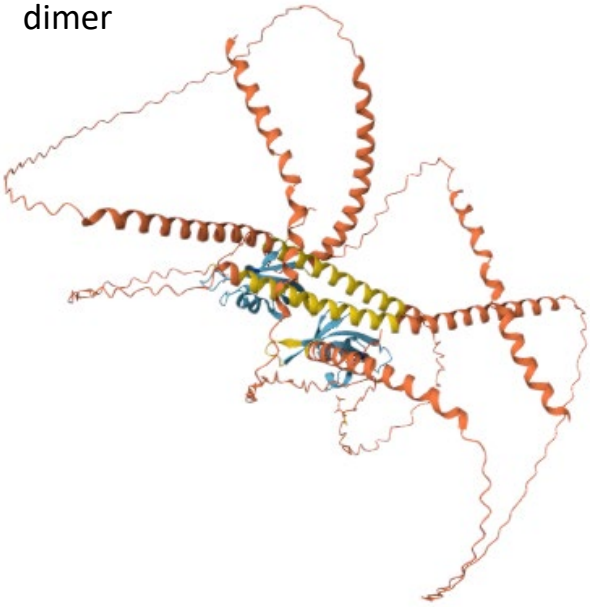
AFP2_T76p(S85,S112,S221,T319)A dimer